Title
Mechanism of Linkage-Specific Ubiquitin Chain Formation

Author
Wickliffe, Katherine

Publication Date
2013

Peer reviewed|Thesis/dissertation

Mechanism of Linkage-Specific Ubiquitin Chain Formation

By

Katherine Elizabeth Wickliffe

A dissertation submitted in partial satisfaction of the
requirements for the degree of
Doctor of Philosophy
in
Molecular and Cell Biology
in the
GRADUATE DIVISION
of the
UNIVERSITY OF CALIFORNIA, BERKELEY

Committee in charge:

Professor Michael Rape, Chair
Professor Rebecca Heald
Professor Eva Nogales
Professor Daniel Zilberman

Spring 2013

Abstract

Mechanism of Linkage-Specific Ubiquitin Chain Formation

by

Katherine Elizabeth Wickliffe

Doctor of Philosophy in Molecular and Cell Biology

University of California, Berkeley

Professor Michael Rape, Chair

The covalent attachment of ubiquitin to a protein controls a range of cellular processes in eukaryotes by altering the protein's stability, localization, or activity. Ubiquitylation requires the activity of three enzymes: a ubiquitin-activating enzyme (E1), a ubiquitin-conjugating enzyme (E2), and a ubiquitin ligase (E3). This enzymatic cascade modifies substrates with either a single ubiquitin or polyubiquitin chains linked through lysine residues of ubiquitin. Because ubiquitin contains seven lysines, different chain types are possible, and chain topology determines the fate of the modified protein. For example, Lys48-linked chains target proteins to the proteasome, while non-proteolytic Lys63 chains are involved in complex reorganization and signaling pathways. Although the physiological roles and formation of these chain types has been extensively studied, the characterization of other chain types is lacking. In this dissertation, I present work describing the biological function and assembly of Lys11-linked ubiquitin chains.

Lys11-linked chains are formed on substrates of the human anaphase-promoting complex (APC/C), an E3 ligase essential for proliferation, promoting their degradation by the proteasome. Because this chain type was proposed to be essential for regulating mitosis, we undertook an extensive investigation into how Lys11 chains are build by the APC/C, with a focus on the role of E2 enzymes. In the Chapters below, we report that APC/C-dependent formation of Lys11-linked chains requires the activity of two E2 enzymes: a chain-initiating E2 Ube2C and a Lys11-specific, chain-elongating E2 Ube2S. These E2s likely bind the APC/C at the same time, representing a unique way for the APC/C to achieve processivity.

In most instances, linkage-specific ubiquitin chain assembly is promoted by E2s, yet this process has only been well characterized for Lys63-linked chains. Therefore, we next investigated the molecular mechanism underlying the Lys11-specificity of Ube2S. We report that Ube2S engages in essential non-covalent interactions with ubiquitin that are required for processive and specific ubiquitylation. Lys11-specificity is generated by substrate-assisted catalysis, in which an acidic residue of the substrate ubiquitin is essential for generating a catalytically competent active site.

To solidify the role of Lys11-linked chains and the APC/C in mitotic control, we developed a Lys11-specific antibody. Using this antibody, we show that the level of Lys11 chains in HeLa cells increases dramatically as cells pass through mitosis, while the level of Lys48 chains remains constant. Importantly, knockdown of the Ube2C/Ube2S E2 module inhibits formation of Lys11 chains, suggesting that the APC/C and its E2s are the major enzymatic machinery responsible for forming K11 chains in mitosis.

For Mary Wickliffe

Table of Contents

Dedication i

Table of Contents ii

Acknowledgements iii

Chapter 1: Introduction 1

Chapter 2: Identification of a Physiological E2 Module for the Human Anaphase-Promoting Complex 6

- Summary 7
- Introduction 7
- Results 8
- Discussion 12
- Methods 14
- Figure Legends 15
- Figures 20

Chapter 3: The Mechanism of Linkage-Specific Ubiquitin Chain Elongation by a Single-Subunit E2 33

- Summary 34
- Introduction 34
- Results 35
- Discussion 42
- Methods 44
- Figure Legends 46
- Figures 54

Chapter 4: K11-Linked Polyubiquitination in Cell Cycle Control Revealed by a K11 Linkage-Specific Antibody 69

- Summary 70
- Introduction 70
- Results 71
- Discussion 73
- Methods 75
- Figure Legends 77
- Figures 79

Chapter 5: Conclusions and Outlook 87

References: 91

Acknowledgements

Thanks to all my family, friends, and labmates who have made the completion of this dissertation possible.

I thank Professor Michael Rape for his continued support, discussion, and guidance over the years. I thank the members of my thesis committee, Professors Rebecca Heald, Eva Nogales, and Daniel Zilberman for their valuable insight.

I have the opportunity to collaborate with many great scientists during my time at Berkeley. I thank my original "in lab" collaborator Adam Williamson; the K11 antibody team at Genentech, especially Vishva Dixit and Marissa Matsumoto; and Sonja Lorenz. I thank my unofficial collaborator and baymate, Hermann-Josef Meyer, for many helpful discussions and generous sharing of constructs, proteins, chocolate, and gummy candies.

I thank all members of the lab, past and present, who have made the Rape lab what it is today. For reagents, help, advice, laughs, lunch breaks, walks to Yali or Starbucks, and tequila shots, I especially thank Annamaria Mocciaro, Achim Werner, John Ashchyan, Allison Craney, Aileen Kelly, Adam Williamson, HJ Meyer, Raquel Dominguez, and Colleen McGourty.

I thank our great support staff: Minda Pagtakhan for preparing hundreds of liters of "golden LB" and Ann Fischer for providing cells and many liters of FBS.

I thank Dr. Stephen Leppla at the NIH where I began my scientific journey and all the postdocs and postbacs I worked with during my time there. I especially thank my mentor Dr. Mahtab Moayeri, who introduced me to research and taught me how to think about science, giving me the freedom to explore, fail, and succeed.

Finally, I thank my family for their love and support over the years: Steve and Mimi, Andy and Monique, and the whole Wickliffe/Livesley/Culotti family.

Chapter 1

Introduction

Introduction to the ubiquitin system

The post-translational modification of proteins produces diverse signals that allow for fine-tuned control of protein activity. The covalent attachment of ubiquitin to a protein controls a wide range of cellular processes in eukaryotes by altering the protein's stability, localization, activity, or interactions. As detailed below, ubiquitylation requires an enzymatic machinery that regulates which substrates are modified, how, and when. Ubiquitin can be added to proteins as single molecules or in polymeric chains, with the fate of the modified protein determined by the manner in which ubiquitin is attached. The versatility of ubiquitylation as a post-translational modification is further heightened by the presence of deubiquitylating enzymes that remove ubiquitin from proteins.

As ubiquitylation is involved in almost all biological pathways, mutations in the ubiquitin system have been linked to many human diseases including cancer, neurodegenerative disorders, cardiovascular disease, and inflammatory disorders (Bedford et al., 2011; Petroski, 2008). Drug discovery efforts aimed at enhancing or inhibiting substrate ubiquitylation require a molecular understanding of how ubiquitylation enzymes function. In this dissertation, I will address mechanisms underlying the formation of specific types of ubiquitin chains essential for mitotic progression.

An enzymatic cascade attaches ubiquitin to protein substrates

Ubiquitylation is achieved by the sequential activity of three enzymes: E1 ubiquitin-activating enzymes, E2 ubiquitin-conjugating enzymes, and E3 ubiquitin ligases. In the initial ATP-dependent step, ubiquitin is activated by an E1 enzyme, resulting in the formation of a thioester bond between the C terminus of ubiquitin and an active site cysteine of the E1 (Schulman and Harper, 2009). Next, ubiquitin is transferred to an active site cysteine of an E2 enzyme (Ye and Rape, 2009). Finally, E3 ligases bind both E2~ubiquitin conjugates and protein substrates and facilitate the transfer of ubiquitin to the ε-amino group of a lysine residue in the target protein (Deshaies and Joazeiro, 2009). There are two major families of E3 ligases, delineated by the presence of a HECT or a RING domain. HECT domain-containing E3 ligases contain an active site cysteine. Ubiquitin transfer to a substrate requires a thioester intermediate in which ubiquitin is first transferred from the E2 to the HECT active site. In contrast, RING domain-containing E3 ligases mediate the direct transfer of ubiquitin from the E2 to a substrate lysine (Deshaies and Joazeiro, 2009).

The topology of ubiquitylation

The addition of a single ubiquitin molecule, termed monoubiquitylation, can occur at one or multiple substrate lysines. Functionally, monoubiquitylation can alter protein localization or recruit binding partners (Sigismund et al., 2004). More often, however, polyubiquitin chains are attached to substrates. To accomplish this, an E2/E3 pair must switch from modifying substrate lysines to modifying lysine residues of ubiquitin itself. As ubiquitin contains seven lysines plus an amino terminus, eight different homogenous ubiquitin chain types linked through the same residue are possible. Additionally, an innumerable variety of mixed chains composed of multiple linkages can be formed. Although all linkage types have been detected in cells by mass spectrometry (Meierhofer et al., 2008; Peng et al., 2003; Xu et al., 2009), only four homogenous

chain types linked through Met1, Lys11, Lys48, and Lys63 have been functionally well-characterized (Komander and Rape, 2012). The physiological roles of so-called "atypical" ubiquitin chains linked through Lys6, Lys27, Lys29, and Lys 33 are not well established.

Structural studies of ubiquitin dimers have revealed that ubiquitin linkages adopt different conformations. Linear and Lys63-linked chains adopt a predominantly "open" conformation, with no intramolecular contacts between the two ubiquitin molecules. In contrast, Lys11 and Lys48 ubiquitin dimers are "compact," with intramolecular interfaces centered on hydrophobic patches of ubiquitin (Bremm et al., 2010; Cook et al., 1992; Eddins et al., 2007; Matsumoto et al., 2010).

Substrate fate is determined by ubiquitin linkage type

Depending on the linkage type, ubiquitylated substrates are subject to different fates. Because ubiquitin chains are structurally distinct, ubiquitin receptors containing ubiquitin binding domains (UBDs) bind ubiquitin chains in a linkage-specific manner and translate ubiquitylation signals into biological outcomes (Husnjak and Dikic, 2012). Ubiquitin chains linked through Lys48 are the most well-studied modification and target proteins for degradation by the 26S proteasome (Finley, 2009). This pathway is important for general protein homeostasis and removal of misfolded proteins (Smith et al., 2011). The regulated degradation of hundreds of cellular proteins modified with Lys48-linked chains provides a rapid mechanism by which cells can inhibit or active signaling pathways, control cell cycle transitions in a switch-like manner, or activate transcription factors (Skaug et al., 2009; Wickliffe et al., 2009). Linear and Lys63-linked ubiquitin chains are non-proteolytic and instead function as molecular scaffolds that recruit effector proteins to modified substrates. Biological processes regulated by these chain types include kinase activation, DNA repair, and endocytosis (Chen and Sun, 2009; Walczak et al., 2012).

Until recently, Lys11-linked ubiquitin chains were considered "atypical," with no known biological role. These linkages were detected in cells by mass spectrometry and their levels increased in response to proteasome inhibition (Meierhofer et al., 2008; Xu et al., 2009), suggesting a role in proteasomal degradation. At the onset of my thesis work, our lab discovered that Lys11-linked ubiquitin chains are required for the degradation of substrates of the human E3 ligase anaphase-promoting complex (APC/C) (Jin et al., 2008). The APC/C is essential for cell proliferation and regulates proper progression through mitosis by triggering the degradation of ~100 substrates, including securin and cyclins (Meyer and Rape, 2011; Peters, 2006). How the APC/C assembles Lys11-linked ubiquitin chains, however, was poorly understood. Work in the following chapters will describe the molecular mechanism by which the APC/C builds Lys11-linked chains on its substrates (Chapters 2 and 3) and the biological link between the APC/C and Lys11 ubiquitin chains in mitotic control (Chapter 4).

E2 ubiquitin conjugating enzymes are key determinants of ubiquitin chain formation

My dissertation will focus on understanding the role of E2 enzymes in catalyzing the processive formation of Lys11-linked ubiquitin chains. It is becoming more apparent that E2 enzymes do more than simply shuttle ubiquitin between E1 and E3 enzymes. For example, the active sites of E2s contribute a number of catalytic residues required for the activation and correct positioning of lysine residues to be modified (Plechanovova et al., 2012; Wu et al., 2003;

Yunus and Lima, 2006). As outlined below, E2s play a number of roles in ubiquitin chain assembly, including the determination of linkage specificity and the processivity of ubiquitylation (Ye and Rape, 2009). Work presented in my thesis uncovers novel mechanisms that E2s employ to build linkage-specific chains.

Ubiquitin chain linkage topology is determined by E2s

Generation of specific ubiquitin linkages requires the correct recognition of *acceptor ubiquitin* surfaces by the E2~*donor ubiquitin* thioester conjugate. Linkage specificity is determined by HECT E3s themselves or, in the case of RING E3s, by E2s (Ye and Rape, 2009). This was initially suggested by the finding that some E2s synthesize linkage-specific ubiquitin chains in the absence of E3s and substrates (Baboshina and Haas, 1996; Haas et al., 1991; Hofmann and Pickart, 1999; Van Nocker and Vierstra, 1991). Importantly, the intrinsic linkage-specificity of the E2s is unchanged in the presence of cognate E3s, as exemplified by the Lys48-specific E2s Ube2R1 (Cdc34 in yeast) and Ube2G2 and their physiological E3s SCF and gp78 (Li et al., 2009; Petroski and Deshaies, 2005).

The molecular basis for lysine selectivity is most well-understood for the Lys63-specific E2 Ube2N. This E2 functions as a heterodimeric E2 with UEV1A, an E2-like protein that lacks an active site cysteine. Structural studies revealed that UEV1A binds acceptor ubiquitin non-covalently in an orientation that places Lys63 near the active site of the Ube2N~ubiquitin thioester (Eddins et al., 2006)

Monomeric E2 enzymes must directly bind and orient acceptor ubiquitin, and kinetic analyses suggest that the Lys48-specific E2s Cdc34 and Ubc1 interact non-covalently with acceptor ubiquitin (Petroski and Deshaies, 2005; Rodrigo-Brenni et al., 2010). Active site residues in these E2s were reported to be required for processive and Lys48-specific ubiquitylation, and their mutation affects the catalytic rate of ubiquitylation without affecting acceptor ubiquitin binding (Gazdoiu et al., 2007; Petroski and Deshaies, 2005; Rodrigo-Brenni et al., 2010). Therefore, it is likely that E2 surfaces near the active site contain residues not only critical to catalyze lysine attack but also for activity towards specific ubiquitin lysines.

The monomeric E2 Ube2S was reported to form Lys11-linked ubiquitin chains *in vitro* in the absence of an E3, although the mechanism of this specificity was unknown (Baboshina and Haas, 1996). In Chapter 2, I will report the identification of Ube2S as a Lys11-specific E2 for human APC/C. Chapter 3 will reveal a novel molecular mechanism of Ube2S linkage specificity, which lies not in specific binding of an acceptor ubiquitin but rather in catalysis.

E2 enzymes regulate the switch between ubiquitin chain initiation and elongation

Ubiquitylation reactions can be separated into two distinct events: chain initiation, the modification of substrate lysine residues; and chain elongation, the subsequent modification of lysine residues of ubiquitin (Ye and Rape, 2009). In some cases, a single E2 both initiates and elongates ubiquitin chains. Kinetic analyses show that chain initiation is the rate-limiting step and that elongation occurs rapidly once the initial ubiquitin is attached to a substrate (Pierce et al., 2009). Even if a single E2 is utilized by an E3 for ubiquitylation, the molecular requirements on the E2 for chain initiation and elongation are distinct, highlighting the separability of the two steps (Gazdoiu et al., 2007; Sadowski et al., 2010; Petroski and Deshaies, 2005).

In a growing number of instances, E3s function with a pair of initiation and elongation E2s. The initiation E2s may monoubiquitylate a substrate lysine (Christensen et al., 2007) or form short, relatively non-specific chains (Kirkpatrick et al., 2006; Rodrigo-Brenni and Morgan, 2007; Wu et al., 2010). These monoubiquitylations or short chains can then be elongated by linkage-specific E2s, leading to the formation of homogenous chain types (Christensen et al., 2007; Hoege et al., 2002; Wu et al., 2010). For example, yeast APC/C uses the E2 Ubc4 to modify lysine residues of substrates and the Lys48-specific E2 Ubc1 to elongate chains (Rodrigo-Brenni and Morgan, 2007). In Chapter 2, we report that human APC/C similarly uses an E2 module to build ubiquitin chains with one critical difference – we identify the Lys11-specific E2 Ube2S as a dedicated chain elongation E2 for human APC/C, uncovering the basic mechanism underlying Lys11 chain formation by this E3.

The processivity of ubiquitylation can be regulated by E2s

As described above, the use of dedicated chain elongation E2s by E3 ligases enhances the processivity of ubiquitin chain formation. There are a number of additional mechanisms by which the processivity of ubiquitylation can be influenced by E2 enzymes. While most E2s are thought to add ubiquitin molecules sequentially to a growing chain (Pierce et al., 2009), the E2 Ube2G2 preassembles ubiquitin chains on its active site before transferring the chains en bloc to a substrate lysine (Li et al., 2007). All E2s bind RING domains relatively weakly through conserved E2/RING surfaces (Ye and Rape, 2009), but some E2s, such as Cdc34 and Ube2G2, contain additional surfaces that interact with non-RING domains of E3s. These secondary binding surfaces increase the ability of the E2s to catalyze ubiquitin chain formation (Das et al., 2009; Kleiger et al., 2009). In addition, non-covalent interactions with ubiquitin are important for chain formation by some E2s (Brzovic et al., 2006; Haldeman et al., 1997). In Chapter 3, we identity non-covalent donor ubiquitin/E2 binding as a novel mechanism to increase the processivity of ubiquitylation.

Three outstanding questions will be addressed in my thesis: 1. How does human APC/C assembly Lys11-linked ubiquitin chains on its substrates? In Chapter 2, we report the identification of Ube2S as a Lys11-specific, dedicated chain elongation E2 for the APC/C. 2. How does Ube2S catalyze the formation of Lys11-linked ubiquitin chains? In Chapter 3, we use a combination of structural and biochemical approaches to show that Ube2S engages in non-covalent interactions with both acceptor and donor ubiquitin that together account for the processivity and specificity of this enzyme. 3. When are Lys11 chains formed *in vivo* and what enzymes are responsible for their formation? In Chapter 4, we develop a Lys11-specific ubiquitin antibody and use it to examine levels of this chain type in human cells.

Chapter 2

Identification of a Physiological E2 Module for the Human Anaphase-Promoting Complex

Adam Williamson*, Katherine E. Wickliffe*, Barbara G. Mellone, Ling Song, Gary Karpen, and Michael Rape

Proceedings of the National Academy of Sciences (2009) *106*, 18213-18218

* equal contribution

Summary

Ubiquitination by the anaphase-promoting complex (APC/C) is essential for proliferation in all eukaryotes. The human APC/C promotes the degradation of mitotic regulators by assembling K11-linked ubiquitin chains, the formation of which is initiated by its E2 UbcH10. Here, we identify the conserved Ube2S as a K11-specific chain elongating E2 for human and *Drosophila* APC/C. Ube2S depends on the cell cycle-dependent association with the APC/C activators Cdc20 and Cdh1 for its activity. While depletion of Ube2S already inhibits APC/C in cells, the loss of the complete UbcH10/Ube2S-module leads to dramatic stabilization of APC/C substrates, severe spindle defects, and a strong mitotic delay. Ube2S and UbcH10 are tightly co-regulated in the cell cycle by APC/C-dependent degradation. We conclude that UbcH10 and Ube2S constitute a physiological E2-module for APC/C, the activity of which is required for spindle assembly and cell division.

Introduction

The proteasomal degradation of proteins is essential for cell division in all eukaryotes. Proteins are targeted to the proteasome by modification with ubiquitin chains, whose assembly depends on a cascade of E1, E2, and E3 enzymes (Dye and Schulman, 2007; Kerscher et al., 2006). E3s containing a RING-domain recruit substrates and ubiquitin-charged E2s, and promote the transfer of ubiquitin from the E2 active site to a substrate lysine. The E2-E3 pair then switches to modifying one of the seven Lys residues in ubiquitin, which results in chain elongation. E2s with dedicated roles in elongating K48- (UBE2K/E2–25K) or K63-linked chains (UBE2N-UEV1A) have been described (Eddins et al., 2006; Rodrigo-Brenni and Morgan, 2007).

The essential RING-E3 anaphase-promoting complex (APC/C) is a key regulator of cell division in eukaryotes (Peters, 2006). Loss of APC/C activity arrests cells at metaphase and results in severe aberrations in the structure of the mitotic spindle (Goshima et al., 2007; Somma et al., 2008; Tugendreich et al., 1995). Human APC/C regulates progression through mitosis by modifying a large family of substrates with K11-linked ubiquitin chains, which triggers their degradation by the proteasome (Jin et al., 2008; Kirkpatrick et al., 2006; Xu et al., 2009). Its specific E2, UBE2C/UbcH10, initiates chain formation by recognizing a substrate motif, the TEK-box, which is homologous to residues around K11 in ubiquitin (Jin et al., 2008). However, depletion of UbcH10 stabilizes APC/C substrates to a lesser extent than inhibition of APC/C or mutation of K11 in ubiquitin (Jin et al., 2008; Xu et al., 2009), suggesting that additional K11-specific E2s operate with human APC/C.

As expected from its central role in proliferation, the capacity of the APC/C to assemble ubiquitin chains is tightly regulated. When cells enter mitosis, the APC/C is partially activated through phosphorylation of core subunits and binding of the WD40-repeat protein Cdc20 (Kimata et al., 2008; Kraft et al., 2003; Yu, 2007). The APC/C becomes fully active after all chromosomes have achieved bipolar attachment to the mitotic spindle, which results in silencing of the spindle checkpoint and dissociation of Cdc20 from its inhibitors Mad2 and BubR1 (Yu, 2007). Soon after anaphase onset, Cdc20 is degraded and replaced by Cdh1, which maintains APC/C activity during late mitosis and early G1 (Pfleger and Kirschner, 2000; Visintin et al., 1997). Accordingly, inactivation of the APC/C before S phase involves phosphorylation and degradation of Cdh1 and binding of the Cdh1-inhibitor Emi1 (Peters, 2006). Cdc20 and Cdh1

recruit substrates to the APC/C (Burton and Solomon, 2001; Kraft et al., 2005), but also increase the catalytic activity of the APC/C by a poorly understood mechanism.

Here, we identify the highly conserved Ube2S as a regulator of human and *Drosophila* APC/C. Ube2S functions as a K11-specific chain elongating E2 of APC/C, which depends on chain initiation by UbcH10. Together, UbcH10 and Ube2S are required for the degradation of all APC/C substrates tested so far, spindle formation, and progression of cells through mitosis. Ube2S and UbcH10 are tightly co-regulated during the cell cycle, and APC/C itself promotes their ubiquitination and degradation. Our data suggest that UbcH10 and Ube2S constitute the physiological E2-module of human APC/C during mitosis.

Results

Ube2S Promotes the Assembly of K11-Linked Ubiquitin Chains by the APC/C

The human APC/C triggers the proteasomal degradation of its substrates by modifying them with K11-linked ubiquitin chains (Jin et al., 2008; Kirkpatrick et al., 2006). Its specific E2, UbcH10, initiates chain formation by recognizing TEK-boxes in substrates and ubiquitin (Jin et al., 2008). UbcH10 is the only known APC/C-E2 with K11-specificity, but its depletion from extracts fails to completely stabilize the APC/C substrate securin (Rape and Kirschner, 2004). Thus, an unidentified E2 must be able to catalyze the formation of K11-linked ubiquitin chains by the APC/C.

To isolate the unknown E2, we purified human E2 enzymes and measured their activity in catalyzing ubiquitination by the APC/C. Using this approach we identified the conserved E2 Ube2S, which dramatically promotes the formation of ubiquitin chains on several APC/C substrates, when added together with the APC/C-specific E2 UbcH10 (Fig. 1A and B and Fig. S1 A–C). Albeit less efficiently, Ube2S also cooperates with the non-specific E2 UbcH5 (Fig. S1E). Ube2S functions with both APC/C^{Cdc20} and APC/C^{Cdh1} (Fig. 1D), while it is inactive with other E3s tested (Fig. S1F).

Ube2S does not modify substrate Lys residues itself (Fig. 1 A and B), and as seen in reactions with methyl-ubiquitin, it does not promote additional chain initiation by UbcH10 (Fig. 1C). These findings indicate that Ube2S elongates ubiquitin chains previously initiated by UbcH10.

The addition of recombinant ubiquitin mutants revealed that chains assembled by Ube2S and APC/C are strictly linked through K11 of ubiquitin, independently of whether UbcH10 or UbcH5c are used to initiate chain formation (Fig. 1E and Fig. S1 A–C and G–I). In promoting chain elongation, Ube2S is reminiscent of E2–25K and Ube2N-Uev1A, which extend K48- or K63-linked ubiquitin chains, respectively (Dye and Schulman, 2007). However, E2–25K and Ube2N-Uev1A do not cooperate with UbcH10 in catalyzing chain formation on APC/C substrates (Fig. S1I).

Ube2S contains a UBC-domain and a conserved C-terminal extension. Mutation of the catalytic Cys of Ube2S (Ube2S^{C95S}) or deletion of the C terminus (Ube2S C) abrogates its activity toward APC/C substrates (Fig. 1F). In a similar manner, addition of a peptide comprising the C terminus of Ube2S (CTP) blocks the activity of Ube2S on APC/C. Ube2S catalyzes the formation of K11-linked ubiquitin-dimers independently of APC/C (22). This activity depends on the active-site Cys of Ube2S, but is not affected by deletion of its C terminus (Fig. 1G),

indicating that the C terminus of Ube2S is specifically required for APC/C-dependent chain formation.

To determine whether Ube2S depends on UbcH10 or APC/C during chain elongation, we separated chain initiation from elongation. We briefly incubated the APC/C substrate cyclin A with APC/C and UbcH10, which results in short ubiquitin chains on cyclin A (Fig. 1H and I). In one experiment, we then added Ube2S together with an excess of inactive $UbcH10^{C114S}$ to block further UbcH10-activity. Under these conditions, Ube2S still elongates ubiquitin chains on cyclin A, indicating that it does not require UbcH10 for chain extension (Fig. 1H). In a parallel experiment, we added Ube2S and the APC/C inhibitor Emi1 or an excess of a competitor APC/C substrate to displace preubiquitinated cyclin A from APC/C. This treatment interferes with chain-extension (Fig. 1I), demonstrating that Ube2S depends on APC/C to elongate chains on APC/C substrates. Together, these experiments point to Ube2S as a K11-specific chain-elongating E2 of human APC/C.

Ube2S Binds APC/C and APC/C Activators

To test whether Ube2S cooperates with APC/C in cells, we precipitated endogenous Ube2S from synchronized HeLa cells and detected co-purifying proteins by Western analysis. We find a strong association between Ube2S and the APC/C activator Cdc20, which occurs specifically during mitosis (Fig. 2A). This interaction is also observed when ^{FLAG}Ube2S or endogenous Cdc20 are immunoprecipitated from mitotic cells (Fig. 2B and Fig. S2A). During late mitosis and early G1, APC/C is activated by Cdh1, and at this cell cycle stage, Ube2S-precipitates only contain Cdh1, and no Cdc20. ^{FLAG}Ube2S also associates with Cdh1 (Fig. 2C), and the reverse affinity- purification of Cdh1 recovers high levels of Ube2S (Fig. 2D). Thus, Ube2S interacts with both APC/C activators Cdc20 and Cdh1 in a cell cycle-dependent manner.

To determine whether Ube2S directly binds Cdc20 or Cdh1, we performed pulldown-assays using ^{MBP}Ube2S. In these experiments, we focused on Cdh1, which does not require mitotic phosphorylations for activity. As expected for a direct interaction, ^{MBP}Ube2S efficiently binds Cdh1 from G1 extracts (Fig. 2E), Cdh1 synthesized by IVT/T (Fig. 2F), and ^{His}Cdh1 purified to homogeneity from insect cells (Fig. 2G). The interaction between Ube2S and Cdh1 in vitro as well as in 293T cells requires the WD40-domain of Cdh1 (Fig. 2D and Fig. S2B). Although the WD40-domain of Cdh1 recognizes APC/C substrates (Burton and Solomon, 2001; Kraft et al., 2005), an excess of APC/C substrates does not block the Cdh1/Ube2S-interaction (Fig. 2E and Fig. S2C), and binding studies show that Cdh1 binds substrates and Ube2S at the same time (Fig. S2D). The association of Ube2S with Cdh1 depends on the C terminus of Ube2S and is blocked by the C-terminal Ube2S-peptide (Fig. 2F and Fig. S2E). Accordingly, Ube2SΔC fails to interact with Cdh1 in cells (Fig. 2H). We conclude that Ube2S directly binds Cdh1 using its C-terminal tail, which is also required for the activity of Ube2S toward APC/C.

In addition to its interaction with Cdc20 and Cdh1, Ube2S binds core APC/C, as Ube2S-precipitates from late G1 and S phase contain the APC/C subunit Cdc27, but little Cdc20 or Cdh1 (Fig. 2A). Indeed, ^{FLAG}Ube2S affinity-purified from stably transfected 293T cells efficiently precipitates core APC/C subunits, as deter- mined by mass spectrometry (Table S1). Surprisingly, the levels of Cdc27 co-purifying with Ube2S are reduced in mitosis and G1, which we attribute to a low efficiency of our antibody to precipitate Ube2S*APC/C*Cdc20/Cdh1-complexes. This hypothesis is supported by the reciprocal purification of APC/C using Cdc27-antibodies, which leads to co-purification of Ube2S during mitosis and G1 (Fig. S3A); by

purification of ^{FLAG}Ube2S from stably transfected, mitotic 293T cells, which co-precipitates Cdc27 (Fig. S3B); and by co-fractionation of Ube2S with core APC/C in sucrose gradient centrifugations of mitotic and G1-extracts (Fig. S3C and D). The regulated interaction between Ube2S and APC/C and its activators demonstrates that Ube2S is a component of the APC/C machinery in cells.

Ube2S Is Crucial for APC/C Activity In Vivo

To determine whether Ube2S functions with APC/C in vivo, we depleted Ube2S and/or UbcH10 in human HeLa and U2OS and in *Drosophila* S2 and Kc cells. The fly Ube2S cooperates with the UbcH10 homolog Vihar in catalyzing chain formation on APC/C substrates (Fig. S4A). If loss of Ube2S and/or UbcH10 abrogates APC/C activity, cells should be delayed in mitosis due to defects in spindle formation, which activate the spindle checkpoint (Goshima et al., 2007; Somma et al., 2008; Tugendreich et al., 1995); failure to disassemble spindle checkpoint complexes (Reddy et al., 2007; Stegmeier et al., 2007; Summers et al., 2008); and stabilization of APC/C substrates, which interferes with mitotic exit (Peters, 2006; Tugendreich et al., 1995).

We depleted Ube2S in *Drosophila* S2 cells stably expressing GFP-tagged histone 2B and mCherry-tagged α-tubulin and analyzed progression through mitosis by time-lapse microscopy. As a control, we depleted *Drosophila* UbcH10/Vihar, which is known to activate APC/C in flies (Mathe et al., 2004). Importantly, the depletion of either Ube2S or UbcH10 results in a strong delay in a metaphase-like state (Fig. 3A and Fig. S4B; $t > 3$ h, compared to ≈ 10 min in control cells). This suggests that like UbcH10/Vihar, *Drosophila* Ube2S is important for progression through mitosis.

We then depleted Ube2S and/or UbcH10 in asynchronous cells and determined the number of mitotic cells in the population. We used five siRNAs against human Ube2S, and three siRNAs against human UbcH10, all of which effectively knock down the respective protein and result in identical phenotypes (compare Fig. 3B and Fig. S4C). In both human and fly cells, reducing Ube2S levels does not strongly affect the mitotic distribution (Fig. 3B and Fig. S4C and D), and depletion of UbcH10 results in a weak increase in the mitotic index (Fig. 3B), as reported previously (Mathe et al., 2004; Rape and Kirschner, 2004). This is consistent with experiments showing that siRNA-dependent depletion of Cdc20, Cdh1, or single APC/C subunits triggers negligible increases in the mitotic index (Baumgarten et al., 2009; Kittler et al., 2004; Wei et al., 2004). Importantly, the co-depletion of Ube2S and UbcH10 strongly increases the mitotic index of human and *Drosophila* cells (Fig. 3B and Fig. S4C and D). By contrast, co-depleting UbcH10 and all UbcH5 homologs does not strongly impact progression through mitosis (Fig. 3C). The effects on mitosis caused by UbcH10/Ube2S depletion are among the most dramatic seen by siRNA against APC/C, underscoring the importance of UbcH10 and Ube2S in APC/C-dependent chain formation.

We next determined whether co-depletion of Ube2S and UbcH10 results in aberrations in spindle structure and function (Fig. S5). Using immunofluorescence and time-lapse microscopy, we observed detachment of spindle poles (Fig. S5A and D) and spindle elongation (Fig. S5F). Chromosome missegregation (Fig. S5C), defects in chromosome congression in early mitosis, and an inability to maintain a metaphase plate were evident in experiments performed by time-lapse microscopy. All of these phenotypes had been reported after APC/C inactivation (Gimenez-Abian et al., 2005; Goshima et al., 2007; Kim et al., 2009; Somma et al., 2008). To

test whether this leads to checkpoint activation, we concurrently depleted Mad2, which abrogates spindle checkpoint function even in the presence of nocodazole or taxol. Switching off the checkpoint partially rescues the mitotic delay caused by Ube2S/UbcH10 depletion (Fig. 3B and Fig. S4D), indicating that the checkpoint had been activated. However, cells co-depleted of Ube2S, UbcH10, and Mad2 are still delayed in progression through mitosis, as seen by time-lapse microscopy in *Drosophila* S2 cells (Fig. 3A), and by accumulation of human cells in prometaphase and metaphase (Fig. S5E). Thus, as expected for inhibition of APC/C, loss of Ube2S and UbcH10 results in spindle defects, activation of the spindle check- point, and in mitotic delay independent of the checkpoint.

Next, we tested for a role of Ube2S in APC/C-dependent spindle checkpoint silencing by analyzing genetic interactions with $p31^{comet}$ and Usp44. $p31^{comet}$ cooperates with UbcH10 and APC/C to promote checkpoint silencing (Reddy et al., 2007; Summers et al., 2008), which is counteracted by the deubiquitinating enzyme Usp44 (Kim et al., 2009; Stegmeier et al., 2007). Accordingly, the depletion of both UbcH10 and $p31^{comet}$ results in synthetic mitotic arrest, and depletion of UbcH10 inhibits spindle checkpoint bypass caused by siRNA against Usp44 (Fig. 3D and E). In a similar manner, Ube2S- and $p31^{comet}$-siRNA strongly synergize in increasing the mitotic index (Fig. 3D), and loss of Ube2S rescues the defective checkpoint response observed after Usp44 depletion (Fig. 3E), showing that Ube2S contributes to APC/C-dependent spindle checkpoint silencing.

Finally, we tested whether Ube2S triggers the degradation of APC/C substrates in vivo. When Ube2S/UbcH10-depleted human cells are released from mitotic arrest, the degradation of several APC/C substrates is strongly delayed (Fig. 4A). When analyzed by fluorescence microscopy, multiple APC/C substrates are stabilized in siRNA-treated cells, including cyclin A, cyclin B, and Tpx2 (Fig. 4B and C and Fig. S6A). Tpx2-levels remain high in siRNA-treated cells even in G1, with Tpx2 accumulating at remnants of the spindle midzone (Fig. 4C). Tpx2 is also stabilized in G1 if only Ube2S is depleted (Fig. S6C). As observed by time-lapse microscopy, the depletion of in *Drosophila* S2 cells stably expressing GFP-tagged cyclin B leads to strong stabilization of cyclin B on the spindle pole (Fig. 4D). Thus, Ube2S plays a critical role in driving the degradation of APC/C substrates in cells.

Several lines of evidence indicate that depletion of Ube2S and UbcH10 directly affect APC/C activity, and not only indirectly through activation of the spindle checkpoint: first, cyclin A is stabilized by UbcH10/Ube2S depletion (Fig. 4B), although it is not regulated by the checkpoint (Geley et al., 2001); second, Tpx2 is stabilized at mitotic stages in which the checkpoint is inactive (Fig. 4C); third, fly GFP-cyclin B1 is stable in Ube2S/Mad2-depleted S2 cells as monitored by time-lapse microscopy (Fig. 4D); and fourth, depletion of Ube2S also stabilizes APC/C substrates during interphase (Fig. S6B). Together, our experiments demonstrate a key role for Ube2S in activating APC/C. The phenotypes of co-depleting Ube2S and UbcH10 are very similar to complete APC/C inhibition: mitotic arrest, spindle defects, prolonged activation of the checkpoint, and stabilization of all tested APC/C substrates.

Ube2S Is Regulated by APC/C-Dependent Degradation

Overexpression of Ube2S transforms cells in culture and promotes tumor growth in mice (Jung et al., 2006; Tedesco et al., 2007). This suggests that Ube2S levels have to be regulated, and indeed, Ube2S is degraded during G1 (Fig. 5A). The proteolysis of Ube2S occurs at similar times as the degradation of UbcH10, but is delayed compared to APC/C substrates. Ube2S is

undetectable in cells arrested in quiescence (Fig. S7A) and synthesized in parallel with UbcH10 when cells re-enter the cell cycle upon stimulation with serum.

Because Ube2S is co-regulated with UbcH10, its levels might be controlled by APC/C itself, as reported for UbcH10 (Rape and Kirschner, 2004). Indeed, APC/C activation, accomplished by depleting its inhibitor Emi1, leads to a dramatic decrease in the concentration of Ube2S, which is also observed for APC/C substrates (Fig. 5B). Conversely, inhibition of the APC/C by depleting its activator Cdh1 or by co-depletion of Apc2 and UbcH10 results in a strong increase in Ube2S (Fig. 5C and Fig. S7B).

Consistent with Ube2S being an APC/C substrate, APC/C^{Cdh1} catalyzes the ubiquitination of Ube2S in vitro, which can be blocked by the APC/C inhibitor Emi1 (Fig. 5D). This reaction requires UbcH5 or UbcH10 to promote the attachment of the first ubiquitin to Ube2S. Although substrates do not compete with Ube2S binding to Cdh1 or APC/C, they interfere with the APC/C-dependent ubiquitination of Ube2S (Fig. S7C). Interestingly, ubiquitination of Ube2S by the APC/C is strongly increased by microtubules (Fig. 5E and Fig. S7 D and E), which is consistent with the known spindle binding of APC/C (Peters, 2006). This efficient ubiquitination of Ube2S depends on its active-site Cys and on its C-terminal tail (Fig. 5E), and the ubiquitin chains attached to Ube2S are specifically linked through K11 (Fig. S7E). 26S proteasomes trigger the degradation of ubiquitinated Ube2S, which is blocked by addition of the proteasome inhibitor MG132 (Fig. 5F). These findings indicate the APC/C promotes the ubiquitination and degradation of both Ube2S and UbcH10 (Rape and Kirschner, 2004), resulting in the tight co-regulation of these E2 enzymes.

Discussion

The APC/C is essential for cell cycle progression in all eukaryotes (Peters, 2006). The human APC/C modifies substrates with K11-linked ubiquitin chains to trigger their proteasomal degradation (Jin et al., 2008). The formation of K11-linked chains is initiated by its E2 UbcH10, which recognizes TEK boxes in substrates and ubiquitin (Jin et al., 2008). Here, we identify the conserved Ube2S as a K11-specific chain elongating E2 for human and *Drosophila* APC/C. Together, UbcH10 and Ube2S promote the efficient degradation of APC/C substrates, spindle assembly, and progression through mitosis. We propose that UbcH10 and Ube2S constitute the physiological E2 module of human APC/C during mitosis.

The cooperation between Ube2S and UbcH10 is reminiscent of yeast APC/C, which uses a chain-initiating E2, Ubc4, and a chain-elongating E2, Ubc1 (Rodrigo-Brenni and Morgan, 2007). However, Ubc4 and Ubc1 function sequentially to assemble K48-linked ubiquitin chains, whereas human UbcH10 and Ube2S most likely bind APC/C at the same time. This hypothesis is supported by competition studies, in which a large excess of UbcH10 does not block the binding of Ube2S to Cdh1 or APC/C, and by ubiquitination assays, in which Ube2S and UbcH10 promote the APC/C-dependent ubiquitination of each other. By binding to different sites on the APC/C, UbcH10 and Ube2S can truly cooperate in the assembly of K11-linked ubiquitin chains, allowing them to promote the degradation of the extended family of human APC/C substrates.

UbcH10 binds the RING subunit Apc11 and the cullin subunit Apc2 (Summers et al., 2008; Tang et al., 2001). Consistent with a different mode of APC/C interaction, Ube2S directly binds the APC/C activators Cdc20 and Cdh1. The deletion of C-terminal amino acids of Ube2S ablates its binding to Cdh1 and abrogates its activity toward APC/C, which implies that the association between Ube2S and Cdh1 is required for Ube2S activity. The interaction between

Ube2S and Cdc20/Cdh1 is cell-cycle regulated and occurs only at times when Cdc20 and Cdh1 activate APC/C. We propose that recruitment of Ube2S in part explains the capability of Cdc20 and Cdh1 to increase the catalytic activity of the APC/C.

The strongest effects on cell cycle progression are observed, if Ube2S and UbcH10 are co-depleted from cells. This indicates that APC/C ubiquitinates at least some substrates, if one E2 is present at low concentrations. It is possible that other E2s partially compensate for loss of either UbcH10 or Ube2S. Such E2s are unlikely to include UBE2D/UbcH5 or UBE2K/E2–25K, which neither assemble specific K11-linked chains (Jin et al., 2008), nor target APC/C substrates for degradation in extracts (Jin et al., 2008), nor show genetic interactions with UbcH10. We believe it is more likely that even low levels of UbcH10 support initiation of short chains, which could then be extended by Ube2S. In support of this notion, mutation of UbcH10 in flies or its efficient depletion in several human cell lines lead to cyclin B stabilization and a delay in mitosis (Berlingieri et al., 2007; Fujita et al., 2009; Mathe et al., 2004; Rape and Kirschner, 2004; Reddy et al., 2007; Wagner et al., 2004), while incomplete depletion of UbcH10 does not produce these phenotypes (Walker et al., 2008).

Consistent with their close cooperation in modifying APC/C substrates, UbcH10 and Ube2S are tightly co-regulated in cells. Both E2s are degraded during G1, which is promoted by APC/C-dependent ubiquitination. The APC/C turns against its own E2s only after most, if not all, APC/C substrates have been degraded. As co-depletion of UbcH10 and Ube2S inactivates APC/C during mitosis, it can be assumed that the degradation of both E2s during G1 also shuts off most of APC/C, as previously proposed (Rape and Kirschner, 2004).

The identification of Ube2S as a K11-specific E2 for the APC/C underscores the importance of K11-linked ubiquitin chains for cell cycle control (Jin et al., 2008). The phenotypes observed after co-depletion of Ube2S and UbcH10 are reminiscent of the strong mitotic delay caused by injection of a K11-deficient ubiquitin mutant into *Xenopus* embryos (Jin et al., 2008). A proteomic analysis revealed that p97/CDC48, whose depletion causes mitotic arrest in HeLa cells (Wojcik et al., 2004), efficiently binds K11-linked ubiquitin chains (Alexandru et al., 2008). K11-linked ubiquitin chains also accumulate in diseases with impaired proteasome activity, such as Huntington's or Alzheimer's (Bennett et al., 2007), and they are abundant in normally dividing cells (Xu et al., 2009). Together, these findings point to K11-linked chains as critical, if not essential, regulators of proteasomal degradation and cell cycle progression in higher eukaryotes.

In conclusion, we have identified the highly conserved Ube2S as a chain-elongating E2 of human and *Drosophila* APC/C. UbcH10 and Ube2S likely constitute the physiological E2 module for the APC/C during mitosis, in which UbcH10 initiates and Ube2S elongates K11-linked ubiquitin chains. The inhibition of mitotic APC/C is an attractive goal for chemotherapy, which, as shown here, could be accomplished by small molecules targeting both UbcH10 and Ube2S.

In this chapter, we asked how human APC/C assembles Lys11-linked chains. We identified Ube2C and Ube2S as a physiological E2 pair for the APC/C. We show that Ube2C acts as an initiation E2, adding short ubiquitin chains to APC/C substrates. These chains are then rapidly elongated by the Lys11-specific Ube2S. Ube2S binds to the APC/C in a cell cycle-dependent manner via the co-adapters Cdh1 and Cdc20. We find that, similar to Ube2C, Ube2S

itself is subject to APC/C-dependent degradation in G1. Importantly, co-depletion of both E2s causes spindle defects and a delay in the degradation of APC/C substrates in cells.

Ube2C displays a preference for assembling Lys11-linked ubiquitin chains, but can also form chains using Lys48 and Lys63. Therefore, we hypothesized that human APC/C may associate with additional specificity factors. The discovery that the Lys11-specific Ube2S functions with the APC/C explains why substrates of this E3 are decorated with Lys11 chains. However, our initial characterization of Ube2S revealed nothing about the structural or catalytic basis of Lys11-specificity. Therefore, we next collaborated with John Kuriyan's lab at UC, Berkeley to investigate how Lys11-specificity is generated by Ube2S. Our findings are presented in Chapter 3.

Methods

Detailed materials and methods can be found in the Supplementary Information. Ube2S was purified as an N-terminal MBP fusion protein, and the MBP-tag was cleaved off by TEV protease before Ube2S was used in assays. UbcH10 and UbcH5c were purified from *E. coli*, while E1 and ^{His}Cdh1 were purified from Sf9 cells. In vitro ubiquitylations were performed as described, with APC/C being obtained from human HeLa S3 cells (Jin et al., 2008). Immunofluorescence analysis was performed in HeLa cells in described (Rape and Kirschner, 2004). siRNAs were obtained from Dharmacon (for sequences see Supplementary Information). Ube2S-binding partners were identified by MudPIT-mass spectrometry performed by the UCB Proteomics/Mass Spectrometry Laboratory (P/MSL).

Supplemental Information is available at:
http://www.pnas.org/content/106/43/18213/suppl/DCSupplemental

Acknowledgments

We thank Deborah Zajchowski and Rick Feldman for providing antibodies against Ube2S, Eric Griffis and Ron Vale for S2 cells expressing cyclin B1*GFP, Claudio Sunkel (IMBC, Portugal) for Mad2 antibody, Chris Fromme for help with sucrose gradients, Isaac Oderberg for technical help, the Drubin/Barnes laboratory for help with microscopy, and Julia Schaletzky for discussions and critically reading the manuscript. This work was supported by National Institutes of Health Grants RO1 GM066272 (to G.H.K.) and RO1 GM083064 (to M.R.) and a National Institutes of Health Director New Innovator Award (to M.R.). M.R. is a Pew fellow.

Figure Legends

Figure 1: Ube2S Promotes Formation of K11-Linked Ubiquitin Chains on APC/C Substrates (A) Ube2S promotes chain formation on cyclin A. ^{35}S-cyclin A was incubated with APC/C^{Cdh1}, E1, ubiquitin, and UbcH10, and/or Ube2S. Reaction products were analyzed by autoradiography. **(B)** Ube2S promotes chain formation on Plk1. The ubiquitylation of ^{35}S-Plk1 was analyzed as described for cyclin A. **(C)** Ube2S does not promote chain initiation. ^{35}S-cyclin A and ^{35}S-Plk1 were incubated with APC/C^{Cdh1} and methylubiquitin, as described above. **(D)** Ube2S cooperates with APC/C^{Cdc20}. APC/C^{Cdc20} was activated as described (Reddy et al., 2007)and used to ubiquitinate endogenous Cdc20, as detected by Western blot. **(E)** Ube2S assembles K11-linked chains on APC/C substrates. The ubiquitylation of ^{35}S-cyclin A by APC/C^{Cdh1} and Ube2S was analyzed in the presence of ubiquitin mutants, as indicated. "K6" describes ubiquitin containing Lys- 6, "R6" is ubiquitin in which K6 has been exchanged to Arg. **(F)** Ube2S requires its catalytic Cys and its C terminus for APC/C-dependent chain formation. Ubiquitylation of ^{35}S-cyclin A was analyzed in the presence of APC/C^{Cdh1}, Ube2S, Ube2S^{C95S}, or Ube2S 1-196 (Ube2S$^{\Delta C}$). In addition, the activity of Ube2S was competed by a C-terminal peptide encompassing the last 26 amino acids of Ube2S (Ube2S+pep). **(G)** Ube2S catalyzes formation of K11-linked ubiquitin dimers independently of an E3. Ube2S and indicated mutants were incubated with E1 and ubiquitin or ubi-R11, and the formation of ubiquitin dimers (ubi-ubi) was detected by Coomassie staining. **(H)** Ube2S does not require UbcH10 during chain elongation. ^{35}S-cyclin A was briefly incubated with APC/C^{Cdh1} and UbcH10, before UbcH10 was inactivated by adding a 100-fold excess of UbcH10^{C114S}. Then, Ube2S was added alone or together with the APC/C inhibitor Emi1. **(I)** Ube2S depends on the APC/C for activity. ^{35}S-cyclin A was briefly incubated with APC/C^{Cdh1} and UbcH10, and then Ube2S alone or Ube2S together with the APC/C inhibitor Emi1 or an excess of the APC/C substrate securin were added.

Figure 2: Ube2S interacts with APC/C (A) Ube2S binds Cdc20 and Cdh1 in a cell cycle-dependent manner. Ube2S was precipitated from extracts of synchronized HeLa cells, and co-purifying proteins were detected by Western blot. **(B)** Cdc20 binds Ube2S in mitosis. Cdc20 was precipitated from mitotic HeLa S3 cells. Co-purifying Ube2S and Mad2 were detected by Western blot. **(C)** Ube2S binds Cdh1. ^{FLAG}Ube2S was precipitated from 293T cells, and co-purifying ^{HA}Cdh1 was detected by Western blot. **(D)** Cdh1 binds Ube2S. ^{HA}Cdh1 or ^{HA}Cdh1$^{\Delta WD40}$ were precipitated from 293T cells, and co-purifying Ube2S was detected by Western blot. **(E)** Ube2S binds Cdh1 from G1 extracts. Immobilized MBP or ^{MBP}Ube2S were incubated with HeLa S3 extracts. Recombinant securin or UbcH10 (≈100x excess over Cdh1) were added as indicated. Bound Cdh1 was detected by Western blot. **(F)** Ube2S binds Cdh1. ^{35}S-Cdh1 was incubated with immobilized ^{MBP}Ube2S or the indicated truncation mutants. Bound Cdh1 was detected by autoradiography. **(G)** Ube2S directly binds Cdh1. ^{His}Cdh1 purified to homogeneity was incubated with MBP and ^{MBP}Ube2S. Bound Cdh1 was detected by Western blot. **(H)** The C terminus of Ube2S is required for its interaction with Cdh1. ^{FLAG}Ube2S or ^{FLAG}Ube2S$^{\Delta C}$ were precipitated from 293T cells, and bound ^{HA}Cdh1 was analyzed by Western blot.

Figure 3: Ube2S regulates progression of cells through mitosis (A) *Drosophila* Ube2S is required for mitosis. S2 cells stably expressing histone H2B-GFP and α-tubulin-mCherry were transfected with RNAi and filmed by time-lapse microscopy. **(B)** Ube2S and UbcH10 cooperate to promote progression through mitosis. HeLa cells were transfected with the indicated siRNAs,

and scored for mitotic cells. Error bars, SEM derived from at least seven independent frames of different experiments, counting at least 1,000 cells in each frame. The right panel shows the depletion efficiency by Western blot. **(C)** UbcH10 shows genetic interactions with Ube2S, but not UbcH5. UbcH10 was depleted by siRNA alone, together with all four UbcH5-homologs, or with Ube2S, and the mitotic index of the cell population was determined. The right panel shows the depletion efficiency, as detected by Western blot. **(D)** Ube2S contributes to APC/C-dependent spindle checkpoint silencing. HeLa cells were transfected with the indicated siRNA and scored for cells arresting in mitosis. **(E)** Ube2S counteracts the DUB Usp44. HeLa cells were transfected with indicated siRNA, and treated with taxol to activate the spindle checkpoint. The number of cells arrested in mitosis were counted.

Figure 5: Ube2S is regulated by the APC/C (A) Ube2S is degraded during G1. Mitotic HeLa cells were released into fresh medium to allow mitotic exit, and the indicated proteins were detected by Western blot. **(B)** Ube2S levels decrease upon activation of the APC/C. HeLa cells were treated with siRNA against the APC/C inhibitor Emi1, and the indicated proteins were detected by Western blot. **(C)** Ube2S-levels increase after depletion of APC/C subunits. HeLa cells were treated with the indicated siRNAs, and the levels of Ube2S were determined by Western blotting. **(D)** Ube2S is ubiquitinated by APC/C^{Cdh1}. Affinity-purified APC/C^{Cdh1} was incubated with ^{35}S-Ube2S in the absence or presence of UbcH5c, UbcH10, or Emi1. Reaction products were detected by autoradiography. **(E)** Microtubules promote the ubiquitination of Ube2S. APC/C^{Cdh1} was incubated with taxol-stabilized microtubules, UbcH5c, and ^{35}S-Ube2S, ^{35}S-Ube2S^{C95S}, ^{35}S-Ube2S$^{\Delta C}$, or ^{35}S-Ube2S, and the C-terminal Ube2S-peptide. Reaction products were detected by autoradiography. **(F)** Ubiquitinated Ube2S is degraded by the 26S proteasome. ^{35}S-Ube2S was ubiquitinated by APC/ C^{Cdh1} in the presence of microtubules. Subsequent to the ubiquitination, purified 26S proteasomes were added. MG132 was added as indicated. The reaction products were visualized by autoradiography.

Figure S1. Ube2S extends K11-linked ubiquitin chains on APC/C substrates (A) Ube2S extends K11-linked ubiquitin chains on cyclin B1. APC/C^{Cdh1} and UbcH10/Ube2S were used to ubiquitinate ^{35}S-cyclin B1. The reactions were performed in the presence of ubiquitin or ubi-R11, and reaction products were detected by autoradiography. **(B)** Ube2S extends K11-linked ubiquitin chains on geminin. The ubiquitination of ^{35}S-geminin by APC/C^{Cdh1} in the presence of ubiquitin and ubi-R11 was performed as described above. **(C)** Ube2S extends K11-linked ubiquitin chains on Tpx2. The ubiquitination of ^{35}S-Tpx2 by APC/C^{Cdh1} in the presence of ubiquitin and ubi-R11 was performed as described above. **(D)** Ube2S extends ubiquitin chains beyond the length achieved by UbcH10 and APC/C alone. APC/C^{Cdh1} and increasing concentrations of UbcH10 ([UbcH10]≈10–50 nM) were used to promote ubiquitination of ^{35}S-cyclin A. Ube2S or Ube2S^{C95S} were added where indicated. The reaction products were separated on long 5–15% SDS gradient gels, and visualized by autoradiography. **(E)** Ube2S can extend ubiquitin chains formed by APC/C and UbcH5c. APC/C^{Cdh1} was used to promote the ubiquitination of ^{35}S-cyclin A. Ube2S and UbcH5c were added when indicated. This reaction contained an increased concentration of ^{35}S-cyclin A, including more reticulocyte lysate. E2 enzymes present in reticulocyte lysate are responsible for weak chain initiation observed in the reaction containing only Ube2S. Reaction products were separated on long 5–15% SDS gradient gels and analyzed by autoradiography. **(F)** Ube2S does not extend ubiquitin chains formed by Brca1. ^{35}S-Brca1 was incubated with E1, UbcH5c, and ubiquitin in the presence of buffer or

Ube2S, and the time course of ubiquitination at 16 °C was analyzed after autoradiography. Addition of Ube2S has no effect on chain length. **(G)** Ube2S is unable to extend ubiquitin chains nucleated by UbcH5c, if ubi-R11 is present. The ubiquitination of ^{35}S-cyclin A by APC/C^{Cdh1} was analyzed in the presence of ubi-R11. (H) Ube2S extends K11-linked ubiquitin chains with APC/C^{Cdc20}. The ubiquitination of Cdc20 was analyzed after APC/C^{Cdc20} was precipitated from mitotic extracts and incubated with E1, p31^{comet}, and UbcH10/Ube2S. The reaction was performed in the presence of wt-ubiquitin or ubi-R11. Ubiquitinated Cdc20 was detected by Western blotting. **(I)** The chain elongating E2 enzymes E2–25K and Ube2N/Uev1A do not cooperate with UbcH10 and APC/C^{Cdh1} in promoting chain assembly. The ubiquitination of ^{35}S-Plk1 by APC/C^{Cdh1} was initiated by incubation with UbcH10, and chain elongation was catalyzed by addition of Ube2S, E2–25K, or Ube2N/Uev1A. The reactions were performed in the presence of wt-ubiquitin and ubi-R11, and products were detected by autoradiography.

Figure S2: Ube2S interacts with APC/C-activators (A) ^{FLAG}Ube2S binds Cdc20 and core APC/C in mitosis. 293T cells were transfected with ^{FLAG}Ube2S and synchronized in mitosis. ^{FLAG}Ube2S was precipitated on FLAG-agarose, and co-purifying proteins were detected by Western blotting. **(B)** The interaction between Ube2S and ^{35}S-Cdh1 is mediated by the WD40-repeat domain of Cdh1. MBP or ^{MBP}Ube2S were coupled to amylose resin and incubated with the indicated Cdh1-truncation mutants. Bound proteins were detected by autoradiography. **(C)** APC/C substrates do not compete for binding of Ube2S to Cdh1. MBP or ^{MBP}Ube2S were immobilized on amylose resin and incubated with ^{35}S-Cdh1 either alone or in presence of an approximate 100-fold excess of the unlabeled APC/C substrate securin. Beads were extensively washed, eluted, and bound proteins were analyzed by autoradiography. **(D)** Cdh1 can bind substrates and Ube2S at the same time. MBP or ^{MBP}Ube2S were incubated with the APC/C substrate ^{35}S-cyclin A alone, or with ^{35}S-cyclin A and recombinant ^{His}Cdh1. The reaction products were analyzed by Coomassie staining and autoradiography. The substrate cyclin A is found in Ube2S complexes only in the presence of ^{His}Cdh1, indicating that Cdh1 can bind to Ube2S and substrate at the same time. **(E)** The C terminus of Ube2S is a binding element for Cdh1. ^{35}S-Cdh1 was incubated with the C-terminal Ube2S peptide and then added to MBP or ^{MBP}Ube2S-beads. Bound proteins were detected by autoradiography.

Figure S3: Ube2S associates with APC/C during mitosis and G1 (A) Ube2S binds APC/C. The core APC/C-subunit Cdc27 was precipitated from extracts of synchronized HeLa cells using monoclonal Cdc27-antibodies, and bound Ube2S and Cdc20 were detected by Western blotting. **(B)** Ube2S binds core APC/C during mitosis. 293T cells stably expressing ^{FLAG}Ube2S were arrested in mitosis. ^{FLAG}Ube2S was precipitated, and co-purifying Cdc27 and Cdc20 were detected by Western blotting. Cdc20 runs very closely to IgG, explaining the background in the control reaction. **(C and D)** Ube2S co-fractionates with APC/C in extracts of HeLa S3 cells in mitosis (C) and G1 (D), as detected by sucrose gradient centrifugation. Sucrose gradient centrifugations of mitotic or G1 extracts were fractionated, proteins were precipitated with TCA, and the indicated proteins were detected by Western blotting using specific antibodies. The signal intensity of the Western blots was quantified using Quantity One; it shows that the peaks of the Ube2S, Cdc20/Cdh1, and APC/C blots overlap.

Figure S4: Effects of Ube2S-depletion (A) *Drosophila* Vihar/UbcH10 and Ube2S catalyze ubiquitin chain formation by APC/C. ^{35}S-cyclin A was incubated with human APC/C^{Cdh1} and

recombinant *Drosophila* Vihar/UbcH10 and *Drosophila* Ube2S. The reaction products were detected by autoradiography. **(B)** The depletion of UbcH10/Vihar by RNAi in S2 cells stably expressing histone H2B-GFP and α-tubulin-mCherry causes a mitotic arrest, which is rescued by co-depletion of Mad2. If Ube2S is depleted in addition to Vihar, Mad2 does not rescue the mitotic arrest, and cells slip into G1 without chromosome segregation. **(C)** The co-depletion of Ube2S and UbcH10 causes mitotic arrest. HeLa cells were treated with the indicated siRNAs. The number of mitotic cells in the bulk population was determined 48 h later. The siRNA against Ube2S is different from the siRNA used for Fig. 5. The right panel shows the efficiency of depletion, as determined by Western analysis. **(D)** The co-depletion of Ube2S and UbcH10/Vihar by RNAi causes a pronounced mitotic arrest in S2 cells, as scored by pH3 staining. The right panel shows depletion of Mad2 in both Kc and S2 cells, as detected by Western blotting.

Figure S5: Depletion of Ube2S and UbcH10 causes widespread spindle defects (A) Ube2S-depletion leads to spindle pole detachment. *Drosophila* S2 cells stably expressing H2B-GFP and α-tubulin-mCherry were treated with RNAi against Ube2S, and imaged by time-lapse microscopy. The arrow indicates a spindle pole, which detaches from the spindle in the RNAi-treated cells. **(B)** Quantification of spindle defects in *Drosophila* Kc cells treated with the indicated siRNA and analyzed by fluorescence microscopy against tubulin. **(C)** Quantification of chromosome missegregation events in postmetaphase Kc cells treated with RNAi as described above. **(D)** Quantification of centrosome defects in RNAi-treated Kc cells measured by immunofluorescence with anti-centrosomin (Cnn) antibodies. **(E)** Depletion of Ube2S and UbcH10 delays mitosis in HeLa cells even in the absence of Mad2. Mitotic cells in metaphase or anaphase were counted after depletion of Mad2, Ube2S/UbcH10, or Mad/Ube2S/UbcH10 by specific siRNA. **(F)** Ube2S and UbcH10 are required for proper spindle formation. Depletion of Ube2S and UbcH10 from HeLa cells results in spindle elongation, chromosome congression defects, and spindle pole abnormalities. Representative figures are shown, in which DNA is detected by DAPI (blue), and the spindle is visualized by immunofluorescence against α-tubulin (red). The length of multiple spindles was measured in control and depleted cells, which is shown in the right panel.

Figure S6: Ube2S is crucial for APC/C-activity in vivo (A) Loss of Ube2S and UbcH10 stabilizes cyclin B1 and Tpx2 on the spindle. HeLa cells were transfected with the indicated siRNA, and stained with antibodies against cyclin B1 (red) and Tpx2 (green). DNA was detected by DAPI-staining (blue). Representative images of all mitotic stages are shown. (Scale bar, 10 μm.) Co-depletion of Ube2S and UbcH10 results in strong stabilization of cyclin B1 and Tpx2. **(B)** Ube2S is required for APC/C^{Cdh1} activity in interphase. HeLa cells were treated with control siRNA or specific siRNAs against Emi1 (to activate APC/C and degrade APC/C substrates), Ube2S, or both. The indicated proteins were detected by Western blots. **(C)** Ube2S is required for Tpx2-degradation in cells. HeLa cells were stained for endogenous Tpx2 by immunofluorescence. The fluorescence intensity in G1 cells was measured and plotted for approximately 100 cells per experiment.

Figure S7: APC/C-dependent ubiquitination and degradation of Ube2S (A) Ube2S is co-regulated with UbcH10 during quiescence. T24 cells were synchronized in quiescence by serum starvation, and allowed to reenter the cell cycle by serum stimulation. The levels of the indicated proteins, including Ube2S, were measured by Western blotting. **(B)** Ube2S levels increase after

APC/C^{Cdh1}-inhibition in vivo. HeLa cells were treated with the indicated siRNAs, and the levels of Ube2S, Cdh1, UbcH10, and α-actin were determined by Western blotting. The asterisk marks a cross-reactive band of the Cdh1-antibody. **(C)** APC/C substrates inhibit ubiquitination of Ube2S by APC/C^{Cdh1}. APC/C^{Cdh1} was incubated with the recombinant APC/C substrate securin or the indicated securin mutants and tested for its capability to ubiquitinate ^{35}S-Ube2S. UbcH5c was added as E2. Reaction products were detected by autoradiography. **(D)** The ubiquitination of Ube2S by APC/C^{Cdh1} is stimulated by microtubules, proceeds by formation of K11-linked ubiquitin chains, and results in Ube2S degradation. ^{35}S-Ube2S was incubated with APC/C^{Cdh1} and UbcH5c in the presence taxol-stabilized microtubules and ubiquitin or ubi-R11. Purified 26S proteasomes were added when indicated. The reaction products were detected by autoradiography.

Figure 1

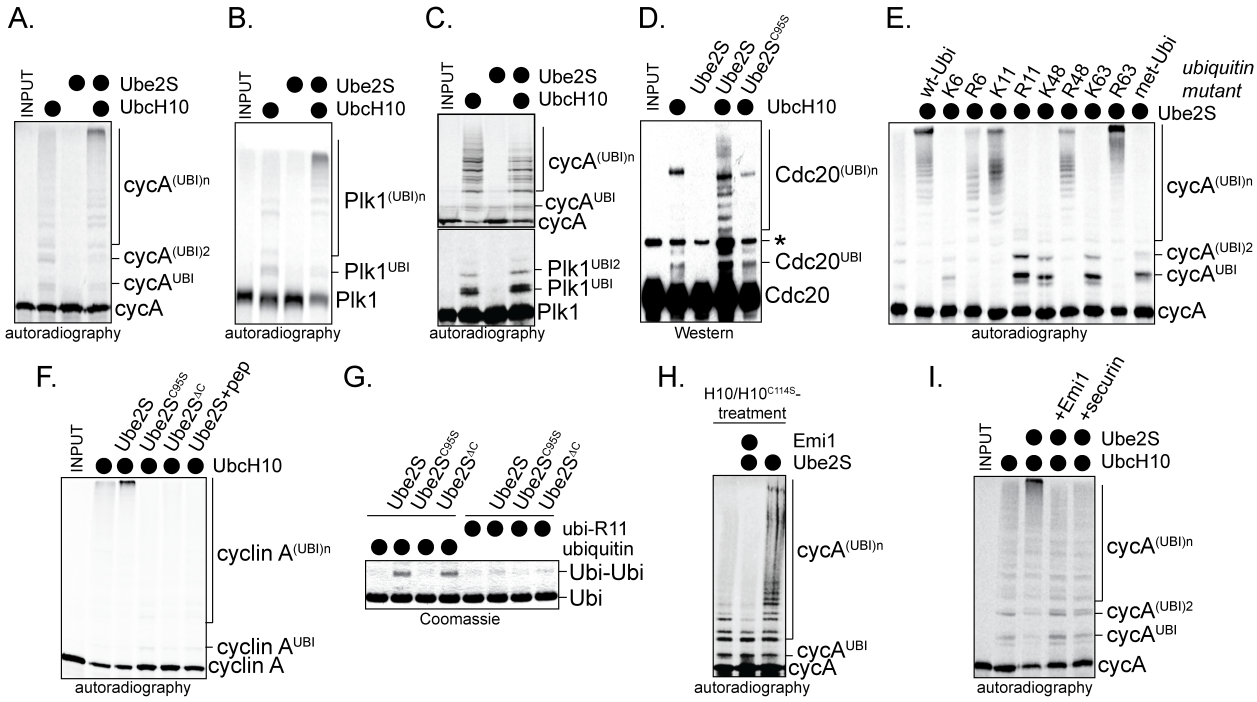
A.
INPUT
Ube2S
UbcH10
cycA(UBI)n
cycA(UBI)2
cycAUBI
cycA
autoradiography
B.
INPUT
Ube2S
UbcH10
Plk1(UBI)n
Plk1UBI
Plk1
autoradiography
C.
INPUT
Ube2S
UbcH10
cycA(UBI)n
cycAUBI
cycA
Plk1UBI2
Plk1UBI
Plk1
autoradiography
D.
INPUT
Ube2S
Ube2S
Ube2SC95S
UbcH10
Cdc20(UBI)n
*
Cdc20UBI
Cdc20
Western
E.
wt-Ubi
K6
R6
K11
R11
K48
R48
K63
R63
met-Ubi
ubiquitin mutant
Ube2S
cycA(UBI)n
cycA(UBI)2
cycAUBI
cycA
autoradiography
F.
INPUT
Ube2S
Ube2SC95S
Ube2SΔC
Ube2S+pep
UbcH10
cyclin A(UBI)n
cyclin AUBI
cyclin A
autoradiography
G.
Ube2S
Ube2SC95S
Ube2SΔC
Ube2S
Ube2SC95S
Ube2SΔC
ubi-R11
ubiquitin
Ubi-Ubi
Ubi
Coomassie
H.
H10/H10C114S-treatment
Emi1
Ube2S
cycA(UBI)n
cycAUBI
cycA
autoradiography
I.
+Emi1
+securin
INPUT
Ube2S
UbcH10
cycA(UBI)n
cycA(UBI)2
cycAUBI
cycA
autoradiography

Figure 2

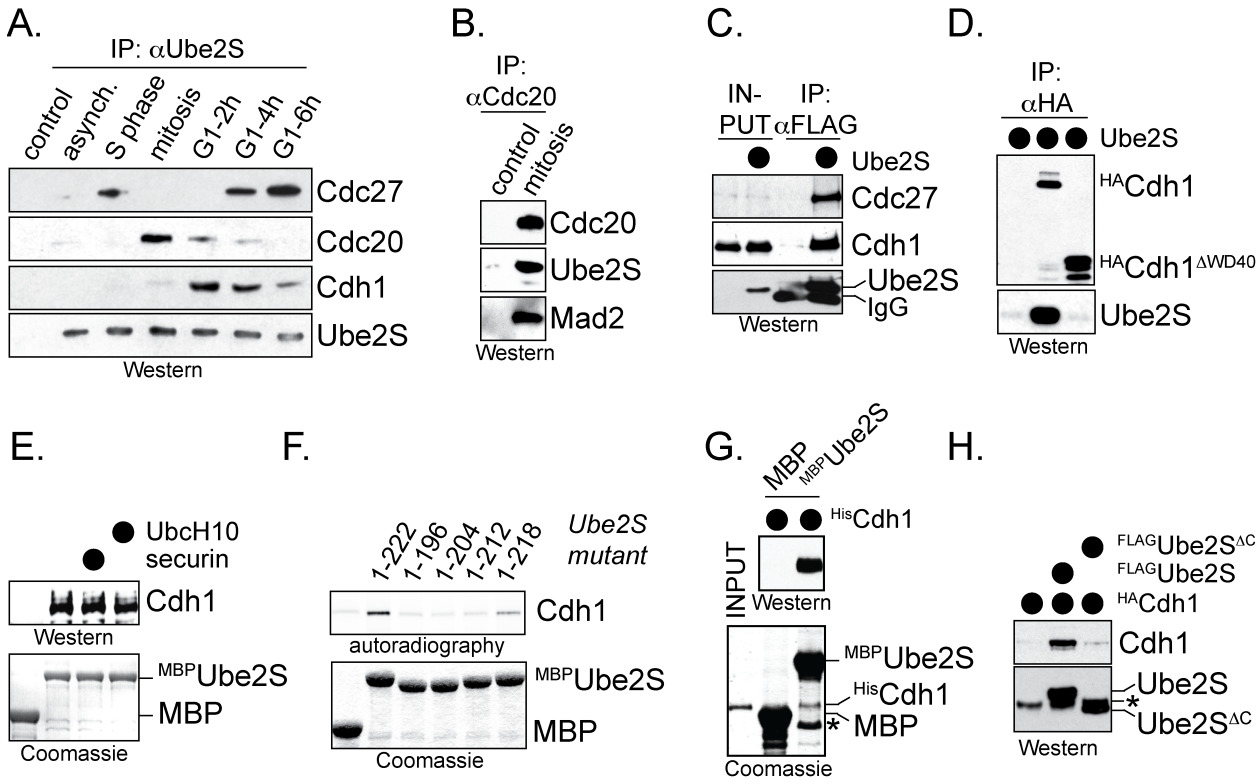
A.
IP: αUbe2S
control
asynch.
S phase
mitosis
G1-2h
G1-4h
G1-6h
Cdc27
Cdc20
Cdh1
Ube2S
Western
B.
IP:
αCdc20
control
mitosis
Cdc20
Ube2S
Mad2
Western
C.
IN-
PUT
IP:
αFLAG
Ube2S
Cdc27
Cdh1
Ube2S
IgG
Western
D.
IP:
αHA
Ube2S
HACdh1
HACdh1ΔWD40
Ube2S
Western
E.
UbcH10
securin
Cdh1
Western
MBPUbe2S
MBP
Coomassie
F.
1-222
1-196
1-204
1-212
1-218
Ube2S
mutant
Cdh1
autoradiography
MBPUbe2S
MBP
Coomassie
G.
MBP
MBPUbe2S
HisCdh1
INPUT
Western
MBPUbe2S
HisCdh1
*
MBP
Coomassie
H.
FLAGUbe2SΔC
FLAGUbe2S
HACdh1
Cdh1
Ube2S
*
Ube2SΔC
Western

Figure 3

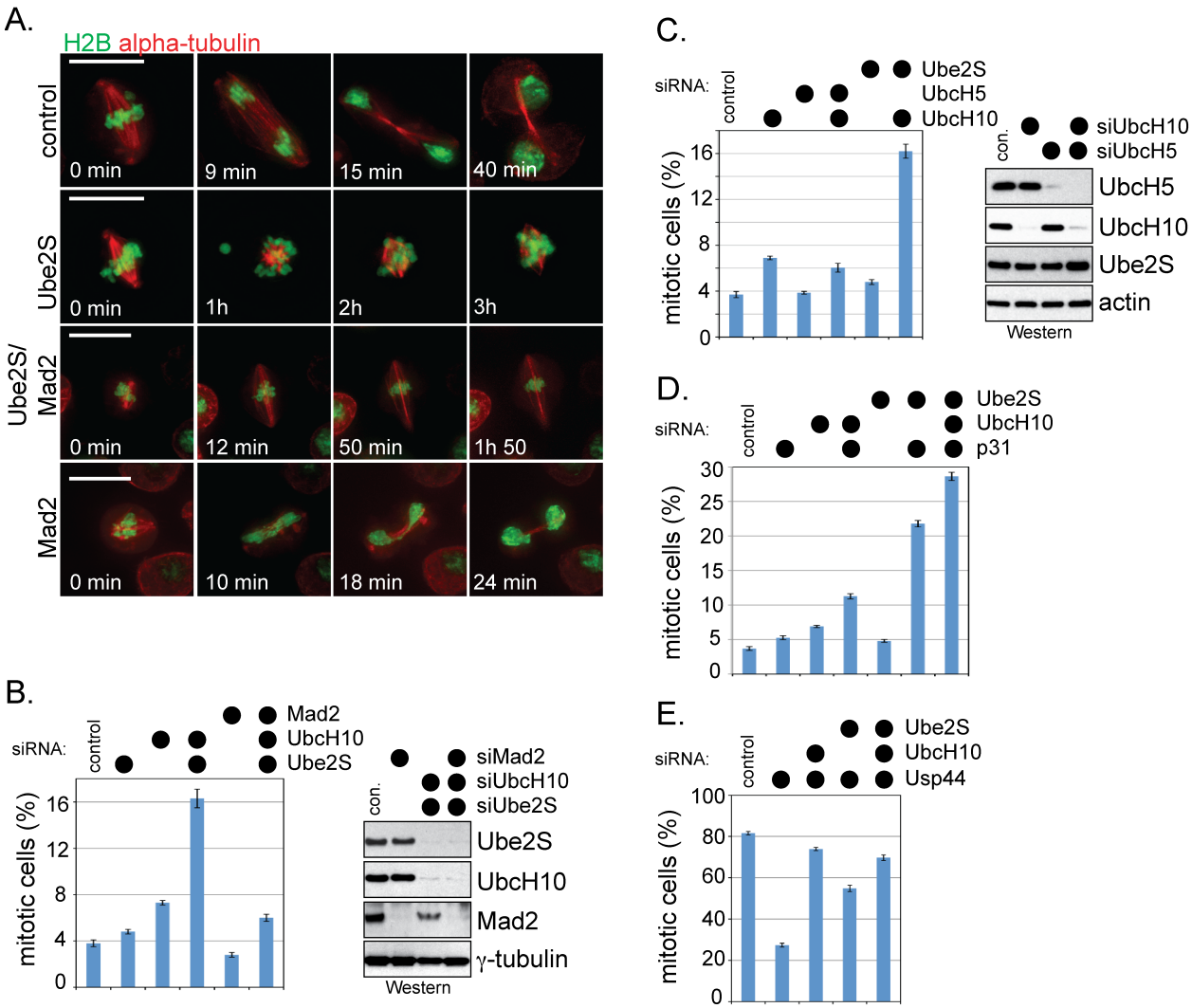
A.
H2B alpha-tubulin
control
Ube2S
Ube2S/ Mad2
Mad2
0 min
9 min
15 min
40 min
1h
2h
3h
12 min
50 min
1h 50
10 min
18 min
24 min
B.
siRNA:
control
Mad2
UbcH10
Ube2S
mitotic cells (%)
siMad2
siUbcH10
siUbe2S
con.
Ube2S
UbcH10
Mad2
γ-tubulin
Western
C.
Ube2S
UbcH5
UbcH10
siUbcH10
siUbcH5
UbcH5
UbcH10
Ube2S
actin
D.
p31
E.
Usp44

Figure 4

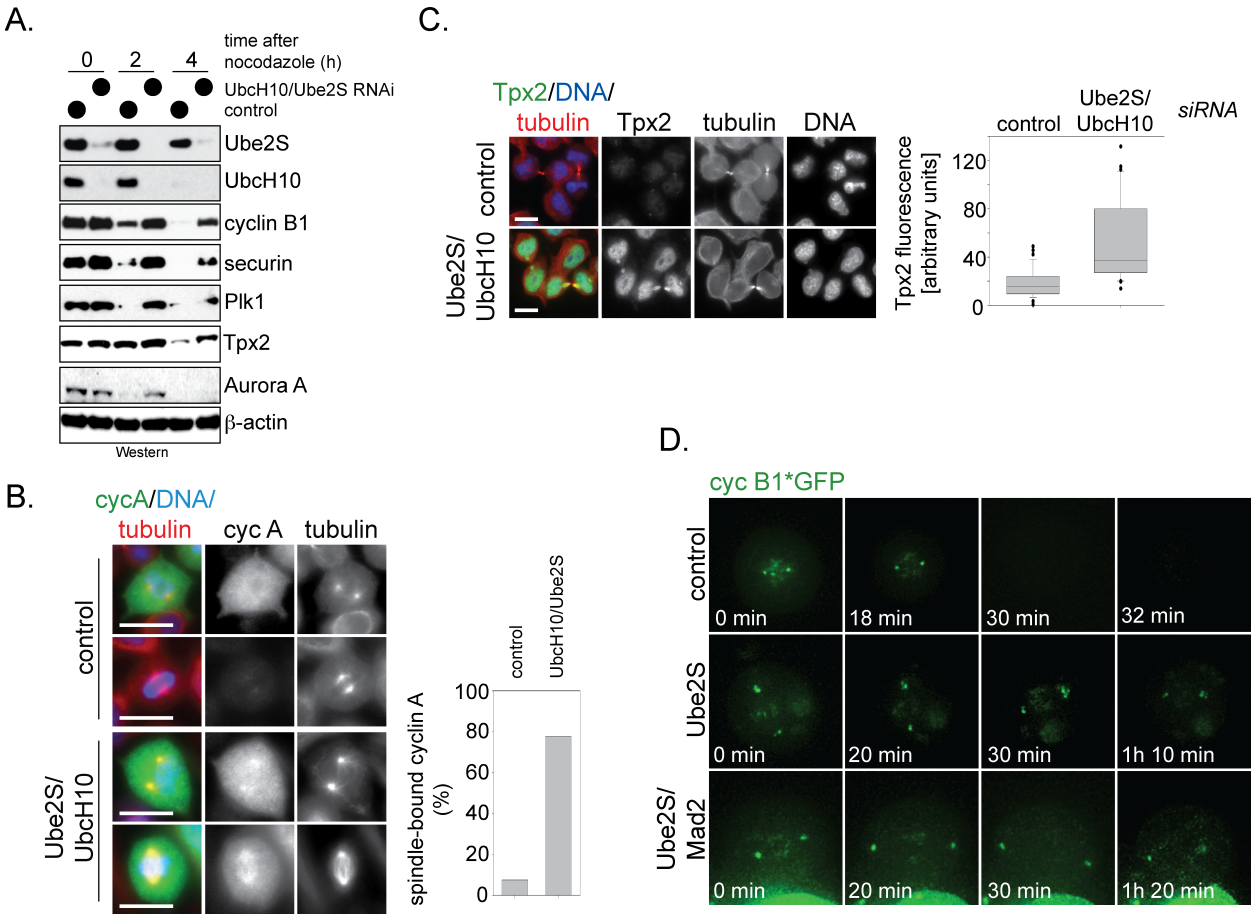
A.
time after nocodazole (h)
0
2
4
UbcH10/Ube2S RNAi
control
Ube2S
UbcH10
cyclin B1
securin
Plk1
Tpx2
Aurora A
β-actin
Western
B.
cycA/DNA/
tubulin
cyc A
tubulin
control
Ube2S/ UbcH10
spindle-bound cyclin A (%)
control
UbcH10/Ube2S
C.
Tpx2/DNA/
tubulin
Tpx2
tubulin
DNA
Ube2S/ UbcH10
control
Tpx2 fluorescence [arbitrary units]
siRNA
control
Ube2S/ UbcH10
D.
cyc B1*GFP
control
Ube2S
Ube2S/ Mad2
0 min
18 min
30 min
32 min
20 min
1h 10 min
1h 20 min

Figure 5

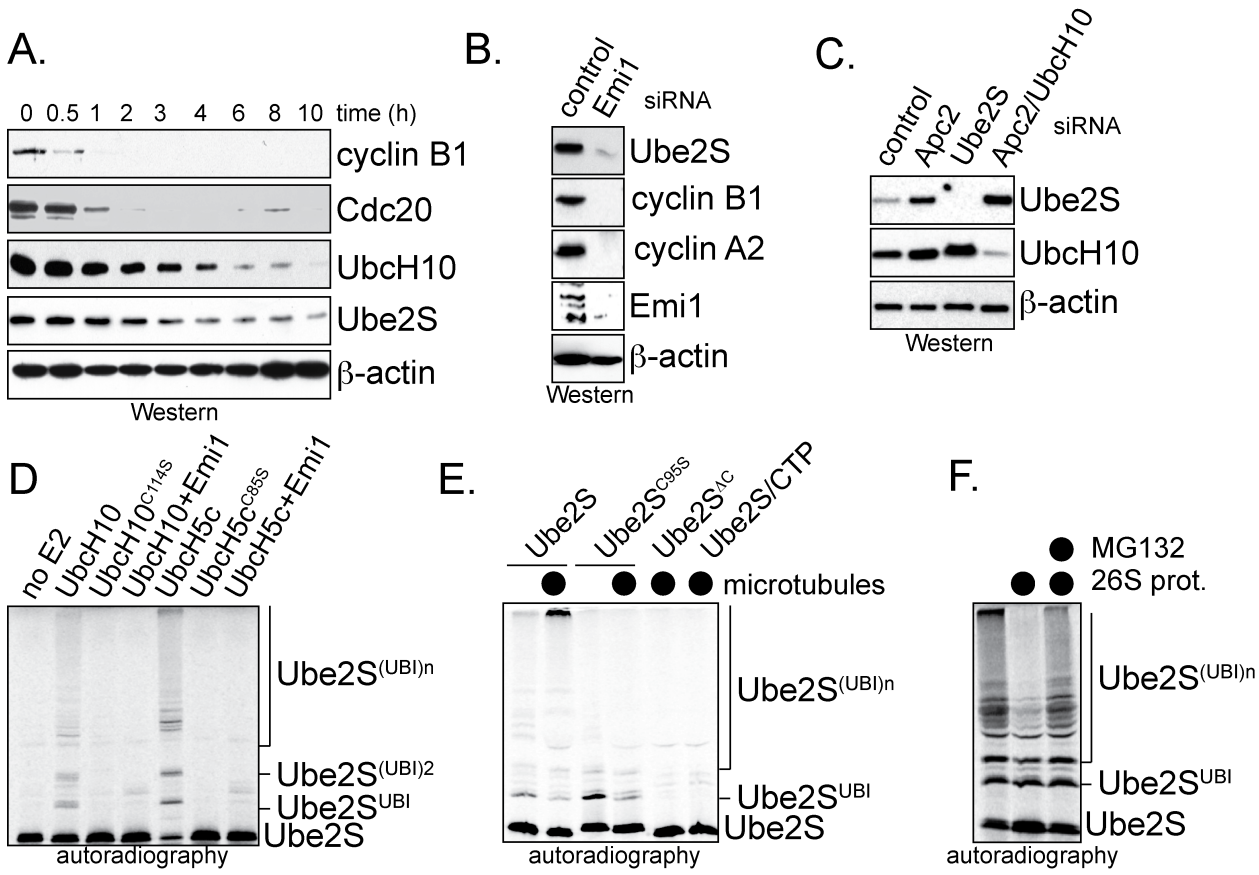
A.
0 0.5 1 2 3 4 6 8 10 time (h)
cyclin B1
Cdc20
UbcH10
Ube2S
β-actin
Western
B.
control
Emi1
siRNA
Ube2S
cyclin B1
cyclin A2
Emi1
β-actin
Western
C.
control
Apc2
Ube2S
Apc2/UbcH10
siRNA
Ube2S
UbcH10
β-actin
Western
D
no E2
UbcH10
UbcH10C114S
UbcH10+Emi1
UbcH5c
UbcH5cC85S
UbcH5c+Emi1
Ube2S(UBI)n
Ube2S(UBI)2
Ube2SUBI
Ube2S
autoradiography
E.
Ube2S
Ube2SC95S
Ube2SΔC
Ube2S/CTP
microtubules
Ube2S(UBI)n
Ube2SUBI
Ube2S
autoradiography
F.
MG132
26S prot.
Ube2S(UBI)n
Ube2SUBI
Ube2S
autoradiography

Figure S1

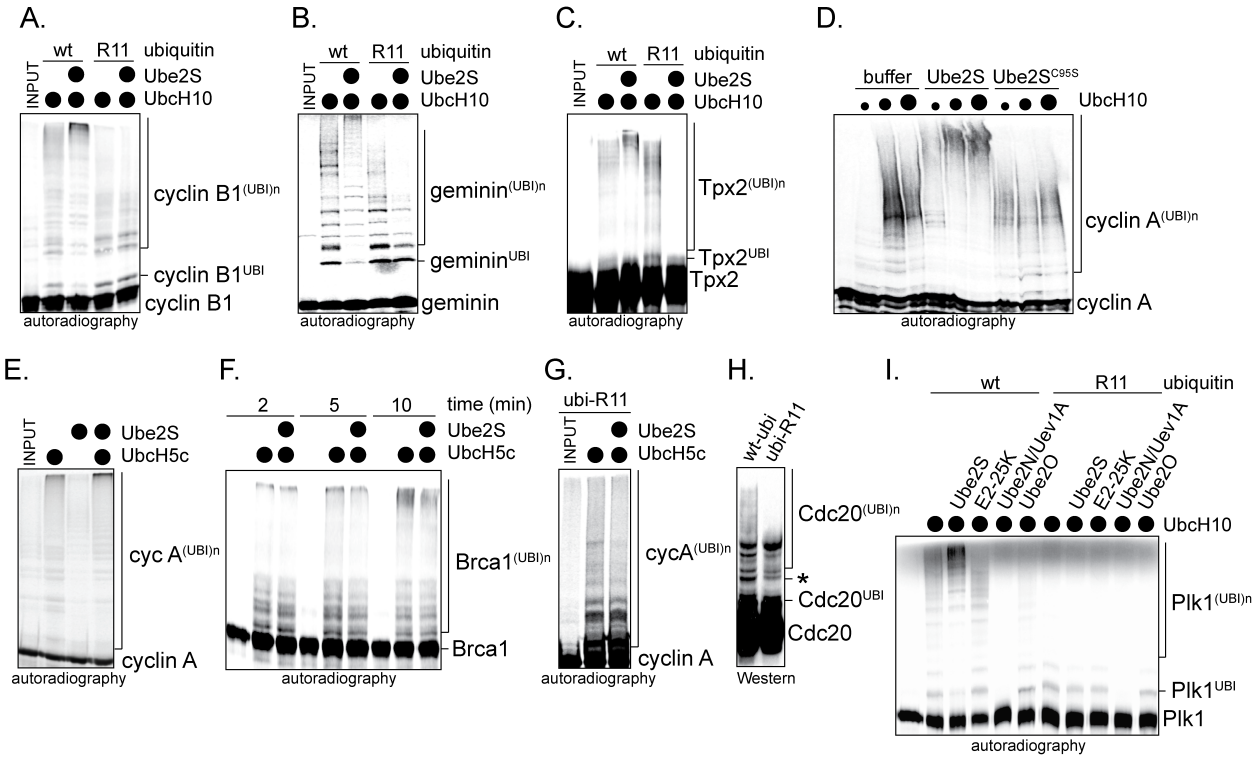
A.
wt
R11
ubiquitin
INPUT
Ube2S
UbcH10
cyclin B1(UBI)n
cyclin B1UBI
cyclin B1
autoradiography
B.
geminin(UBI)n
gemininUBI
geminin
C.
Tpx2(UBI)n
Tpx2UBI
Tpx2
D.
buffer
Ube2S
Ube2SC95S
cyclin A(UBI)n
cyclin A
E.
UbcH5c
cyc A(UBI)n
F.
2
5
10
time (min)
Brca1(UBI)n
Brca1
G.
ubi-R11
cycA(UBI)n
H.
wt-ubi
ubi-R11
Cdc20(UBI)n
*
Cdc20UBI
Cdc20
Western
I.
Ube2S
E2-25K
Ube2N/Uev1A
Ube2O
Plk1(UBI)n
Plk1UBI
Plk1

Figure S2

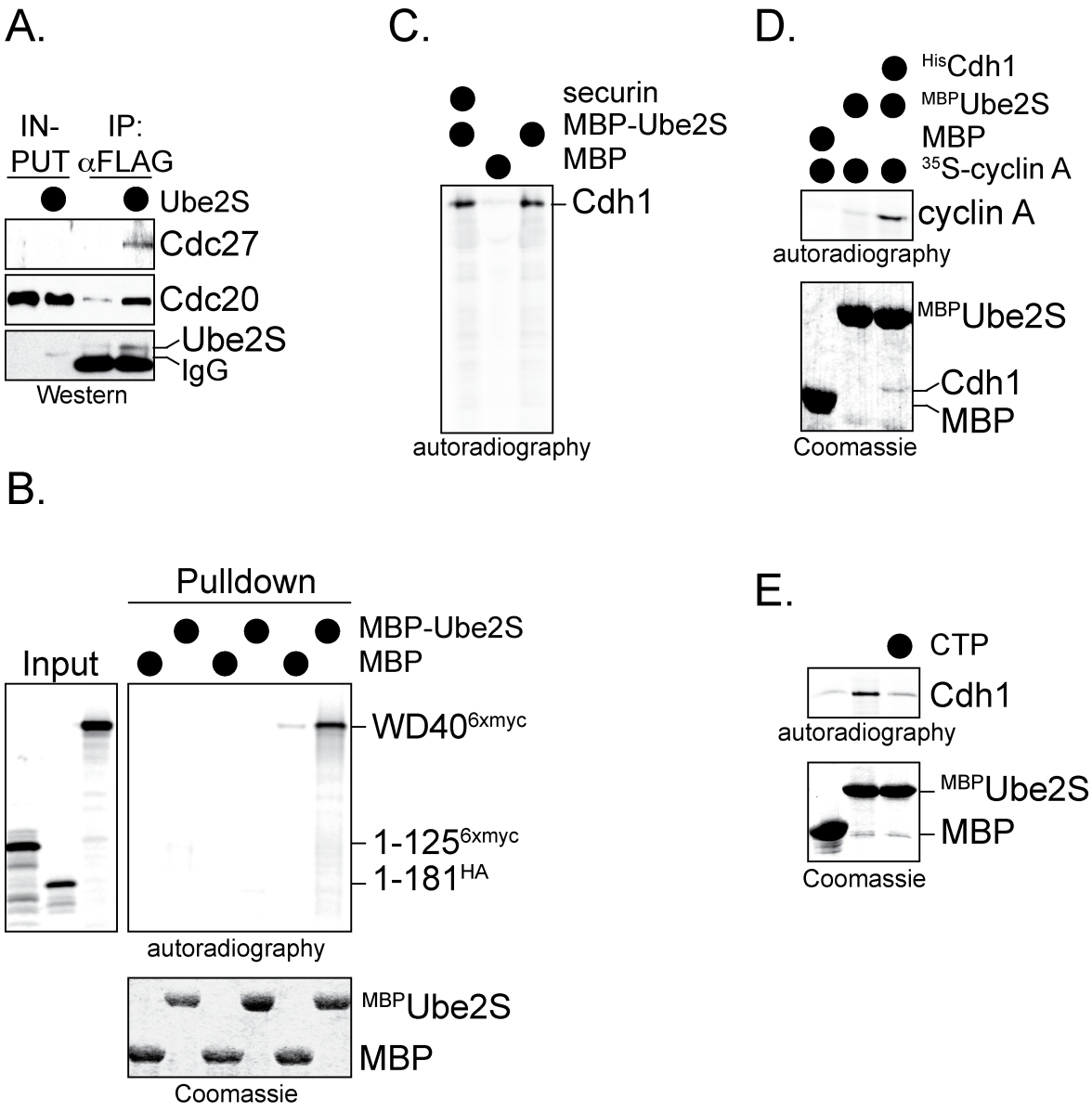
A.
IN-
PUT
IP:
αFLAG
Ube2S
Cdc27
Cdc20
Ube2S
IgG
Western
C.
securin
MBP-Ube2S
MBP
Cdh1
autoradiography
D.
HisCdh1
MBPUbe2S
MBP
35S-cyclin A
cyclin A
autoradiography
MBPUbe2S
Cdh1
MBP
Coomassie
B.
Pulldown
Input
MBP-Ube2S
MBP
WD406xmyc
1-1256xmyc
1-181HA
autoradiography
MBPUbe2S
MBP
Coomassie
E.
CTP
Cdh1
autoradiography
MBPUbe2S
MBP
Coomassie

Figure S3

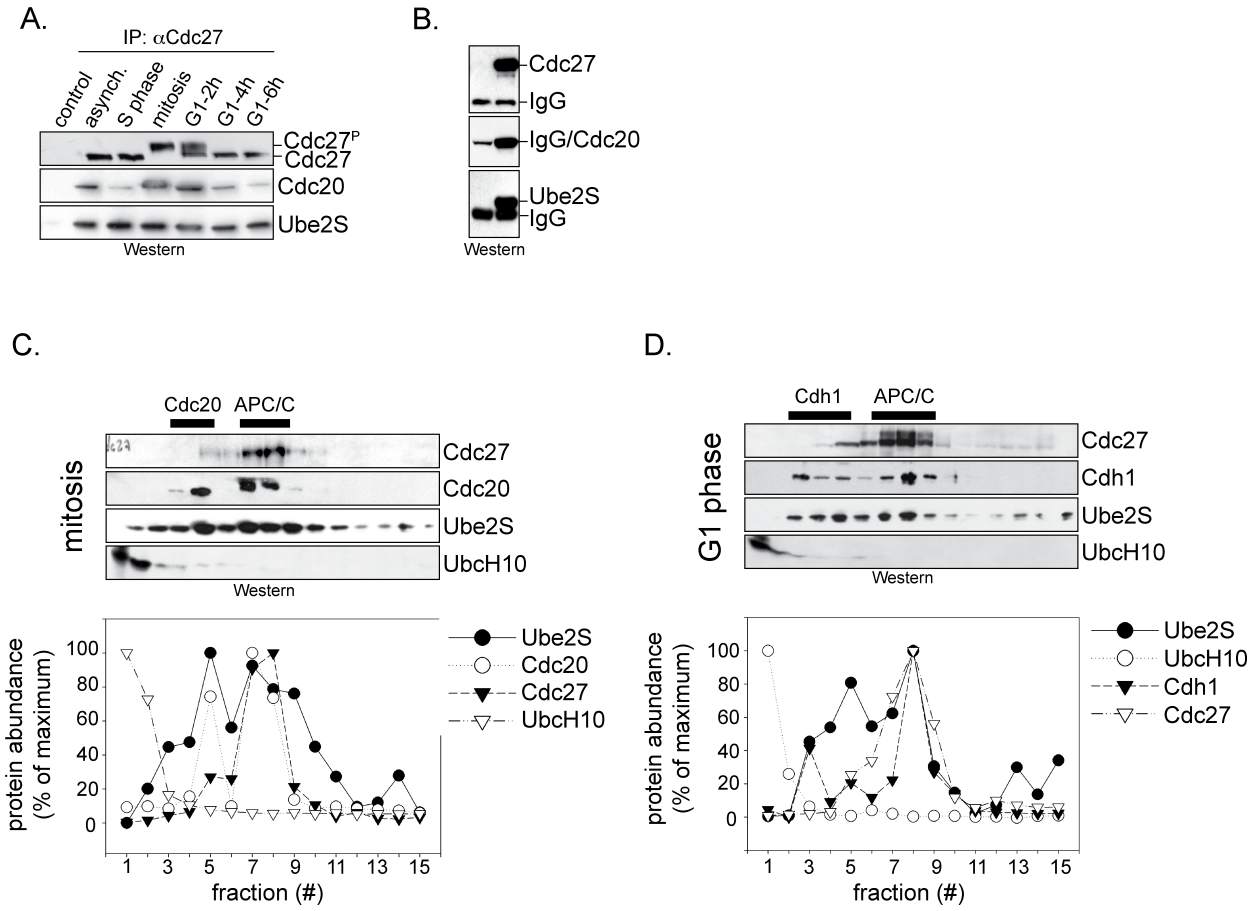
A.
IP: αCdc27
control
asynch.
S phase
mitosis
G1-2h
G1-4h
G1-6h
Cdc27P
Cdc27
Cdc20
Ube2S
Western
B.
Cdc27
IgG
IgG/Cdc20
Ube2S
IgG
Western
C.
Cdc20
APC/C
mitosis
Cdc27
Cdc20
Ube2S
UbcH10
Western
protein abundance (% of maximum)
fraction (#)
Ube2S
Cdc20
Cdc27
UbcH10
D.
Cdh1
APC/C
G1 phase
Cdc27
Cdh1
Ube2S
UbcH10
Western
protein abundance (% of maximum)
fraction (#)
Ube2S
UbcH10
Cdh1
Cdc27

Figure S4

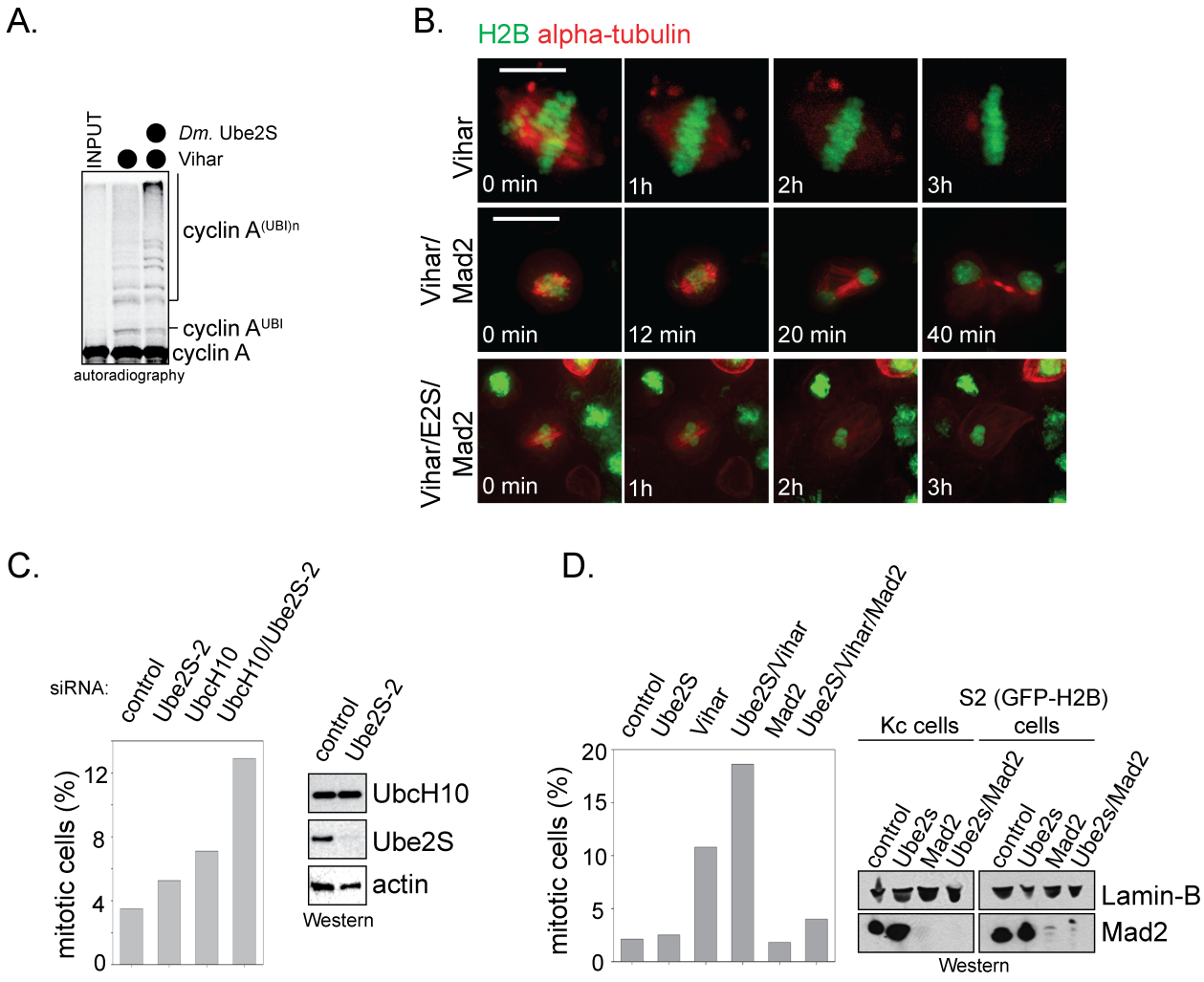
A.
INPUT
Dm. Ube2S
Vihar
cyclin A(UBI)n
cyclin AUBI
cyclin A
autoradiography
B.
H2B alpha-tubulin
Vihar
Vihar/ Mad2
Vihar/E2S/ Mad2
0 min
1h
2h
3h
12 min
20 min
40 min
C.
siRNA:
control
Ube2S-2
UbcH10
UbcH10/Ube2S-2
mitotic cells (%)
UbcH10
Ube2S
actin
Western
D.
control
Ube2S
Vihar
Ube2S/Vihar
Mad2
Ube2S/Vihar/Mad2
mitotic cells (%)
S2 (GFP-H2B)
Kc cells
cells
Ube2s/Mad2
Lamin-B
Mad2
Western

Figure S5

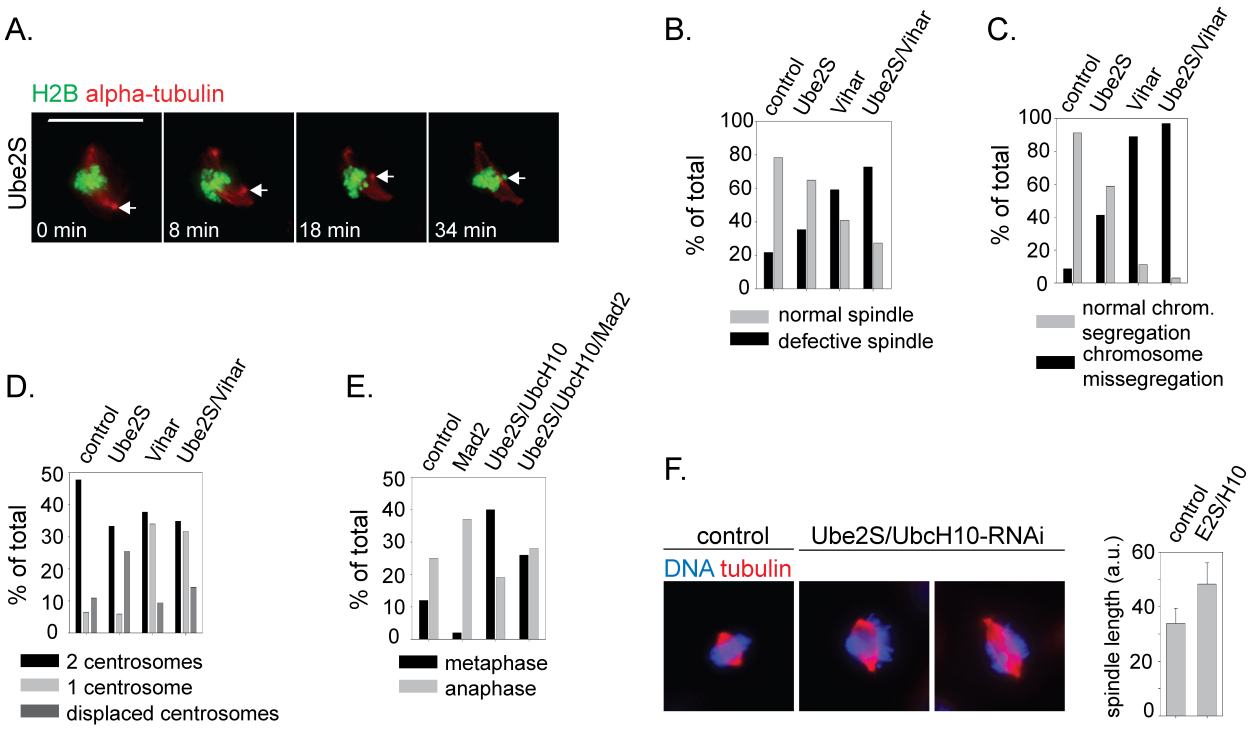
A.
H2B alpha-tubulin
Ube2S
0 min
8 min
18 min
34 min
B.
control
Ube2S
Vihar
Ube2S/Vihar
% of total
normal spindle
defective spindle
C.
normal chrom. segregation
chromosome missegregation
D.
2 centrosomes
1 centrosome
displaced centrosomes
E.
control
Mad2
Ube2S/UbcH10
Ube2S/UbcH10/Mad2
metaphase
anaphase
F.
control
Ube2S/UbcH10-RNAi
DNA tubulin
E2S/H10
spindle length (a.u.)

Figure S6

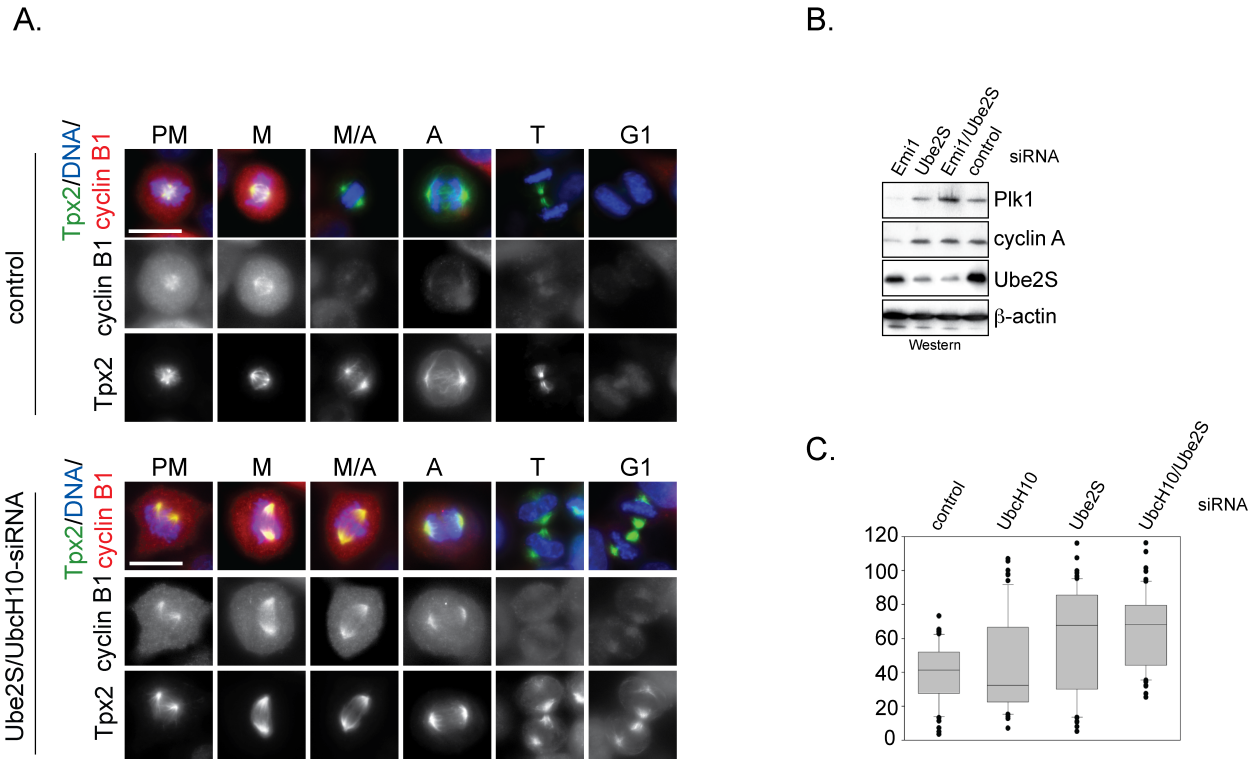
A.
B.
C.
control
Ube2S/UbcH10-siRNA
Tpx2/DNA/cyclin B1
cyclin B1
Tpx2
PM
M
M/A
A
T
G1
Emi1
Ube2S
Emi1/Ube2S
control
siRNA
Plk1
cyclin A
Ube2S
β-actin
Western
control
UbcH10
Ube2S
UbcH10/Ube2S
siRNA
120
100
80
60
40
20
0

Figure S7

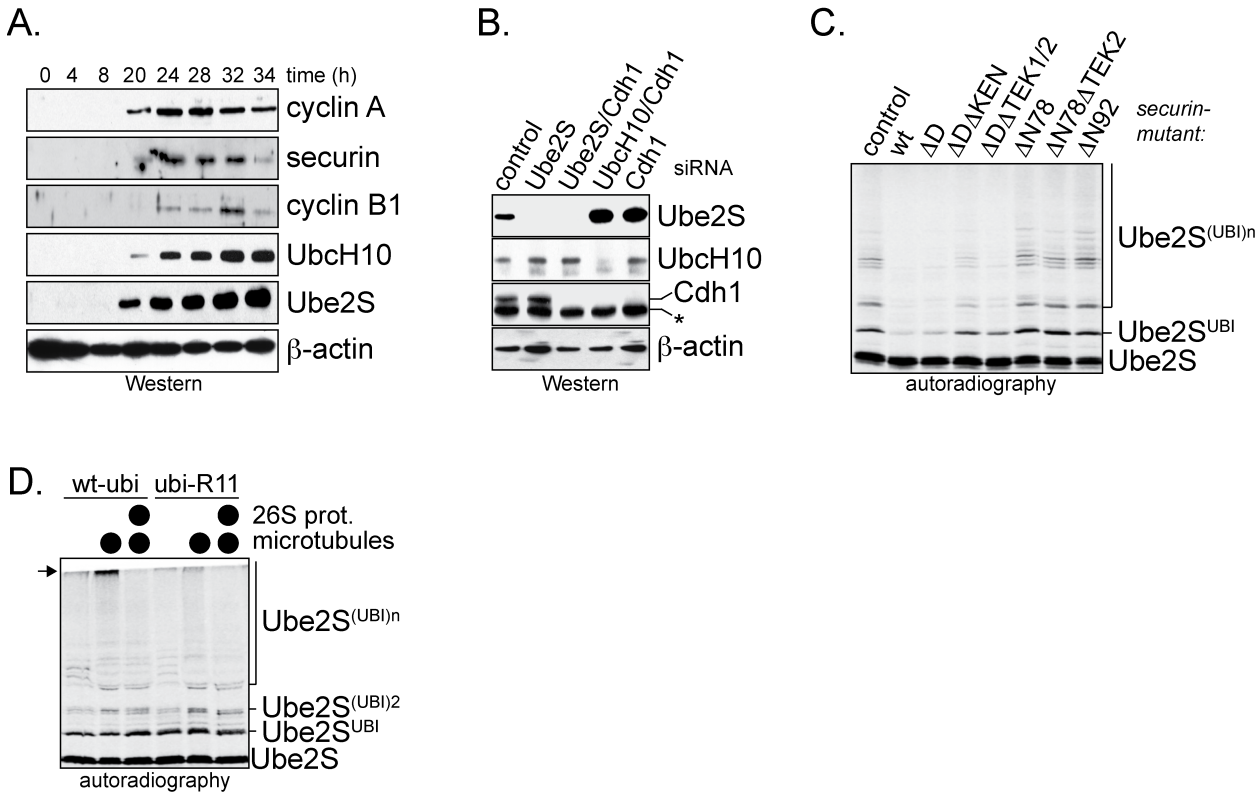
A.
0 4 8 20 24 28 32 34 time (h)
cyclin A
securin
cyclin B1
UbcH10
Ube2S
β-actin
Western
B.
control
Ube2S
Ube2S/Cdh1
UbcH10/Cdh1
Cdh1
siRNA
Ube2S
UbcH10
Cdh1
*
β-actin
Western
C.
control
wt
ΔD
ΔDΔKEN
ΔDΔTEK1/2
ΔN78
ΔN78ΔTEK2
ΔN92
securin-mutant:
Ube2S(UBI)n
Ube2SUBI
Ube2S
autoradiography
D.
wt-ubi
ubi-R11
26S prot.
microtubules
Ube2S(UBI)n
Ube2S(UBI)2
Ube2SUBI
Ube2S
autoradiography

Table S1. Ube2S interaction partners in asynchronously grown 293T cells

APC/C	APC1 (6); APC2 (3); APC4 (5); APC5 (4); APC6 (3); APC7 (7); APC10 (2); Cdc23 (4); Cdc27 (2)
Ribosome	RPS3 (5); RPS3a (3); RPS5 (5); RPS6 (3); RPS7 (4); RPS8 (4); RPS8c (2); RPS9 (3); RPS13 (3); RPS14 (2); RPS15a (2); RPS16 (3); RPS19 (3); RPS20 (2); RPS21 (2); RPS25 (3); RPS27a (9); RPS28 (3); RPSA (4); RPL5 (6); RPL6 (5); RPL7 (4); RPL7a (6); RPL8 (4); RPL9 (3); RPL9 (3); RPL10a (3); RPL11 (5); RPL12 (2); RPL13 (5); RPL13a (2); RPL17-like (2); RPL18 (3); RPL18a (2); RPL19 (2); RPL24 (5); RPL26 (2); RPL27a (2); RPL28 (3); RPL30 (2); RPL38 (2); RPLP0 (3); RPLP2 (3); LOC388339 (3); LOC389342 (5); LOC439992 (3); LOC100129902 (2)
Ribosome-associated	EIF6 (2); SRP14 (2); PA2G4 (3); EF2 (11); PABPC1 (2); EIF3; ILF2 (2); RACK1 (2)
Other	α-tubulin (2); β-tubulin (4); nucleolin (3); ASPM (2); Nek2; Aurora A; MAST1

Interaction partners of Ube2S in asynchronously grown 293T cells. ^{FLAG}Ube2S was immunopurified from a stable 293T cell line by FLAG-agarose and eluted by FLAG-peptide. Elutions were concentrated, and proteins were identified by MudPIT-mass spectrometry (Berkeley Proteomic Center). Proteins specifically identified in Ube2S-IPs are listed, and the number of unique peptides is shown in the brackets.

Chapter 3

The Mechanism of Linkage-Specific Ubiquitin Chain Elongation by a Single-Subunit E2

Katherine E. Wickliffe*, Sonja Lorenz*, David E. Wemmer, John Kuriyan, and Michael Rape

Cell (2011) *144*, 769-781

* equal contribution

Summary

Ubiquitin chains of different topologies trigger distinct functional consequences, including protein degradation and reorganization of complexes. The assembly of most ubiquitin chains is promoted by E2s, yet how these enzymes achieve linkage specificity is poorly understood. We have discovered that the K11-specific Ube2S orients the donor ubiquitin through an essential noncovalent interaction that occurs in addition to the thioester bond at the E2 active site. The E2-donor ubiquitin complex transiently recognizes the acceptor ubiquitin, primarily through electrostatic interactions. The recognition of the acceptor ubiquitin surface around Lys11, but not around other lysines, generates a catalytically competent active site, which is composed of residues of both Ube2S and ubiquitin. Our studies suggest that monomeric E2s promote linkage-specific ubiquitin chain formation through substrate-assisted catalysis.

Introduction

By regulating protein stability, activity, or localization, ubiquitination exerts control over almost every cellular process. As this includes pathways responsible for the duplication and separation of genetic material, aberrant ubiquitination often results in tumorigenesis. Despite the importance for cellular regulation, the mechanisms determining the specificity and efficiency of ubiquitination reactions are still incompletely understood.

Ubiquitination requires at least three enzymatic activities. An E1 enzyme forms a thioester between a cysteine at its active site and the C terminus of ubiquitin (Schulman and Harper, 2009). The activated ubiquitin is transferred to a cysteine of an E2 (Ye and Rape, 2009). In the third step, the charged E2 cooperates with E3s to catalyze formation of an isopeptide bond between the C terminus of ubiquitin and the ε-amino group of a substrate lysine (Deshaies and Joazeiro, 2009). The ~600 human RING-E3s interact with E2s and substrates at the same time, allowing them to promote the transfer of ubiquitin directly from the E2 to the substrate.

The modification of a substrate with a single ubiquitin usually leads to changes in protein interactions (Dikic et al., 2009). In many cases, additional ubiquitin molecules are attached to a substrate-linked ubiquitin, giving rise to polymeric ubiquitin chains. Such chains can be connected through the N terminus of ubiquitin or through one of its seven Lys residues, and all linkages have been detected in cells (Xu et al., 2009; Ye and Rape, 2009). Ubiquitin chains of different topologies can have distinct structures and functions (Dikic et al., 2009; Matsumoto et al., 2010). K48-linked chains, for example, drive protein degradation, whereas K63-linked chains regulate the assembly of protein complexes (Ye and Rape, 2009). Thus, the efficiency and specificity of chain formation have profound consequences for the modified protein.

We recently identified K11-linked ubiquitin chains as critical cell-cycle regulators in human cells (Jin et al., 2008). Most K11-linked chains are synthesized during mitosis by the E3 anaphase-promoting complex (APC/C) and its E2s Ube2C/UbcH10 and Ube2S (Matsumoto et al., 2010; Williamson et al., 2009; Wu et al., 2010). Together, these enzymes modify mitotic regulators, such as cyclin B, securin, or HURP, to trigger their degradation (Jin et al., 2008; Song and Rape, 2010). As a result, inhibiting the formation of K11-linked chains blocks mitotic progression in *Xenopus*, *Drosophila*, and humans (Garnett et al., 2009; Jin et al., 2008; Williamson et al., 2009), whereas their untimely assembly causes inaccurate cell division and tumorigenesis (Jung et al., 2006; Wagner et al., 2004). How the APC/C and its E2s assemble K11-linked chains, however, is poorly understood.

Linkage between two ubiquitin moieties involves the covalent connection of one ubiquitin, the donor, to the active site cysteine of the E2, followed by nucleophilic attack by a lysine of an acceptor ubiquitin (Figure 1A). Much of our knowledge about the basis of linkage specificity is limited to the E2 Ube2N-Uev1A (Ubc13-Mms2) (VanDemark et al., 2001). In this system, the catalytically inactive Uev1A orients the acceptor ubiquitin, such that Lys63 of the acceptor is at the active site of Ube2N charged with the donor (Eddins et al., 2006). In contrast, K11- and K48-linkage-specific E2s promote chain elongation in reconstituted systems lacking UEVs (Li et al., 2009; Pierce et al., 2009; Williamson et al., 2009). Although kinetic analyses suggest that these E2s also engage acceptor ubiquitin residues (Petroski and Deshaies, 2005; Rodrigo-Brenni et al., 2010), the molecular details of acceptor recognition by monomeric E2s and its importance for linkage-specific chain formation have not been established.

Here, we have combined functional studies with nuclear magnetic resonance (NMR) and computational docking to dissect the mechanism of linkage-specific chain formation by single-subunit E2s. We show that the K11-specific Ube2S orients the *donor* ubiquitin by a noncovalent interaction that is in addition to the flexible covalent linkage between these molecules at the E2 active site. We find that a similar tethering mechanism is used by other E2s independently of linkage specificity. The Ube2S-donor ubiquitin complex transiently engages the acceptor ubiquitin through electrostatic interactions. As indicated by our analysis, only binding of the acceptor surface around Lys11, but not around other lysines, leads to formation of a catalytically competent active site composed of residues of both Ube2S and ubiquitin. Hence, linkage-specific ubiquitin chain formation by Ube2S is the result of substrate-assisted catalysis.

Results

A Noncovalent Interaction with Ubiquitin Is Required for Ube2S Activity

In the absence of the APC/C, Ube2S generates K11-linked ubiquitin dimers (ubi_2) and chains attached to Lys residues of its UBC domain and its C-terminal tail (Figure S1A available online). The UBC domain of Ube2S (UBC^{Ube2S}) promotes ubi_2 formation with similar kinetics and specificity as Ube2S (Figure S1A). Like Ube2S, UBC^{Ube2S} is monomeric in ubiquitination buffers, as suggested by gel filtration, small-angle x-ray scattering (SAXS), and other biophysical techniques (Figures S1B and S1C; data not shown). Thus, UBC^{Ube2S} contains all elements required for the synthesis of K11 linkages, making it an appropriate system for analyzing the mechanism of linkage-specific chain formation.

The prevailing model of linkage-specific chain formation posits that an elongating E2, charged with the donor ubiquitin, binds the acceptor in such a way that a preferred acceptor lysine is at the E2 active site (Eddins et al., 2006). To test for such a noncovalent interaction between Ube2S and ubiquitin, we performed titrations of ^{15}N-enriched ubiquitin with Ube2S and UBC^{Ube2S}, respectively, and monitored ^{1}H-^{15}N HSQC spectra. The presence of either E2 caused significant resonance-specific chemical shift perturbations in the ubiquitin spectrum, indicating a specific interaction (Figure 1B).

Chemical shift mapping on the surface of ubiquitin revealed that the hydrophobic patch surrounding Ile44 is involved in the noncovalent interaction with Ube2S (Figure S2B). Mutation of the isoleucine to alanine (ubi^{I44A}) disrupted the interaction with Ube2S (Figure 1B and Figure 2A). Furthermore, mutating residues in the hydrophobic patch (L8A, I44A, V70A) interfered strongly with the formation of K11-linked ubi_2 by Ube2S (Figure 1C).

Ube2S extends K11-linked chains on APC/C substrates after initiation by Ube2C (Williamson et al., 2009; Wu et al., 2010). To test whether mutations in ubiquitin interfere with chain elongation by Ube2S and APC/C, we bypassed the need for Ube2C by generating a fusion between ubiquitin and the APC/C substrate cyclin A (Ub-L-cycA). Ube2S and APC/C rapidly elongated ubiquitin chains on Ub-L-cycA, which did not require Ube2C and was not inhibited by an excess of inactive Ube2C^{C114S} (Figure 1D). Mutation of the hydrophobic patch of ubiquitin interfered strongly with this activity of Ube2S (Figure 1E; Figure S1D), without affecting charging by E1 (Figure S1F). The same mutations in ubiquitin blocked ubiquitination of APC/C substrates in an assay containing both Ube2C and Ube2S (Figure S1E). Thus, a noncovalent interaction with ubiquitin is required for the ability of Ube2S to assemble K11-linked ubiquitin chains.

The Hydrophobic Patch Is Required on the Donor Ubiquitin

To determine whether Ube2S interacts with donor or acceptor ubiquitin, we made a ubiquitin mutant lacking its two C-terminal Gly residues, ubi$^{\Delta GG}$. ubi$^{\Delta GG}$ is not activated by E1 and can only act as acceptor. Ube2S produced dimers between ubi$^{\Delta GG}$ and ubiquitin (ubi$^{\Delta GG}$-ubi; Figure 1F), and mutation of Lys11 on the acceptor ubi$^{\Delta GG}$, but not the donor ubiquitin, blocked this reaction (Figures 1F and 1G). The mutation of Leu8, Ile44, or Val70 on the acceptor ubi$^{\Delta GG}$ had no effect on the formation of ubi$^{\Delta GG}$-ubi dimers (Figure 1F; Figure S1G). Instead, when the hydrophobic patch was mutated on the donor ubiquitin, dimer formation was prevented (Figure 1G).

We conclude that Ube2S recognizes the *donor* ubiquitin. Several aspects of our analysis indicate that this is the only thermodynamically stable interaction between ubiquitin and Ube2S in solution. The NMR-derived binding isotherms are well described by a single-site binding model (Figure S2D); significant chemical shift perturbations map to one contiguous binding region (Figure S2B); and disruption of the donor interface did not result in the population of an alternate binding site (Figure 1B). Variation of the experimental conditions, such as ionic strength and pH, also did not provide evidence for a second binding site (data not shown). Thus, Ube2S forms a noncovalent interface with the hydrophobic patch of the donor ubiquitin, which is required for its activity to promote the formation of K11-linked ubiquitin chains.

The Donor Ubiquitin Interacts with Helix αB of Ube2S

We identified the donor-binding site on Ube2S by titrating ^{15}N-enriched UBC^{Ube2S} with ubiquitin and measuring ^{1}H-^{15}N HSQC spectra. Significant ubiquitin-induced chemical shift perturbations mapped to a surface region around the C-terminal part of helix αB of Ube2S (Figure 2A; Figure S2B). The same region was found to interact with covalently bound donor ubiquitin (Figure S2A). Mutation of two Ube2S residues in this region (C118A, I121A) impaired ubiquitin binding (Figure 2A; Figure S2C) without affecting the structural integrity of Ube2S (data not shown). The dissociation constant (K_D) for this interaction (1.11 ± 0.08 mM or 1.7 ± 0.08 mM for ubiquitin binding to UBC^{Ube2S} or Ube2S; Figure S2D) was comparable to the estimated concentration of donor ubiquitin linked to the Ube2S active site (~3 mM) (Petroski and Deshaies, 2005). Our results, therefore, suggest that covalently linked donor ubiquitin occupies the noncovalent binding site on Ube2S around helix αB.

Based on our previous results, we expected the donor interface of Ube2S to be required for activity. Indeed, $Ube2S^{C118A}$ and $Ube2S^{I121A}$ were strongly impaired in ubi_2 formation (Figure 2B); K11-linked chain assembly on Ub-L-cycA with APC/C (Figure 2C); or modification of cyclin A in an APC/C assay containing Ube2C and Ube2S (Figure 2D). Disrupting this Ube2S surface did not affect charging by E1 (Figure S2E) or binding to the APC/C (Figure S2F).

To test for the importance of donor binding at physiological ubiquitin levels, we generated HeLa cell lines that stably express Ube2S or $Ube2S^{I121A}$. Endogenous Ube2S was specifically depleted from cells by siRNAs against the 3′ untranslated region (UTR) of the Ube2S mRNA, and formation of K11-linked chains was monitored upon exit from mitosis by a K11-linkage-specific antibody. As expected, long K11-linked chains were absent from cells lacking Ube2S, which was rescued by expression of siRNA-resistant wild-type (WT)-Ube2S (Figure 2E). By contrast, the donor-binding-deficient $Ube2S^{I121A}$ failed to promote K11-linked chain formation. Thus, recognition of the donor ubiquitin by Ube2S is essential for K11-linked ubiquitin chain formation in vitro and in vivo.

NMR-Based Docking of the Donor Ubiquitin on Ube2S

The binding site for the donor ubiquitin on Ube2S, as defined by chemical shift mapping, makes it plausible that this interaction occurs in *cis*, i.e., involves the same E2 that the donor is covalently attached to. To test this idea, we determined whether a catalytically inactive Ube2S mutant with an intact donor-binding site ($Ube2S^{C95A}$) could complement the loss-of-function phenotype of a Ube2S mutant with a defective noncovalent interface ($Ube2S^{C118A}$, $Ube2S^{I121A}$). As this was not the case (Figure 2F), the observed noncovalent interaction most likely occurs in *cis*.

To obtain a structural model of the interaction between UBC^{Ube2S} and donor ubiquitin, we used the docking program HADDOCK (De Vries et al., 2007). The NMR chemical shift data were used to specify residues at the interface, and we defined only one explicit distant restraint that required the C-terminal carbon atom of Gly76 of ubiquitin to be close to the S^{γ} atom of Cys95 in Ube2S. HADDOCK produced an ensemble of 200 structures after automated refinement, which were clustered using a backbone root-mean-square deviation (rmsd) cut-off of 7.5 Å. The resulting three clusters contain 71%, 25.5%, and 2.5% of all docked models, respectively (Table S1). As shown later, structures in cluster 1, but not those of clusters 2 and 3, could be validated by biochemical data.

As a representative structure of the Ube2S-donor ubiquitin complex, we selected a model from cluster 1 that among the top 3 according to HADDOCK scoring had the largest buried surface area, the most negative interaction energy, and the smallest number of distant restraint violations (Figure 3A; Table S1). A similar model with a low backbone rmsd of 1.1 Å was obtained by a different docking program, Cluspro (Comeau et al., 2007), without restraints (Figure S3A). Our model resembles the structure of the charged E2 Ubc9, when bound to its E3 (Reverter and Lima, 2005), and an NMR-based, docked model of the E2 Ubc1 and ubiquitin (Hamilton et al., 2001).

Within our model, the donor ubiquitin docks onto a hydrophobic area on Ube2S, comprising the C-terminal half of helix αB, the C-terminal part of helix αC, and the N-terminal part of helix αD (Figures 3A and 3B). The corresponding interaction surface on donor ubiquitin contains the hydrophobic patch (Figure 3C), which is extended to form a contact area that buries

a total of ~830 Å^2 on ubiquitin. The model includes ionic contacts between Lys6, Arg42, and Lys48 of ubiquitin, and Glu51, Glu126, and Glu142 of Ube2S (Figure S3B). An ionic contact between Arg74 of ubiquitin and Asp102 of Ube2S serves as a linchpin to guide the C terminus of ubiquitin toward the active site of Ube2S (Figure S3C). The ubiquitin tail is also anchored by hydrogen bonds between the peptide backbone and Ube2S residues close to the active site. The distance between the S^{γ} atom of Cys95 of Ube2S and the C-terminal carbon atom of ubiquitin, 3.9 Å, is too long for a covalent bond, but small adjustments around the active site of Ube2S could readily close this gap.

Validation of the Ube2S-Donor Ubiquitin Model

Based on the selected model for this complex, we designed additional mutations to test the structural details of the predicted interface. We found that altering residues at the binding interface (Ube2S: E51K, R101A, D102A, S127A, Y141A; ubiquitin: K6E, K48E, T66E, H68A, L71A, R72A) interfered with Ube2S activity in vitro (Figures 3D–3G) and, as seen for ubi^{K6E}, disrupted the Ube2S-donor ubiquitin interaction (Figure 2A). Residues that do not make intermolecular contacts (Ube2S: D29, G30, L114, E142; ubiquitin: A46) were not required for activity (data not shown). Introducing mutations into ubi$^{\Delta GG}$ showed that most ubiquitin residues were required in the donor but not the acceptor (Figures S3D and S3E). The role of Lys6 in the acceptor ubiquitin is described below. With the exception of ubi^{R72A}, no Ube2S or ubiquitin mutant was impaired in charging by E1 (Figures S3F and S3G). To confirm this analysis in vivo, we generated cell lines that express Ube2S mutants with defective donor-binding interfaces (E51K; D102A; S127A). Importantly, all of these failed to promote the formation of K11-linked ubiquitin chains in HeLa cells that lacked endogenous Ube2S (Figure 3H).

To further test our model, we used charge-swap analysis to analyze the role of the predicted ion pair between Glu51 of Ube2S and Lys6 of ubiquitin. While the K6E mutation in donor ubiquitin interfered with formation of ubi$^{\Delta GG}$-ubi dimers, this was rescued by a complementary mutation in Ube2S, Ube2S^{E51K} (Figure 3I). Ube2S^{E51K} did not establish ubi_2 formation for other ubiquitin mutants, such as ubi^{I44A}, attesting to the specificity of this rescue (Figure S3H). Together, the mutational studies, charge-swap analysis, and in vivo experiments validate the selected NMR-based model for the Ube2S-donor ubiquitin interaction and show its importance for chain formation by this E2.

Noncovalent Donor Ubiquitin Binding Is Required for Processive Chain Formation

We next determined the role of donor binding for catalysis by Ube2S. It was unlikely that recognizing the donor ubiquitin was important for specificity, and indeed, any ubi_2 formed in the presence of ubi^{I44A} was lost upon mutation of K11 (Figure 4A). The same was observed when Ube2S mutants with a defective donor-binding interface (Ube2S^{I121A}; Ube2S^{C118A}; Ube2S^{E51K}) were analyzed for ubi_2 formation (Figure 4A). Thus, donor binding does not determine the K11 specificity of Ube2S.

Alternatively, the noncovalent interaction between the donor and Ube2S might prevent a flexible donor molecule from interfering with acceptor recognition. If this is the case, higher concentrations of the acceptor ubi$^{\Delta GG}$ should rescue the defect in ubi_2 formation when the Ube2S-donor ubiquitin interface is disturbed. Consistent with this hypothesis, high levels of ubi$^{\Delta GG}$ allowed linkage formation with ubi^{I44A} or Ube2S^{I121A} (Figure 4B). The acceptor concentration

required under these conditions was above the endogenous ubiquitin levels in HeLa cells (90 μM) (Ryu et al., 2006), consistent with the lack of Ube2S^{I121A} activity in vivo. These findings suggest that noncovalent binding of the donor ubiquitin facilitates acceptor recognition by Ube2S.

Based on these observations, we expected that donor binding would increase the processivity of chain formation by Ube2S. Indeed, a time-resolved analysis of chain elongation on Ub-L-cycA suggested that Ube2S assembles chains with high processivity (Figure 4C), whereas chain formation occurred in a step-like, distributive fashion if donor-binding was impaired (Figure 4C). To directly measure the processivity of chain elongation, we supplied the reactions with a UBA domain. As previously described (Rape et al., 2006), the UBA domain captures any substrate dissociating from the APC/C, thereby preventing it from rebinding the E3 and revealing the number of ubiquitin molecules transferred in a single substrate-binding event. Ube2S could transfer up to ~13 ubiquitin molecules to Ub-L-cycA per binding event (Figure 4D, top), whereas less than four molecules of the hydrophobic patch mutant ubi^{V70A} were transferred (Figure 4D, bottom). As this UBA domain only recognizes K11-chains with at least ~5 ubiquitin moieties (data not shown), the number of ubi^{V70A} molecules transferred in a single binding event is likely even smaller. Thus, the noncovalent interaction between Ube2S and donor ubiquitin increases the processivity of chain formation, at least in part by facilitating acceptor ubiquitin recognition.

Noncovalent Donor Ubiquitin Binding Is a Feature of Chain Elongation in Other E2s

To test whether other E2s bind the donor ubiquitin noncovalently, we turned to Ube2R1 and Ube2G2, which extend K48-linked chains (Li et al., 2009; Pierce et al., 2009). Disruption of the hydrophobic patch on ubiquitin strongly impaired the formation of K48 linkages by these E2s (Figure S4A), while having no effect on their charging by E1 (Figure S4B). Analogous to our results for Ube2S, we found that the activity of Ube2R1 and Ube2G2 was dependent on recognition of the hydrophobic patch on the donor but not the acceptor ubiquitin (Figure 5A). As revealed by ubi$^{I44A/K48R}$- and ubi$^{V70A/K48R}$-double mutants, noncovalent donor binding did not determine linkage specificity (Figure 5B) but was required for catalysis at low substrate concentrations (Figure 5C).

To test whether a common E2 surface recognizes the donor ubiquitin, we studied Ube2R1 mutations of sites that are structurally homologous to the Ube2S-donor interface (Figure 5D). These mutations (Ube2R1^{T122E}; Ube2R1^{L125A}; Ube2R1^{I128E}) strongly inhibited the formation of K48 linkages (Figure 5D; Figure S4C), without affecting charging by E1 (Figure S4D). The same mutations also impaired the SCF- and Ube2R1-dependent formation of ubiquitin chains on IκBα (Figure 5E). Thus, similar surfaces on the conserved E2 fold and ubiquitin are used for chain elongation by E2s of different linkage specificity. The tethering of the donor ubiquitin by an E2, therefore, provides a conserved mechanism to facilitate acceptor recognition.

Ube2S Recognizes the TEK-Box in Acceptor Ubiquitin

We next identified the binding site for the acceptor ubiquitin on Ube2S. Consistent with previous analyses (Petroski and Deshaies, 2005; Rodrigo-Brenni et al., 2010), acceptor binding was too transient to be detected by NMR, independently of whether the donor ubiquitin had been linked to the Ube2S active site or not (data not shown). We therefore used HADDOCK to dock a

second ubiquitin molecule, the acceptor, onto the validated Ube2S-donor ubiquitin complex. The only restraint used for this docking defined the N^{ζ}-atom of the acceptor Lys11 to be close to the S^{γ} atom of Cys95 at the Ube2S active site. HADDOCK generated two clusters of models, which were similar in terms of energy and buried surface area (Figure S5; Table S2).

Intriguingly, models in cluster 1 orient the TEK-box of ubiquitin toward the active site of Ube2S. The TEK-box is a surface region of ubiquitin that was previously identified to mediate the preference of Ube2C/UbcH10 for assembling K11-linked chains (Jin et al., 2008). We found that mutation of the TEK-box strongly interfered with the ability of Ube2S to synthesize K11-linked ubi_2 (Figure 6A), to elongate chains on Ub-L-cycA (Figure 6B), and to modify cyclin A in a full APC/C assay (Figure S6A). Residues outside of the TEK-box (Thr9, Glu16, Lys33) were not required for activity (data not shown). Introducing mutations into $ubi^{\Delta GG}$ revealed that the TEK-box was essential on the acceptor (Figure 6C) but, with exception of Lys6, not the donor ubiquitin (Figure 6D). The TEK-box was dispensable for Ube2S charging by E1 (Figure S6B) or binding of donor ubiquitin to Ube2S (Figure S6C). Thus, the TEK-box of the acceptor ubiquitin is required for K11-linkage formation by Ube2S.

On the basis of these results, we performed another docking run that defined four TEK-box residues to be at the interface (Table S2). All HADDOCK solutions grouped into a single cluster reproducing the binding topology of cluster 1 of the previous run (Figure 6E). With backbone rmsd values of ~1 Å, the best models of this ensemble were remarkably similar, and we focused on the top-scoring model (cluster 1, no. 1; Table S2, bottom).

In this model of the ternary complex, the acceptor ubiquitin interacts mostly with Ube2S (Figure 6E), with a total buried surface area between the acceptor ubiquitin and the Ube2S-donor complex of ~980 $Å^2$ (Figures 6F and 6G). The acceptor ubiquitin uses its β strand region to bind a surface of Ube2S comprising the active site helix αCat, the loop region between helices αB and αC, and helix αC (Figure 6F). Although the interaction leads to the burial of few hydrophobic residues, these are not closely packed, and the interface is predominantly electrostatic. In particular, a network of ionic contacts involving Lys6 and Lys63 of ubiquitin, Glu131 and Glu139 of Ube2S, and a series of hydrogen bonds including Glu64 of ubiquitin and Arg135 of Ube2S are key features of the interface (Figure S6D). The electrostatic Ube2S-acceptor interface is consistent with the low affinity between these molecules (Sheinerman and Honig, 2002).

Mutating residues in the predicted binding site on Ube2S (N97A, E131K, R135E), but not outside of this interface (K76, N91, E93, K100, E126, E132), impaired production of ubi_2 (Figure 6H; data not shown), chain elongation on Ub-L-cycA (Figure 6I), and substrate modification in a full APC/C assay (Figure S6E). As seen in cells expressing $Ube2S^{E131K}$ or $Ube2S^{R135E}$, these mutations also inhibited formation of K11-linked chains in vivo (Figure 6J). Asn97, Glu131, and Arg135 were not required for Ube2S charging by E1 (Figure S6F) or Ube2S binding to the APC/C (Figure S2F).

We next probed the predicted ionic contacts between Ube2S and the acceptor ubiquitin by charge-swap analyses. Our model found the acceptor Lys6 to face Glu131 of Ube2S (Figure 7A). Consistent with this, the loss of $ubi^{\Delta GG}$-ubi formation caused by a K6E mutation in the acceptor $ubi^{\Delta GG}$ could be rescued by $Ube2S^{E131K}$ or $Ube2S^{E131A}$ (Figure 7A; Figure S7A), but not by other Ube2S mutants in this interface (N97A, R135E) (Figure S7B). Thus, the acceptor Lys6 is recognized by Glu131 of Ube2S, whereas the donor Lys6 contacts Glu51 of Ube2S (Figure 3); indeed, $Ube2S^{E51K/E131K}$ completely rescued ubi_2 formation by ubi^{K6E} (Figure 7B; Figure S7C). Our model also showed Arg135 of Ube2S in proximity of Glu64 of ubiquitin.

Accordingly, the diminished activity of Ube2S^{R135E} was significantly rescued by ubi^{E64K} (Figure S7D), but not other ubiquitin mutants in the proximity of this surface (Figure S7E). Finally, less ubi_2 was formed in the presence of ubi^{K63E}, which could be rescued by mutation of the opposing Glu139 of Ube2S (Figure S7F). The mutational and charge-swap analyses provide strong support for our model of acceptor recognition by Ube2S.

Linkage Specificity Is Determined by Substrate-Assisted Catalysis

The low affinity of Ube2S for acceptor ubiquitin raised the question of how this E2 achieves the stringent selection of K11 over other linkages. In one scenario, recognition of other Lys residues would be even less favored, with differences in binding energies accounting for the K11 specificity of Ube2S. To address this issue, we carried out docking calculations that placed each of the other Lys residues of ubiquitin in proximity to the active site of charged Ube2S. Among the clusters returned by HADDOCK, several had buried surface areas and energy characteristics comparable to our K11-centered model (Figure S8; Table S3). This suggests that other Lys residues can be exposed to the active site of Ube2S, yet these binding events do not result in linkage formation. Thus, selective acceptor binding is not sufficient to explain the K11 specificity of Ube2S.

Alternatively, the composition of the active site of Ube2S might force the reaction toward K11 linkages. Our models of the ternary complex found that the active site of Ube2S was similar to the E2 Ubc9 ((Reverter and Lima, 2005) (Figure 7C). For Ubc9, several residues in addition to the active site cysteine were attributed roles in catalysis: Tyr87 and Asn85 of Ubc9 contribute to pK_a suppression of the substrate lysine through desolvation. Further, Asn85 serves to stabilize the oxyanion intermediate during ubiquitin transfer, and Tyr87 provides a hydrophobic platform to position the attacking lysine side chain (Yunus and Lima, 2006). Whereas Asn85 of Ubc9 is conserved in Ube2S (Asn87) (Figure 7C), the attacking lysine is likely positioned by Leu129 of Ube2S (Figure 7C). Asn87 and Leu129 are essential for Ube2S activity in vitro (Figures 7D and 7E) and, as seen with HeLa cell lines expressing Ube2S^{L129E}, in vivo (Figure 7F). The mutation of Asn87 or Leu129 did not impede charging of Ube2S by E1 (Figure S7G).

In addition to Asn85 and Tyr87, Asp127 of Ubc9 was assigned a catalytic role in reducing the pK_a of the substrate lysine (Yunus and Lima, 2006). In Ube2S, this residue is replaced by serine (Ser127), which our models place into a position to interact with the donor ubiquitin rather than activate an acceptor lysine (Figure 3). Strikingly, instead of an E2 residue, our models show an amino acid of ubiquitin, Glu34, to be in an appropriate position to orient the acceptor Lys11 and to promote its desolvation (Figure 7C). The mutation of Glu34 inhibited K11-linkage formation (Figures 7G and 7H), and kinetic analyses found this to be due to a strong reduction in the apparent catalytic rate constant (k_{cat}) but not the Michaelis-Menten constant (K_M) (Figure 7I). Thus, a residue in the substrate, Glu34 of ubiquitin, plays an important role in catalysis by Ube2S.

Due to its position in the ternary complex, Glu34 is expected to orient Lys11, but not other Lys residues, and to suppress its pK_a. The E34Q mutant of ubiquitin might maintain the position of Lys11 but fail to promote its deprotonation. If this assumption is correct, the inability of ubi^{E34Q} to produce ubi_2 may be rescued by increasing the pH of the reaction, which facilitates lysine deprotonation. Indeed, Ube2S efficiently linked ubi^{E34Q} molecules at higher pH (Figure 7J), which was due to a change in the apparent k_{cat}, but not K_M (Figure 7I). By contrast, an acceptor TEK-box mutant defective in Ube2S binding (ubi^{T14E}) and a donor ubiquitin mutant

($ubi^{I44A/V70A}$) were inactive at pH 9 (Figure 7J). These findings support the notion that Glu34 of ubiquitin participates in catalysis by suppressing the pK_a of the acceptor Lys11.

As the catalytic role of Glu34 could be bypassed by increasing the pH, the same treatment might reduce the specificity of Ube2S. Consistent with this hypothesis, Ube2S modified Lys residues in a peptide derived from its C-terminal tail much more efficiently at pH 9 than at pH 7.5 (Figure S7H). Moreover, at pH 9, but not at pH 7.5, Lys63 and Lys48 of ubiquitin could act as acceptor for Ube2S (Figure S7I), although the bulk of linkage formation still occurred through K11 (Figure S7J). These findings further suggest that Ube2S requires a residue in ubiquitin, Glu34, for specific formation of K11 linkages. We conclude that Ube2S promotes linkage-specific ubiquitin chain formation by substrate-assisted catalysis.

Conclusions

K11- and K48-linked ubiquitin chains are often assembled by single-subunit E2s that cooperate with RING-E3s (Ye and Rape, 2009). Most of these E2s are specific and processive, but how these properties are achieved in the absence of cofactors was poorly understood. Here, we addressed this question by dissecting the mechanism of ubiquitin chain assembly by the K11-specific E2 Ube2S.

We found that Ube2S requires a noncovalent interaction with the donor ubiquitin for chain formation. Although the affinity of Ube2S for the donor ubiquitin is weak, this interaction occurs in addition to the covalent thioester bond at the E2 active site. It tethers the donor ubiquitin to the E2, thereby restricting its flexibility and facilitating acceptor recognition. It also places the C terminus of the donor ubiquitin in an optimal position for nucleophilic attack by the acceptor lysine.

The Ube2S-donor ubiquitin complex binds the acceptor ubiquitin very transiently through primarily electrostatic interactions. Ube2S recognizes the TEK-box on acceptor ubiquitin, a motif previously identified as being required for formation of K11 linkages by Ube2C (Jin et al., 2008). As seen in crystal structures of K11-linked ubiquitin dimers (Bremm et al., 2010; Matsumoto et al., 2010), all TEK-box residues in the distal ubiquitin are fully accessible for recognition by Ube2S.

The low affinity of Ube2S for the acceptor is in agreement with observations for other E2s (Petroski and Deshaies, 2005; Rodrigo-Brenni et al., 2010) and likely protects cells from spurious chain elongation in the absence of E3s. However, together with our comparative docking analysis, the transient nature of acceptor binding suggests that selective acceptor recognition does not explain the linkage specificity of Ube2S.

Indeed, our model of the ternary complex between Ube2S, donor, and acceptor ubiquitin revealed that Ube2S lacks a residue required for suppressing the pK_a of the substrate lysine. This function is instead provided by Glu34 of ubiquitin, which is in direct proximity to Lys11. Mutation of Glu34 had strong effects on the apparent k_{cat}, but not the K_M, of linkage formation by Ube2S, supporting a role in catalysis. Other Lys residues of ubiquitin do not have a suitably positioned acidic residue when docked into the active site of Ube2S or display features incompatible with catalysis (Figure S8). The same likely applies to Lys residues of APC/C substrates, which may explain why Ube2S is unable to promote chain initiation (Garnett et al., 2009; Williamson et al., 2009). Thus, our findings suggest that formation of a competent catalytic center requires residues of Ube2S and ubiquitin, which only occurs when K11 of the

acceptor is exposed to the active site of Ube2S. We conclude that linkage-specific chain assembly by Ube2S occurs through substrate-assisted catalysis.

Do other E2 enzymes use similar mechanisms for ubiquitin transfer? We found that noncovalent donor binding is a property shared by E2s with different linkage specificity. Ube2R1 and Ube2G2 also tether the donor ubiquitin for efficient catalysis, but not for K48 specificity, and Ube2R1 uses a similar surface on its UBC domain as Ube2S uses for donor recognition. In addition, the HECT-E3 Nedd4L binds E2-linked donor ubiquitin, a feature required for rapid ubiquitin transfer to the catalytic cysteine of the E3 (Kamadurai et al., 2009); the E3 RanBP2 binds SUMO to restrict its conformational freedom (Reverter and Lima, 2005); and in some cases, a ubiquitin-binding domain can promote E2-dependent ubiquitination reactions (Hoeller et al., 2007). We, therefore, propose that noncovalent donor binding is a general property of ubiquitination enzymes to increase the processivity of substrate modification.

Other E2s may also use substrate-assisted catalysis for chain assembly. Mms2-Ubc13 positions Glu64 of ubiquitin close to the E2 active site, and mutation of this residue resulted in a decrease of K63-linkage formation (Eddins et al., 2006). Thus, although acceptor binding to Mms2 helps to orient Lys63 toward the active site of Ubc13, a catalytic ubiquitin residue might increase the specificity of chain formation. Moreover, mutation of a Tyr residue in ubiquitin reduced the catalytic rate of K48-linkage formation by yeast Ubc1 (Rodrigo-Brenni et al., 2010). Together, these findings allow us to propose that several E2 enzymes achieve linkage-specific ubiquitin chain formation through a mechanism of substrate-assisted catalysis.

In this chapter, we asked how monomeric E2 enzymes achieve linkage-specificity, using Ube2S as a model E2. We discovered that Ube2S and Lys48-specific E2s engage in an essential and conserved non-covalent interaction with the donor ubiquitin, which promotes recognition of the acceptor ubiquitin. When presented to the Ube2S active site, the surface of ubiquitin surrounding Lys11, but no other lysines, triggers catalysis. We conclude that linkage-specificity of Ube2S is accomplished by a mechanism of substrate-assisted catalysis, in which a residue of acceptor ubiquitin helps active Lys11.

All of the initial evidence linking human APC/C and its E2s to Lys11-linked ubiquitin chains relied on *in vitro* studies using ubiquitin lysine mutants (e.g. K11R or K11-only). Similarly, the only *in vivo* evidence that the APC/C makes Lys11-linked chains was derived from the overexpression of ubiquitin mutants. Work presented in the previous chapter uncovered some caveats of using such mutants. While not sites of ubiquitin attachment, Lys6 and Lys48 are nevertheless important for Ube2S activity, and their mutation may unknowingly affect chain formation. Additionally, direct evidence that the APC/C and its E2s assemble Lys11 chains during mitosis and that these chains promote degradation in cells was lacking. To address these concerns, we collaborated with Genentech to develop and test a Lys11-linkage-specific antibody. Experiments conducted with the antibody are presented in the next chapter.

Methods

A detailed methods description can be found in the Extended Experimental Procedures:
http://www.sciencedirect.com/science/article/pii/S0092867411001115#sec3.9

All tables can be found online at:
http://www.sciencedirect.com/science/article/pii/S0092867411001115#mmc1

Reagents

Table S4 shows a complete list of all constructs.

Protein Purification

Most proteins were purified from BL21/DE3 (RIL) cells. E1 was purified from Sf9 cells. For uniform isotopic enrichment, Ube2S and ubiquitin were expressed in M9-medium using ^{15}N-enriched $(NH_4)_2SO_4$ and/or ^{13}C-enriched glucose.

To generate ester-linked complex, 75 μM ^{15}N-enriched $UBC^{Ube2S/C95S}$ and 230 μM unlabeled ubiquitin were incubated at 37°C for 3 hr. The diluted reaction was subjected to two rounds of anion-exchange chromatography.

Formation of ubi_2

60 μM ubiquitin and/or $ubi^{\Delta GG}$ and 5 μM E2s were incubated with E1 and energy mix at 30°C for 1 hr and analyzed by Coomassie or Silver staining. In assays comparing activity at different pH, Tris/HCl was replaced with 50 mM Bis-tris propane, pH 7.5, 8, or 9.

Ube2S Kinetics Assays

Time courses of ubi_2 formation were performed with different concentrations of WT- or E34Q-ubiquitin. Levels of ubi_2 were quantified by Quantity One and compared to a known amount of Ube2S on each gel. Initial velocity rates and kinetic constants were calculated with GraphPad Prism and Michaelis-Menten equations.

APC/C Ubiquitination Assays

^{35}S substrates were synthesized by IVT/T. Ub-L-cycA was synthesized in the presence of 175 μM ubi^{K29R} to inhibit the UFD-pathway, which is active in reticulocyte lysate. To purify ^{35}S-Ub-L-cycA, ^{His}Cdk2 was bound to NiNTA. IVT/T was added to beads for 3 hr at 4°C. Beads were eluted with imidazole, and Ub-L-cycA/Cdk2-complexes were concentrated with 30 MWCO Microcon filters. APC/C was purified from G1-HeLa extracts and used for ubiquitination as described (Rape et al., 2006).

Analysis of Ube2S Activity In Vivo

HeLa cells were transfected in 6-well plates with 4 μg Ube2S vectors and Lipofectamine 2000. Twenty-four hours later, 10% of transfected cells were expanded to 10 cm dishes and selected with hygromycin B. Individual hygromycin-resistant colonies were picked with cloning discs and tested for Ube2S expression by western.

Cells expressing Ube2S or mutants were transfected with 100 nM siRNA with Oligofectamine and synchronized in prometaphase by thymidine/nocodazole. Samples were taken at 0 hr and 2 hr post-release and processed for αK11-western.

Computational Docking

Donor docking was performed with HADDOCK 2.1, using crystal structures of UBC^{Ube2S} (Protein Data Bank (PDB) ID: 1ZDN, chain A) and ubiquitin (PDB ID: 1UBQ). Active residues were based on chemical shift perturbation data and solvent accessibility. For thioester linkage between donor and Ube2S, we applied an unambiguous intermolecular distance restraint between C95 of Ube2S and G76 of ubiquitin. Residues 70–76 of ubiquitin were defined fully flexible.

To generate a model of the ternary complex, we docked a second ubiquitin onto the selected E2-donor complex (cluster 1, no. 3; Table S1). We initially applied a single unambiguous restraint between K11 of the acceptor and C95 of Ube2S (Table S2, top), followed by a refined run with ambiguous restraints based on functional data (Table S2).

Additional donor-docking experiments used ClusPro 2.0 and default parameters.

NMR

Data were recorded at 25°C on Bruker DRX spectrometers (500, 600, 800, and 900 MHz) and processed with NMRPipe. Backbone chemical shift assignments for UBC^{Ube2S} and ubiquitin were obtained by standard triple resonance experiments. Titration experiments were performed by mixing stock solutions containing 240 μM ^{15}N-enriched UBC^{Ube2S} or 200 μM ^{15}N-enriched ubiquitin and no or an ~6-fold molar excess of unlabeled partner. Phase-sensitive gradient-enhanced ^{1}H-^{15}N HSQC spectra were recorded. To compare chemical shift perturbations, a weighted combined chemical shift difference $\Delta\delta(^{1}H^{15}N)$ was calculated.

^{1}H-^{15}N HSQC experiments of ester-linked complex between ^{15}N-enriched $UBC^{Ube2S/C95S}$ and ubiquitin were recorded with 22 μM complex.

Acknowledgments

We thank H.J. Meyer for Ub-L-cycA; A. Williamson for golden extracts; members of the Rape and Kuriyan labs, J. Winger, S. Kassube, and J. Kirsch for discussions; J. Schaletzky for reading the manuscript and suggestions; J. Pelton for help with NMR experiments; D. King and T. Iavarone for mass spectrometry; and the staff at beamline 12.3.1 at LBNL for technical support. NMR instrumentation and operation were supported by NIH-GM 68933, NIH GM68933, NSF BBS 0119304 and NIH RR15756, and NSF BBS 8720134. S.L. is a fellow of The Leukemia & Lymphoma Society. M.R. is a Pew fellow and is supported by NIH GM83064 and an NIH New Innovator Award.

Accession Numbers

The 1H, 15N, and 13C backbone chemical shift assignments for Ube2S (1–156) and ubiquitin have been submitted to the Biological Magnetic Resonance Bank (BMRB), http://www.bmrb.wisc.edu, with accession numbers 17437 and 17439, respectively.

Figure Legends

Figure 1. Ube2S Recognizes the Hydrophobic Patch of Donor Ubiquitin (A) Overview of K11-specific linkage formation. Lys11 of acceptor ubiquitin attacks the thioester bond between Cys95 of Ube2S and the C terminus of the donor ubiquitin. **(B)** Ube2S interacts with ubiquitin noncovalently. Weighted combined chemical shift perturbations, $\Delta\delta(^{1}H^{15}N)$, are plotted over residue number. The asterisk indicates the disappearance of the resonance for His68 of ubiquitin in the presence of Ube2S due to intermediate exchange. **(C)** Mutation of the hydrophobic patch in ubiquitin interferes with formation of K11-linked ubiquitin dimers (ubi~ubi) by Ube2S, as monitored by Coomassie staining. **(D)** Ube2S and APC/C extend ubiquitin chains on a fusion between ubiquitin and cyclin A (Ub-L-cycA), as analyzed by autoradiography. **(E)** The hydrophobic patch of ubiquitin is required for chain elongation by APC/C^{Cdh1} and Ube2S, as analyzed by autoradiography. **(F)** The hydrophobic patch is not required on acceptor ubiquitin. Ube2S was mixed with acceptor ^{His6}ubiquitin$^{\Delta GG}$ mutants (ubi$^{\Delta GG}$; purple) and WT-ubiquitin (blue) and analyzed by α-ubiquitin-western. **(G)** The hydrophobic patch is required on the donor ubiquitin. Ube2S was mixed with WT-ubi$^{\Delta GG}$ and ubiquitin mutants and analyzed by α-ubiquitin-western.

Figure 2. Noncovalent Donor Ubiquitin Binding Is Required for Ube2S Activity (A) Identification of Ube2S residues involved in noncovalent binding of ubiquitin. Weighted combined chemical shift perturbations, $\Delta\delta(^{1}H^{15}N)$, are plotted over the residue number. **(B)** Donor binding is required for formation of ubi_2 dimers (ubi~ubi) by Ube2S mutants, as analyzed by Coomassie staining. **(C)** Donor binding by Ube2S is required for chain elongation on Ub-L-cycA with APC/C, as analyzed by autoradiography. **(D)** Donor binding by Ube2S is required for chain formation in a full APC/C assay. Ubiquitination of cyclin A by APC/C, Ube2C, and Ube2S mutants was analyzed by autoradiography. **(E)** Donor binding is required for Ube2S activity in vivo. HeLa cell lines expressing Ube2S or Ube2S^{I121A} were treated with siRNAs against the 3′ UTR of Ube2S, which specifically depletes endogenous Ube2S. Cells were synchronized in prometaphase (t = 0 hr) or late mitosis (t = 2 hr), and K11-linked ubiquitin chains were detected by αK11-western. **(F)** Donor binding occurs in *cis*. Ube2S^{C118A} or Ube2S^{I121A} (lack the noncovalent ubiquitin-binding site) and Ube2S^{C95A} (no active site) were mixed, and ubi_2 formation was monitored by Coomassie staining.

Figure 3. Structural Model of the Ube2S-Donor Ubiquitin Complex (A) NMR-based HADDOCK model of the UBC^{Ube2S}-donor ubiquitin complex (cluster 1, no. 3; see Table S1). The C-terminal tail of ubiquitin (cyan) was allowed full flexibility during docking. **(B and C)** Surface representation of the binding interface on UBC^{Ube2S} (B) and donor ubiquitin (C). Residues that make intermolecular contacts within a radius of 4 Å are shown in pink. **(D)** Ube2S residues at the donor-binding interface are required for formation of ubi_2 dimers (ubi~ubi), as monitored by Coomassie staining. **(E)** Donor-binding-deficient Ube2S mutants do not promote chain elongation on Ub-L-cycA with APC/C, as analyzed by autoradiography. **(F)** Ubiquitin residues at the Ube2S interface are required for linkage formation, as seen by Coomassie staining. **(G)** Ubiquitin residues at the Ube2S interface are required for chain elongation on Ub-L-cycA with APC/C, as analyzed by autoradiography. **(H)** Donor binding is required for Ube2S activity in cells. HeLa cell lines expressing donor-binding-deficient Ube2S (E51K; D102A; S127A) were depleted of endogenous Ube2S, synchronized in prometaphase (t = 0) or allowed to exit mitosis

(t = 2 hr), and tested for K11-linked ubiquitin chains by αK11-western. **(I)** Charge-swap analysis of the ionic interaction between Lys6 of donor ubiquitin and Glu51 on Ube2S. ubi$^{\Delta GG}$ was mixed with ubiquitin or ubi^{K6E} in the presence of Ube2S or Ube2S^{E51K}. Reactions were monitored by Silver staining.

Figure 4. Noncovalent Donor Binding Increases the Processivity of Ube2S (A) Donor binding is not required for the K11-linkage specificity of Ube2S. Ube2S or donor-binding mutants were incubated with ubiquitin or ubi^{K11R}, or as indicated with ubi^{I44A} and ubi$^{I44A/K11R}$. Reactions were incubated longer and at higher ubiquitin concentrations to observe formation of ubi$_2$ and analyzed by Coomassie staining. **(B)** Donor binding promotes catalysis at low acceptor concentrations. Dimer formation between increasing levels of ubi$^{\Delta GG}$ and ubi^{K11R} or ubi$^{K11R/I44A}$, respectively, by Ube2S was monitored by Silver staining. **(C)** Time-course analysis of chain elongation on Ub-L-cycA by APC/C^{Cdh1} and Ube2S in the presence of ubiquitin mutants, as analyzed by autoradiography. **(D)** Donor binding is required for processive chain formation by Ube2S. Chain elongation on Ub-L-cycA by APC/C and Ube2S was monitored in the presence of the UBA domains of Rad23A. Reactions were performed with ubiquitin or ubi^{V70A} and analyzed by autoradiography (top) and line scanning (bottom).

Figure 5. Noncovalent Donor Binding Is Utilized by E2s Independently of Linkage Specificity (A) Ube2R1 and Ube2G2 require the hydrophobic patch in the donor but not acceptor ubiquitin for K48-linkage formation. Ube2S, Ube2R1, or Ube2G2 and its E3 gp78 were incubated with ubi$^{\Delta GG}$ or ubi$^{\Delta GG/I44A/V70A}$ (purple) and ubiquitin or ubi^{I44A} (blue). Reactions were analyzed by Silver staining. **(B)** The hydrophobic patch of donor ubiquitin is not required for K48 specificity of Ube2R1 or Ube2G2. ubi$_2$ formation by Ube2R1 or Ube2G2/gp78 with ubiquitin mutants was analyzed by Coomassie staining. **(C)** Donor binding is required for rapid catalysis by Ube2R1. Time courses of ubi$_2$ formation by Ube2R1 in the presence of increasing concentrations of ubiquitin or ubi^{I44A} were analyzed by Coomassie staining. **(D)** A similar surface as the donor-binding interface of Ube2S (yellow) is required in Ube2R1 (green; PDB ID: 2OB4). Ube2R1 mutants were analyzed for K48-specific ubi$_2$ formation by Coomassie staining. **(E)** Donor binding is required for processive chain formation by SCF$^{\beta TrCP}$ and Ube2R1. Phosphorylated IκBα was incubated with SCF$^{\beta TrCP}$, Ube2R1 or Ube2R1^{I128E}, and ubiquitin or ubi$^{I44A/V70A}$ and analyzed by autoradiography.

Figure 6. Acceptor Ubiquitin Recognition by the Ube2S-Donor Ubiquitin Complex (A) The TEK-box in ubiquitin is required for K11-linkage formation by Ube2S. Ube2S was incubated with ubiquitin mutants, and ubi$_2$ formation (ubi~ubi) was monitored by Coomassie staining. **(B)** TEK-box mutants in ubiquitin inhibit chain formation on Ub-L-cycA by Ube2S and APC/C, as analyzed by autoradiography. **(C)** The TEK-box is required on acceptor ubiquitin. ubi$^{\Delta GG}$ mutants (purple) were incubated with ubiquitin (blue) and Ube2S and analyzed by Silver staining. **(D)** The TEK-box is not required in donor ubiquitin. TEK-box mutants of ubiquitin were mixed with WT-ubi$^{\Delta GG}$ and Ube2S, and reactions were analyzed by Coomassie staining. **(E)** HADDOCK-based model of the ternary complex between the UBC^{Ube2S} (yellow), donor ubiquitin (blue), and acceptor ubiquitin (pink; cluster 1, no. 1; see Table S2, bottom). **(F)** Surface representation of the Ube2S-binding interface on acceptor ubiquitin. Contact residues within a radius of 4 Å are shown in pink. **(G)** Surface representation of the acceptor-binding interface on the Ube2S-donor complex. **(H)** Acceptor binding is required for Ube2S activity. Ube2S mutants

were incubated with ubiquitin and analyzed by Coomassie staining. **(I)** Ube2S residues at the acceptor interface are required for chain elongation by APC/C. The modification of Ub-L-cycA by APC/C and Ube2S mutants was analyzed by autoradiography. **(J)** Ube2S residues at the acceptor-binding interface are required in vivo. HeLa cell lines expressing $Ube2S^{E131K}$ and $Ube2S^{R135E}$ were treated with siRNAs to deplete endogenous Ube2S, arrested in prometaphase (t = 0 hr) or allowed to exit mitosis (t = 2 hr), and tested for K11-linked chains by αK11-western.

Figure 7. Substrate-Assisted Catalysis Contributes to the K11-Linkage Specificity of Ube2S **(A)** Charge-swap analysis of the ionic contact between acceptor Lys6 and Glu131 of Ube2S. Ube2S or $Ube2S^{E131K}$ was mixed with $ubi^{\Delta GG}$ or $ubi^{\Delta GG/K6E}$ and reactions were analyzed by Silver staining. **(B)** $Ube2S^{E51K/E131K}$ rescues mutation of Lys6 in both acceptor and donor ubiquitin. Lys6 was mutated in acceptor $ubi^{\Delta GG}$ (purple) or donor ubiquitin (blue), and $ubi^{\Delta GG}$-ubi formation by Ube2S or $Ube2S^{E51K/E131K}$ was analyzed by Silver staining. **(C)** Ube2S (left) and Ubc9 (PDB ID: 2GRN; right) show similar active site constellations. The highest scoring Ube2S model of the HADDOCK run in the absence of ambiguous restraints is shown (Table S2, top; cluster 1, no 1). **(D)** Candidate active-site residues are required for the activity of Ube2S to catalyze ubi_2 formation (ubi~ubi), as analyzed by Coomassie staining. **(E)** Active-site residues in Ube2S are required for chain elongation by APC/C. Ub-L-cycA was incubated with APC/C^{Cdh1} and Ube2S mutants and analyzed by autoradiography. **(F)** Leu129 is required for Ube2S activity in vivo. HeLa cell lines expressing Ube2S or $Ube2S^{L129}$ were tested for formation of K11-linked chains after endogenous Ube2S was depleted by siRNAs. K11-chain formation in cells arrested in prometaphase or exiting mitosis was monitored by αK11-western. **(G)** Glu34 of acceptor ubiquitin is required for K11-linkage formation. Ubiquitin mutants were incubated with Ube2S and analyzed by Coomassie staining. **(H)** Glu34 of acceptor ubiquitin is required for chain elongation by APC/C and Ube2S. The modification of Ub-L-cycA by APC/C, Ube2S, and ubiquitin mutants was analyzed by autoradiography. **(I)** ubi^{E34Q} displays catalytic, but not binding defects. The rates of ubi_2 formation at different concentrations of ubiquitin and ubi^{E34Q} at the indicated pH were determined from two or three independent time courses. Apparent kinetic constants were obtained by fitting the rate constants to a Michaelis-Menten equation. **(J)** Rescue of ubi^{E34Q}, but not other TEK-box or hydrophobic patch mutants, by increasing the reaction pH. Ubiquitin or indicated mutants were incubated with Ube2S at pH 7.5 (left) or pH 9 (right) and analyzed by Coomassie staining.

Figure S1. Characterization of Ube2S and Its Interaction with Donor Ubiquitin, Related to Figure 1 **(A)** The UBC domain of Ube2S (UBC^{Ube2S}) promotes formation of K11 linkages between ubiquitin molecules. UBC^{Ube2S} or Ube2S were incubated with E1, ubiquitin or ubi^{K11R}, and ATP for the indicated times. Reaction products were analyzed by SDS-PAGE and Coomassie staining. **(B)** Radius of gyration, R_g, of Ube2S and UBC^{Ube2S} at various protein concentrations, as derived from Guinier analysis in PRIMUS (Konarev et al., 2003). Analysis with the indirect transform package GNOM (Svergun et al., 1988) yielded similar R_g values (data not shown). For both proteins, R_g does not change significantly with increasing protein concentration, consistent with a lack of oligomerization. The R_g–values of ~17 and 28 Å correlate well with the hydrodynamic radius/molecular mass of the monomeric states of UBC^{Ube2S} and Ube2S, respectively, as derived by gel filtration and multi-angle light scattering (data not shown). **(C)** Comparison of experimental and simulated scattering curves generated with CRYSOL (Svergun et al., 1995) based on a UBC^{Ube2S} monomer (PDB ID: 1ZDN, chain A)

and a crystallographic dimer (PDB ID: 1ZDN, both chains). I(q) is plotted as a function of the momentum transfer $q = (4\pi^*\sin(\Theta))/\lambda)$, where 2Θ is the scattering angle and λ is the wavelength of the incident x-ray beam. **(D)** The hydrophobic patch of ubiquitin is required for Ube2S- and APC/C-dependent chain formation over a wide range of ubiquitin concentrations. Ub-L-cycA was produced by IVT/T and incubated with APC/C^{Cdh1}, Ube2S, E1, ATP, and the indicated concentrations of either WT-ubiquitin or ubi^{I44A}. The formation of K11-linked ubiquitin chains on Ub-L-cycA was monitored by SDS-PAGE and autoradiography. As a comparison, the concentration of ubiquitin in HeLa cells has been estimated at 90 μM (Ryu et al., 2006). **(E)** The hydrophobic patch in ubiquitin is required for APC/C-dependent ubiquitin chain elongation. ^{35}S-labeled APC/C substrate cyclin A was incubated with APC/C^{Cdh1}, E1, low concentrations of Ube2C (for chain initiation) and Ube2S (for chain elongation). Reaction products were separated by SDS-PAGE and analyzed by autoradiography. Due to the presence of Ube2S, the majority of modified cyclin A is decorated with long ubiquitin chains. **(F)** The hydrophobic patch of ubiquitin is not required for charging of Ube2S by the E1. Ube2S was incubated with E1 and ubiquitin or the indicated ubiquitin mutants in the absence of reducing agents. When indicated, β-mercaptoethanol was added to gel-loading buffer to reduce thioester linkages. Charging of Ube2S with ubiquitin results in a βME-sensitive conjugate representing the thioester (Ube2S-Cys95~ubi) and in a βME-insensitive conjugate, most likely a covalent modification of a lysine residue in the UBC domain of Ube2S (Ube2S-ubi). **(G)** A functional hydrophobic patch is not required in the acceptor ubiquitin. The L8A and I44A/V70A-mutations were introduced into the acceptor $ubi^{\Delta GG}$. $ubi^{\Delta GG}$ and indicated mutants were mixed with ubiquitin, E1, ATP, and Ube2S, and the formation of $ubi^{\Delta GG}$-ubi and ubi-ubi dimers was monitored by SDS-PAGE and Silver staining.

Figure S2. Characterization of Donor Ubiquitin Binding to Ube2S, Related to Figure 2 (A) Ubiquitin causes similar chemical shift perturbations on UBC^{Ube2S} regardless of whether it is added in *trans* or is covalently linked to the active site. To obtain a more stable oxy-ester complex, the C95S mutant of UBC^{Ube2S} was used instead of WT. Weighted combined chemical shift perturbations, $\Delta\delta(^1H^{15}N)$, are plotted over the residue number. ^{1}H-^{15}N HSQC spectra were recorded of 22 μM ^{15}N-enriched UBC^{Ube2S} C95S ester-linked to unlabeled ubiquitin (yellow) and 140 μM ^{15}N-enriched UBC^{Ube2S} C95S in the presence of an 11-fold molar excess of unlabeled ubiquitin (red) and were referenced to the spectrum of 140 μM ^{15}N-enriched UBC^{Ube2S} C95S in the absence of ubiquitin. Gaps are due to proline residues or missing assignments. (B) Residues with significant binding-induced chemical shift perturbations and significant surface accessibility (see Table S1) are mapped onto the surface of UBC^{Ube2S} (PDB ID: 1ZDN) and ubiquitin (PDB ID: 1UBQ), respectively. **(C)** Mutations in the UBC^{Ube2S}-donor ubiquitin interface interfere with the interaction detected by NMR. Weighted combined chemical shift perturbations, $\Delta\delta(^1H^{15}N)$, are plotted over residue number. The data are based on ^{1}H-^{15}N HSQC spectra of mixtures of 200 μM ^{15}N-enriched ubiquitin and a 6-fold molar excess of UBC^{Ube2S}. Gaps are due to proline residues or missing assignments. As justified under Materials and Methods, we interpret the amplitude of $\Delta\delta(^1H^{15}N)$ as a measure of binding affinity. **(D)** Determination of the dissociation constants, K_D, for the interaction between Ube2S and ubiquitin in solution. NMR-derived isotherms for the binding of ubiquitin to Ube2S (left panel) and UBC^{Ube2S} (right panel) were fitted globally to a single-site model. Only those resonances were included that show a weighted combined chemical shift perturbation, $\Delta\delta(^1H^{15}N)$, of at least 0.05 ppm at the highest excess of ubiquitin used. The concentration of Ube2S and UBC^{Ube2S} was 240 μM. **(E)** Mutations in the

noncovalent donor ubiquitin binding interface of Ube2S do not inhibit charging of Ube2S by E1. Ube2S or indicated mutants were incubated with ubiquitin E1 and ATP, resulting in formation of a βME-sensitive thioester (Ube2S-Cys95~ubi) and a βME-insensitive conjugate (Ube2S-ubi). Reactions were analyzed by αUbe2S-western. **(F)** Mutations of Ube2S do not interfere with binding of Ube2S to the APC/C. APC/C subunits were synthesized by in vitro-transcription/translation. The radiolabeled proteins are incorporated into full APC/C present in reticulocyte lysate (our unpublished observations). The ^{35}S-labeled proteins were then incubated with ^{MBP}Ube2S, which was immobilized on amylose-resin; MBP was used as a control. After extensive washing, binding reactions were analyzed by SDS-PAGE and Coomassie staining (for inputs; bottom panel) or autoradiography (for binding; top panel).

Figure S3. Characterization of the NMR-Based Model of the Ube2S-Donor Ubiquitin Interface, Related to Figure 3 **(A)** Comparison of docked models generated by two different programs, HADDOCK, including NMR-based restraints (blue/yellow), and ClusPro without any restraints (green). Major differences are only seen for the C-terminal tail of ubiquitin, which is highlighted red in the ClusPro model. The chosen ClusPro model represents 9 out of 965 models generated, 38 of which have the S^{γ} atom of Cys95 of Ube2S within a distance of 7.5 Å from the C-terminal carbon atom of donor ubqiutin. **(B)** Surface electrostatic potentials of the donor interface, as calculated using APBS (Baker et al., 2001; Dolinsky et al., 2007; Dolinsky et al., 2004). Intermolecular salt bridges, as predicted by the PISA server at the European Bioinformatics Institute (http://www.ebi.ac.uk/msd-srv/prot_int/pistart.html) (Krissinel and Henrick, 2007), are illustrated by solid lines. **(C)** Illustration of the ionic contact between Arg74 of donor ubiquitin and Asp102 on Ube2S, as seen in our model of the Ube2S-donor ubiquitin complex. **(D)** Residues in ubiquitin that are at the Ube2S-donor ubiquitin interface are not required on the acceptor ubiquitin. Mutations were introduced into the acceptor ubi$^{\Delta GG}$. ubi$^{\Delta GG}$ and indicated mutants were incubated with E1, Ube2S, ubiquitin, and ATP, and formation of ubi$^{\Delta GG}$-ubi and ubi-ubi dimers was monitored by SDS-PAGE and Silver staining. Except for Lys6, no residue was required in the acceptor ubiquitin. **(E)** Lys6 is required in the donor ubiquitin. Ubiquitin and the respective mutants K6A and K6E were incubated with the acceptor ubi$^{\Delta GG}$, E1, Ube2S, and ATP. Reaction products were analyzed by SDS-PAGE and Coomassie staining. Mutation of Lys6 to Glu affects both acceptor and donor ubiquitin, and thus, neither ubi$^{\Delta GG}$-ubi nor ubi-ubi dimers are formed. Mutation of Lys6 to Ala only affects acceptor ubiquitin function, and thus, ubi$^{\Delta GG}$-ubi dimers are formed with this mutant. Both ubi^{K6E} and ubi^{K6A} showed higher mobility in SDS-PAGE compared to WT-ubiquitin. **(F)** With exception of Arg72, all ubiquitin residues at the Ube2S-donor ubiquitin interface can be mutated without affecting Ube2S-charging by E1. Ube2S was incubated with ubiquitin or indicated mutants, E1, and ATP, resulting in formation of a βME-sensitive thioester (Ube2S-Cys95~ubi) and a βME-insensitive conjugate (Ube2S-ubi). Reaction products were analyzed by SDS-PAGE and αUbe2S-western. **(G)** Ube2S-residues at the binding interface with donor ubiquitin are not required for charging of Ube2S by E1. Ube2S and indicated mutants were incubated with E1, ubiquitin, and ATP. Reaction products were analyzed by SDS-PAGE and αUbe2S-western. **(H)** The E51K mutant of Ube2S does not rescue defective ubiquitin dimer formation in the presence of the I44A-mutation on ubiquitin. Ubiquitin or ubi^{I44A} were incubated with acceptor ubi$^{\Delta GG}$, Ube2S or Ube2S^{E51K}, E1, and ATP. Reaction products were analyzed by SDS-PAGE and Silver staining.

Figure S4. Characterization of Donor Ubiquitin Recognition by Ube2R1 and Ube2G2, Related to Figure 5 (A) The hydrophobic patch of ubiquitin is required for ubiquitin-dimer formation by the K48-specific E2s Ube2G2 (top panel) and Ube2R1 (bottom panel). Ubiquitin and indicated mutants were incubated with Ube2R1 or Ube2G2/gp78, E1, and ATP. Reaction products were separated by SDS-PAGE and analyzed by Coomassie staining. **(B)** The hydrophobic patch of ubiquitin is not required for charging of Ube2G2 (top panel) or Ube2R1 (bottom panel) by E1. Ubiquitin and indicated mutants were incubated with E1, ATP, and Ube2G2 or Ube2R1 in the absence of reducing agents. Where indicated, βME was added to gel loading buffer to show thioester formation. Reaction products were monitored by αHis-western, detecting a His-epitope used to purify the E2 proteins. **(C)** The same surface used by Ube2S for donor ubiquitin-binding is required on Ube2R1 for E2 activity. Ube2R1 or indicated mutants were incubated with E1, ubiquitin, and ATP. Formation of K48-linked ubiquitin dimers (ubi~ubi) was monitored by SDS-PAGE and Coomassie staining. **(D)** Ube2R1 residues at the donor ubiquitin binding interface are not required for charging of Ube2R1 by the E1. Ube2R1 or indicated mutants were incubated with E1, ATP, and ubiquitin, and analyzed for charging as described above.

Figure S5. HADDOCK Output for the Docking of Acceptor Ubiquitin onto the UBC^{Ube2S}-Donor Ubiquitin Complex, Related to Figure 6 Cartoon representation of the top-scoring models of the two clusters of run 1 without experimental restraints (see Table S2).

Figure S6. Characterization of Acceptor Ubiquitin Recognition by the Ube2S-Donor Ubiquitin Complex, Related to Figure 6 (A) The TEK-box of ubiquitin is required for APC/C-dependent chain formation catalyzed by the E2s Ube2C and Ube2S. Ubiquitin or indicated mutants were incubated with ^{35}S-labeled cyclin A, APC/C^{Cdh1}, Ube2C, Ube2S, E1, and ATP. Reaction products were separated by SDS-PAGE and analyzed by autoradiography. **(B)** The TEK-box residues of ubiquitin are not required for charging of Ube2S by E1. Ubiquitin or indicated mutants were incubated with E1, Ube2S, and ATP, and analyzed for charging as described above. **(C)** Mutations in the Ube2S-acceptor ubiquitin interface do not influence the interaction between Ube2S and donor ubiquitin, as detected by NMR. Weighted combined chemical shift perturbations, $\Delta\delta(^{1}H^{15}N)$, are plotted over residue number. The data are based ^{1}H-^{15}N HSQC spectra of mixtures of 200 μM ^{15}N-enriched ubiquitin and a 6-fold molar excess of UBC^{Ube2S}. Gaps are due to proline residues or missing assignments. **(D)** Surface electrostatic potentials of the acceptor interface for the selected HADDOCK complex between Ube2S, donor, and acceptor ubiquitin (cluster 1, no. 1; Table S2, bottom), as calculated using APBS (Baker et al., 2001; Dolinsky et al., 2007; Dolinsky et al., 2004). Intermolecular salt bridges and hydrogen bonds, as predicted by the PISA server are illustrated by solid and dashed lines, respectively. **(E)** Ube2S residues at the acceptor binding interface are required for APC/C-dependent ubiquitin chain formation. Ube2S or indicated mutants were incubated with ^{35}S-labeled cyclin A, APC/C^{Cdh1}, E1, Ube2C, and ubiquitin, and reaction products were analyzed by SDS-PAGE and autoradiography. **(F)** Ube2S residues at the acceptor binding interface are not required for charging of Ube2S by E1. Ube2S or indicated mutants were incubated with E1, ATP, and ubiquitin, and analyzed for charging as described above.

Figure S7. Characterization of Acceptor Ubiquitin Recognition by Ube2S, Related to Figure 7 (A) The E131A mutant of Ube2S rescues the phenotype of the K6E mutation in

acceptor ubiquitin. ubi$^{\Delta GG}$ or ubi$^{\Delta GG/K6E}$ were incubated with ubiquitin, E1, ATP, and Ube2S or indicated Ube2S mutants. Formation of ubi$^{\Delta GG}$-ubi and ubi-ubi dimers was analyzed by SDS-PAGE and Coomassie staining. In contrast to Ube2S^{E131K}, Ube2S^{E131A} does not interfere with recognition of Lys6 in WT-ubiquitin, explaining the formation of ubi-ubi dimers in the presence of Ube2S^{E131A}, but not Ube2S^{E131K}. **(B)** Specific rescue of the K6E-mutation in acceptor ubiquitin by Ube2S^{E131K}, but not other mutants at the acceptor ubiquitin-binding interface. Ube2S or indicated mutants were incubated with E1, ATP, ubi$^{\Delta GG}$ or ubi$^{\Delta GG/K6E}$, and ubiquitin. Formation of ubi$^{\Delta GG}$-ubi and ubi-ubi dimers was analyzed by SDS-PAGE and Coomassie staining. **(C)** Complete rescue of the ubi^{K6E}-phenotype by Ube2S$^{E51K/E131K}$. Ubiquitin or ubi^{K6E} were incubated with Ube2S or Ube2S$^{E51K/E131K}$, E1, and ATP, and formation of ubiquitin dimers was monitored by SDS-PAGE and Silver staining. **(D)** Validation of the Ube2S-acceptor ubiquitin interaction by charge-swap analysis between Glu64 of ubiquitin and Arg135 of Ube2S. The indicated mutants of ubiquitin and Ube2S were tested for their ability to produce ubiquitin dimers (ubi~ubi). Reaction products were analyzed by SDS-PAGE and Coomassie staining. **(E)** Specific rescue of the deleterious effects of a R135E mutant of Ube2S by a E64K mutant of ubiquitin. Ube2S or Ube2S^{R135E} were incubated with ubiquitin or indicated TEK-box mutants, and formation of ubiquitin dimers (ubi~ubi) was monitored by SDS-PAGE and Coomassie staining. **(F)** Rescue of impaired ubiquitin dimer formation by a K63E mutant of ubiquitin by Ube2S^{E139K}. Ube2S or Ube2S^{E139K} were incubated with ubiquitin or ubi^{K63E}, E1, and ATP, and formation of ubiquitin dimers was analyzed by SDS-PAGE and Coomassie staining. **(G)** Ube2S residues required for ubiquitin-linkage formation are not required for charging of Ube2S by the E1. Ube2S or indicated mutants were incubated with E1, ATP, and ubiquitin, and analyzed for charging as described above. **(H)** Reduced substrate-specificity of Ube2S at higher pH. A peptide of 26 C-terminal residues of Ube2S tagged with biotin (^{B}CTP) was incubated with Ube2S, E1, ATP, and ubiquitin at either pH 7.5 or at pH 9. Modification of lysine residues in ^{B}CTP was detected by western blotting using HRP-coupled streptavidin. **(I)** Increasing the pH allows Ube2S to modify ubiquitin lysine residues other than K11. The indicated single lysine ubiquitin mutants were incubated with Ube2S, E1, and ATP at either pH 7.5 or pH 9. Formation of ubiquitin dimers (ubi~ubi) was detected by western blotting using an α-ubiquitin antibody. **(J)** Increasing the pH does not completely obliterate the K11-specificity of Ube2S. Ubiquitin or the indicated mutants were incubated with Ube2S, E1, and ATP at pH 9. The formation of ubiquitin dimers (ubi~ubi) was monitored by SDS-PAGE and Silver staining.

Figure S8. HADDOCK Analysis of Ube2S-Donor-Acceptor Complexes Exposing Each of the Seven Lysine Residues of the Acceptor Ubiquitin to the Active Site of Ube2S, Related to Figure 7 Details of the active site are shown for the top-scoring model of each of seven HADDOCK runs in *stereo* representation with relevant side chains rendered as ball-and-stick. Only the C-terminal tail (residues 71–76) of donor ubiquitin is displayed (blue). Ribbons for acceptor ubiquitin and Ube2S are shown in pink and gray, respectively. While structures docked around K11 show a favorable active site constellation (see Figure 7C), complexes exposing other lysine residues have features incompatible with efficient catalysis. In the following we describe these features for the top representatives of the most populated clusters for each of seven HADDOCK runs; note, however, that these conclusions also hold for the lower-ranked clusters. Around K6 and K48 no acidic groups are found on the acceptor within a radius of ~8 Å and ~10 Å, respectively. K33 is neighbored by an acidic residue, E34; in this case, however, the acidic side chain points away from the active site, which puts K33 in an unfavorable orientation

for the nucleophilic attack. Structures docked around K27 display productive active site geometry including a proximal acidic residue, D52. However, these complexes contain an additional acidic residue, D39, near the active site cysteine of Ube2S, which might interfere with catalysis by destabilizing the thiolate intermediate formed during the nucleophilic substitution reaction. Complexes docked around K29 contain D21 of the acceptor ubiquitin in a distance of ~5 Å from K29, but their overall geometry appears sterically unfavorable. K63 can be docked in a reasonable orientation, but the position of the neighboring acidic side chain, E64, appears less optimal than in the case of K11.

Figure 1

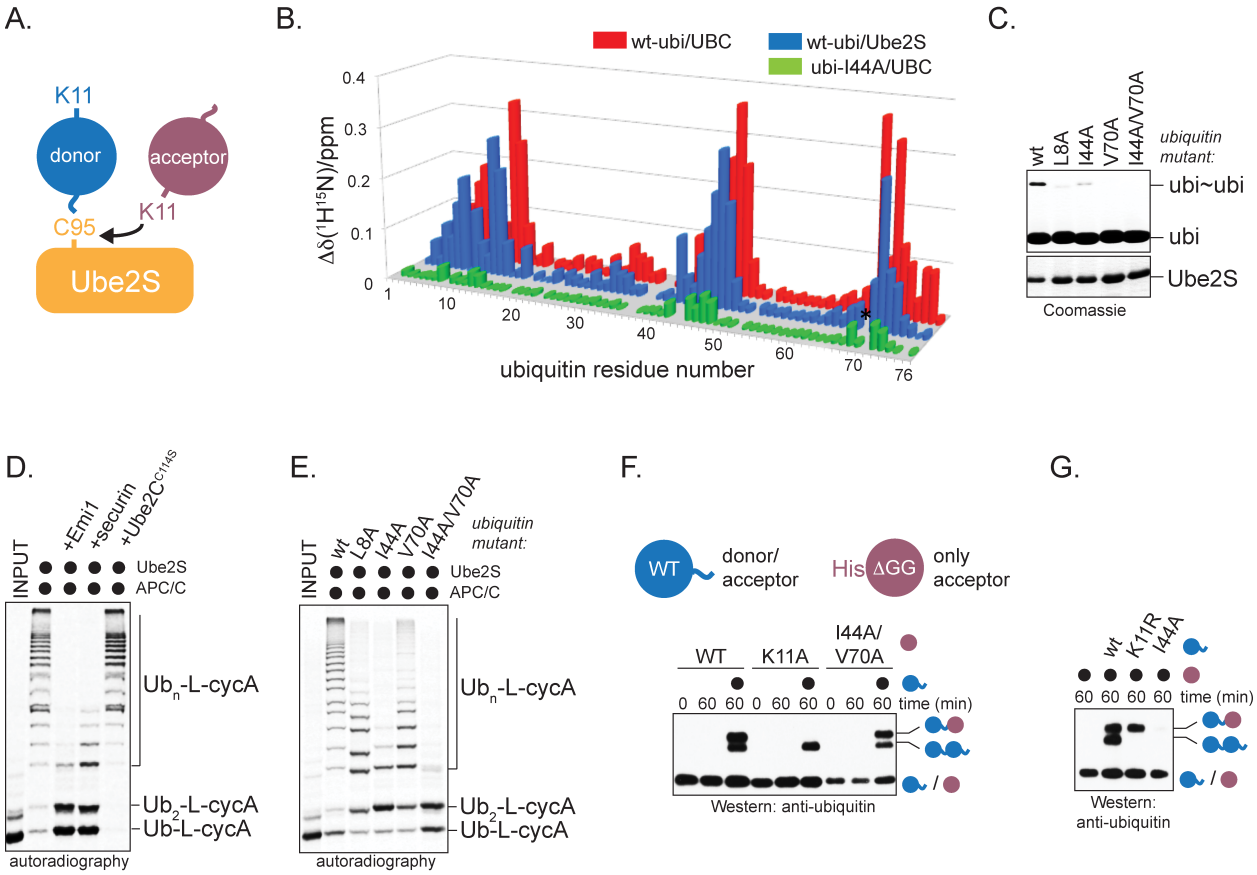
A.
K11
donor
acceptor
K11
C95
Ube2S
B.
wt-ubi/UBC
wt-ubi/Ube2S
ubi-I44A/UBC
Δδ(¹H¹⁵N)/ppm
0.4
0.3
0.2
0.1
0
1
10
20
30
40
50
60
70
76
ubiquitin residue number
C.
wt
L8A
I44A
V70A
I44A/V70A
ubiquitin mutant:
ubi~ubi
ubi
Ube2S
Coomassie
D.
INPUT
+Emi1
+securin
+Ube2C^C114S
Ube2S
APC/C
Ub_n-L-cycA
Ub_2-L-cycA
Ub-L-cycA
autoradiography
E.
INPUT
wt
L8A
I44A
V70A
I44A/V70A
ubiquitin mutant:
Ube2S
APC/C
Ub_n-L-cycA
Ub_2-L-cycA
Ub-L-cycA
autoradiography
F.
WT
donor/ acceptor
His ΔGG
only acceptor
WT
K11A
I44A/ V70A
0 60 60 0 60 60 0 60 60 time (min)
Western: anti-ubiquitin
G.
wt
K11R
I44A
60 60 60 60 time (min)
Western: anti-ubiquitin

Figure 2

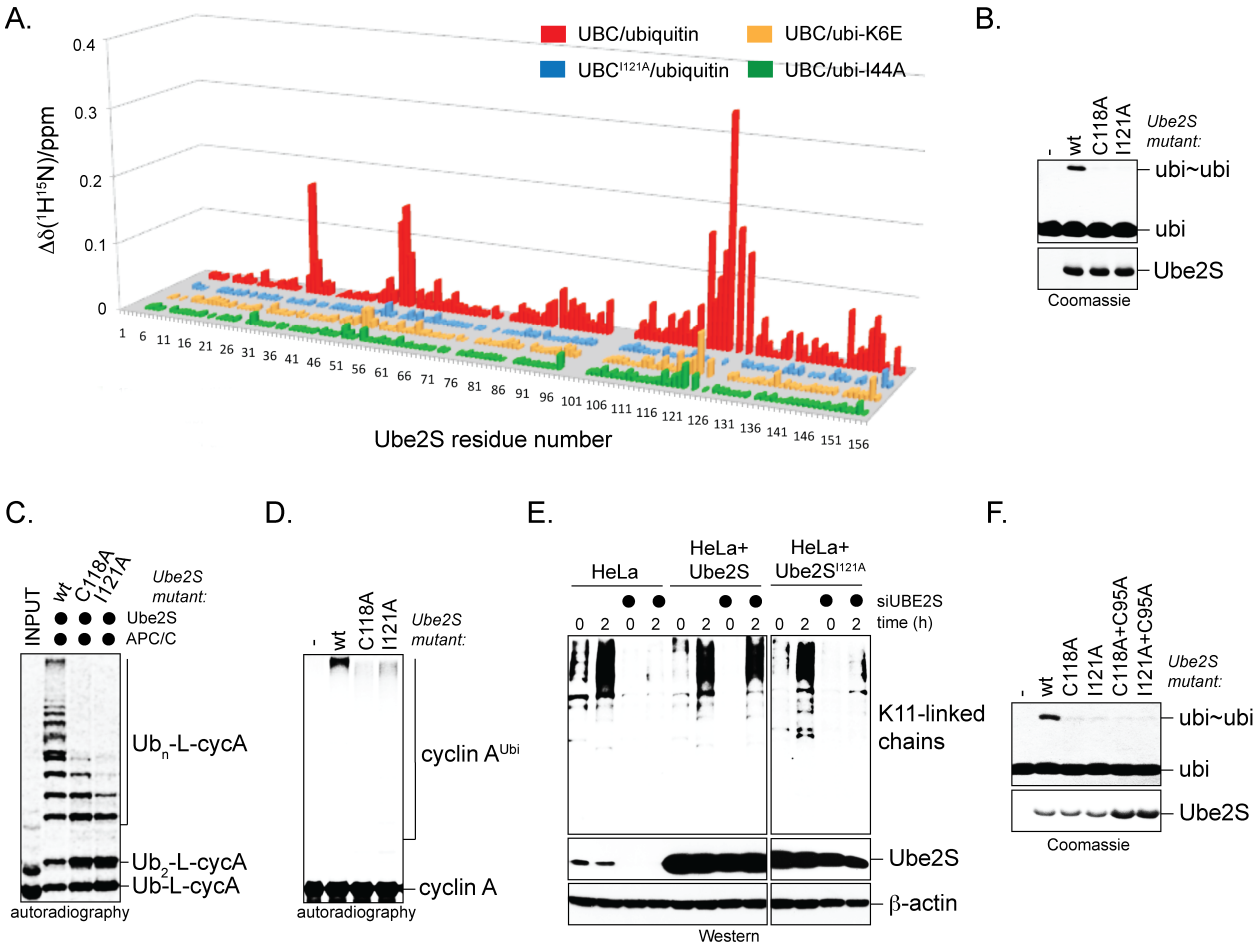
A.
UBC/ubiquitin
UBC/ubi-K6E
UBC^I121A/ubiquitin
UBC/ubi-I44A
Δδ(¹H¹⁵N)/ppm
Ube2S residue number
B.
Ube2S mutant:
wt
C118A
I121A
ubi~ubi
ubi
Ube2S
Coomassie
C.
INPUT
Ube2S mutant:
Ube2S
APC/C
Ub_n-L-cycA
Ub_2-L-cycA
Ub-L-cycA
autoradiography
D.
Ube2S mutant:
cyclin A^Ubi
cyclin A
autoradiography
E.
HeLa
HeLa+ Ube2S
HeLa+ Ube2S^I121A
siUBE2S
time (h)
K11-linked chains
Ube2S
β-actin
Western
F.
Ube2S mutant:
C118A+C95A
I121A+C95A
ubi~ubi
ubi
Ube2S
Coomassie

Figure 3

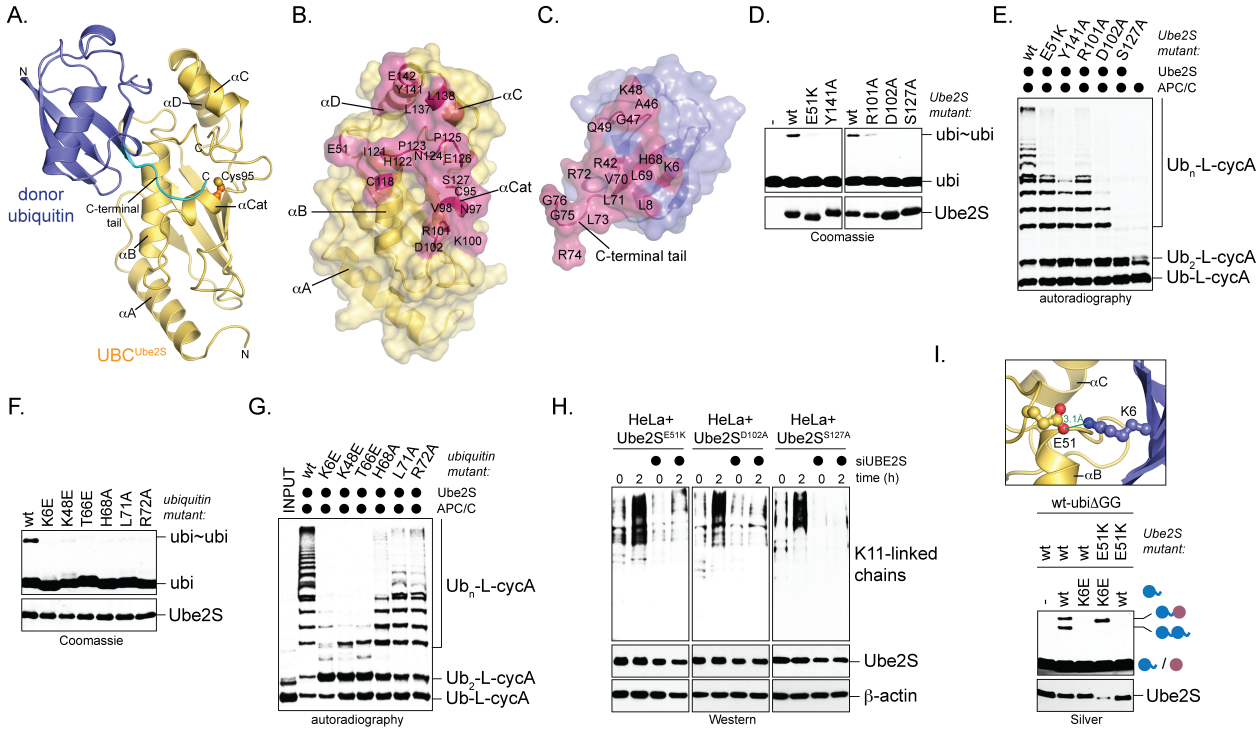
A.
B.
C.
D.
E.
donor ubiquitin
C-terminal tail
UBC^Ube2S
αC
αD
αCat
αB
αA
Cys95
K48
A46
G47
Q49
R72
R42
H68
K6
V70
L69
G76
L71
L8
G75
L73
R74
C-terminal tail
wt
E51K
Y141A
R101A
D102A
S127A
Ube2S mutant:
ubi~ubi
ubi
Ube2S
Coomassie
Ube2S APC/C
Ub_n-L-cycA
Ub_2-L-cycA
Ub-L-cycA
autoradiography
F.
G.
H.
I.
ubiquitin mutant:
K6E
K48E
T66E
H68A
L71A
R72A
INPUT
HeLa+ Ube2S^E51K
HeLa+ Ube2S^D102A
HeLa+ Ube2S^S127A
siUBE2S
time (h)
K11-linked chains
β-actin
Western
wt-ubiΔGG
3.1Å
K6
E51
Silver

Figure 4

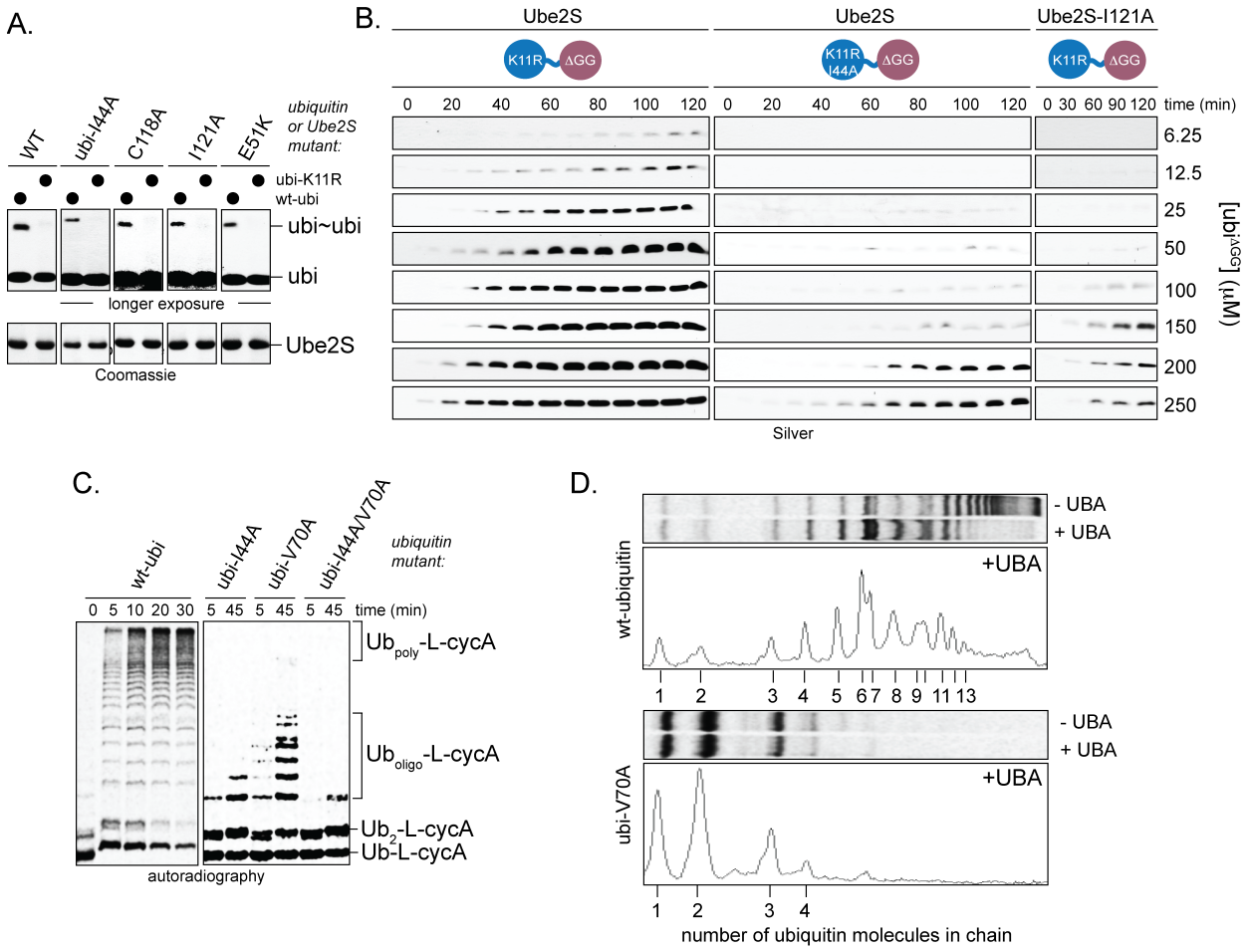
A.
WT
ubi-I44A
C118A
I121A
E51K
ubiquitin or Ube2S mutant:
ubi-K11R
wt-ubi
ubi~ubi
ubi
longer exposure
Ube2S
Coomassie
B.
Ube2S
Ube2S
Ube2S-I121A
K11R
ΔGG
K11R I44A
0 20 40 60 80 100 120
0 30 60 90 120 time (min)
6.25
12.5
25
50
100
150
200
250
[ubiΔGG] (μM)
Silver
C.
wt-ubi
ubi-I44A
ubi-V70A
ubi-I44A/V70A
ubiquitin mutant:
0 5 10 20 30
5 45 5 45 5 45 time (min)
Ub poly -L-cycA
Ub oligo -L-cycA
Ub2-L-cycA
Ub-L-cycA
autoradiography
D.
- UBA
+ UBA
wt-ubiquitin
+UBA
1 2 3 4 5 6 7 8 9 11 13
ubi-V70A
1 2 3 4
number of ubiquitin molecules in chain

Figure 5

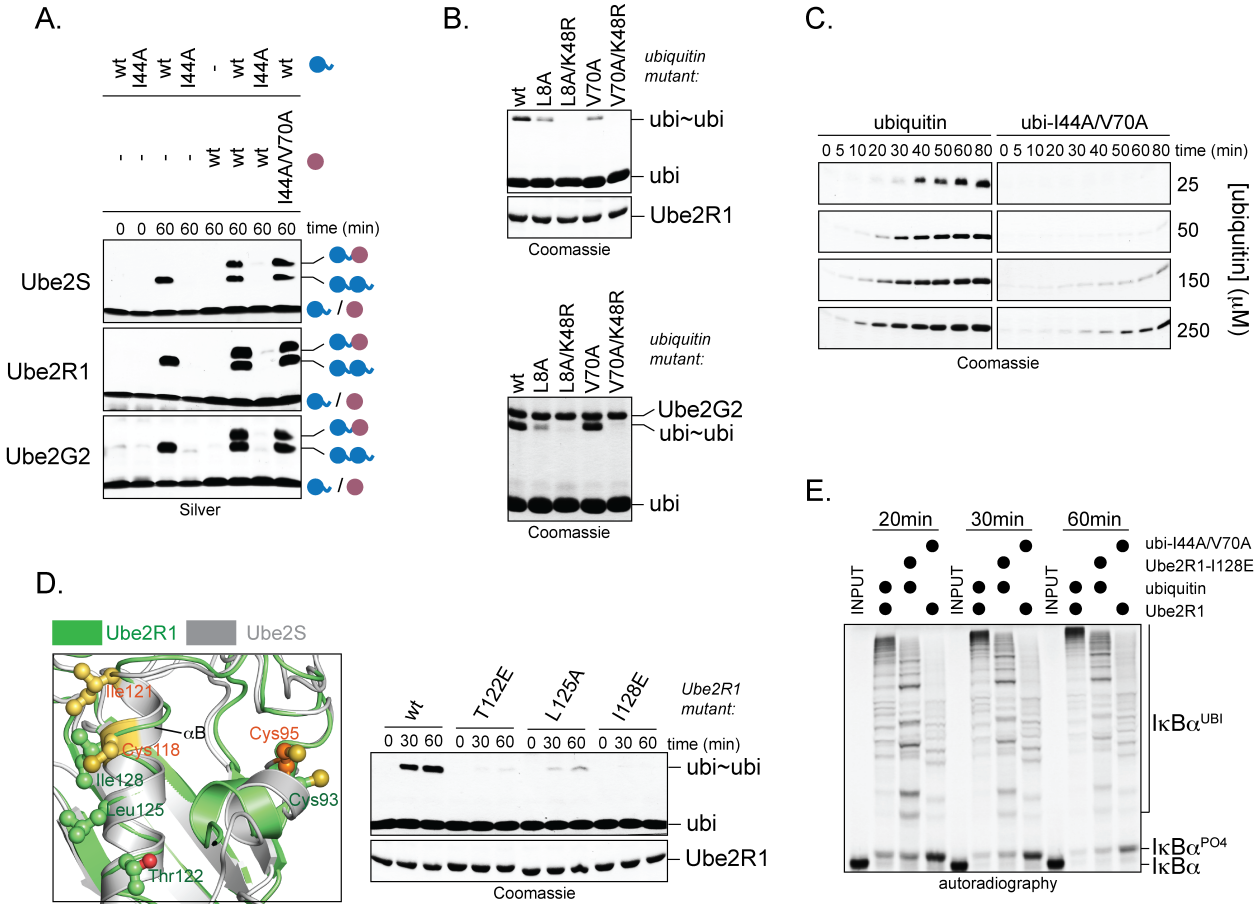
A.
wt
I44A
wt
I44A
-
wt
I44A
wt
I44A/V70A
0 0 60 60 60 60 60 60 time (min)
Ube2S
Ube2R1
Ube2G2
Silver
B.
ubiquitin mutant:
wt
L8A
L8A/K48R
V70A
V70A/K48R
ubi~ubi
ubi
Ube2R1
Coomassie
Ube2G2
ubi~ubi
ubi
C.
ubiquitin
ubi-I44A/V70A
0 5 10 20 30 40 50 60 80 0 5 10 20 30 40 50 60 80 time (min)
25
50
150
250
[ubiquitin] (μM)
Coomassie
D.
Ube2R1
Ube2S
Ile121
αB
Cys95
Cys118
Ile128
Leu125
Cys93
Thr122
Ube2R1 mutant:
wt
T122E
L125A
I128E
0 30 60 0 30 60 0 30 60 0 30 60 time (min)
ubi~ubi
ubi
Ube2R1
Coomassie
E.
20min
30min
60min
INPUT
INPUT
INPUT
ubi-I44A/V70A
Ube2R1-I128E
ubiquitin
Ube2R1
IκBα^UBI
IκBα^PO4
IκBα
autoradiography

Figure 6

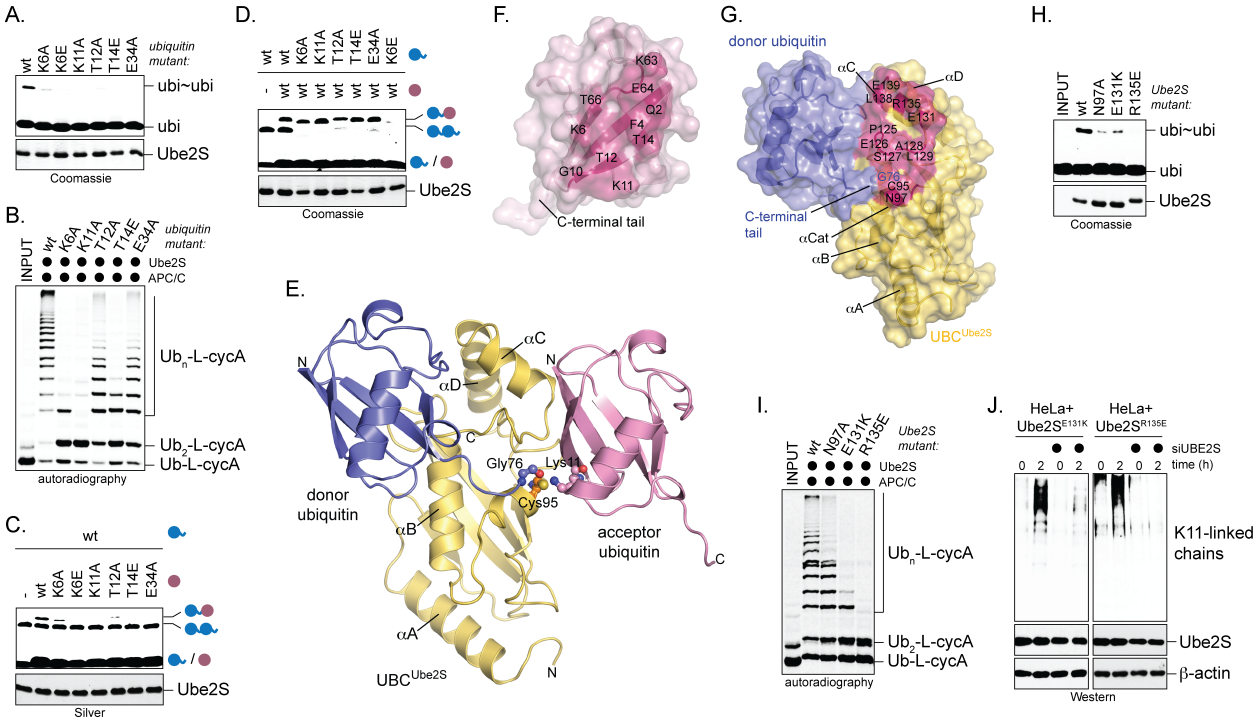
A.
ubiquitin mutant:
wt K6A K6E K11A T12A T14E E34A
ubi~ubi
ubi
Ube2S
Coomassie
B.
INPUT wt K6A K11A T12A T14E E34A
ubiquitin mutant:
Ube2S
APC/C
Ub$_n$-L-cycA
Ub$_2$-L-cycA
Ub-L-cycA
autoradiography
C.
wt
- wt K6A K6E K11A T12A T14E E34A
/
Ube2S
Silver
D.
wt wt K6A K11A T12A T14E E34A K6E
- wt wt wt wt wt wt wt
/
Ube2S
Coomassie
E.
αC
αD
N
C
Gly76
Lys11
Cys95
donor ubiquitin
acceptor ubiquitin
αB
αA
UBC^{Ube2S}
F.
K63
E64
T66
Q2
K6
F4
T14
T12
G10
K11
C-terminal tail
G.
donor ubiquitin
αC
αD
E139
L138
R135
E131
P125
E126
A128
S127
L129
C76
C95
N97
C-terminal tail
αCat
αB
αA
UBC^{Ube2S}
H.
INPUT wt N97A E131K R135E
Ube2S mutant:
ubi~ubi
ubi
Ube2S
Coomassie
I.
INPUT wt N97A E131K R135E
Ube2S mutant:
Ube2S
APC/C
Ub$_n$-L-cycA
Ub$_2$-L-cycA
Ub-L-cycA
autoradiography
J.
HeLa+ Ube2S^{E131K}
HeLa+ Ube2S^{R135E}
siUBE2S
0 2 0 2 0 2 0 2
time (h)
K11-linked chains
Ube2S
β-actin
Western

Figure 7

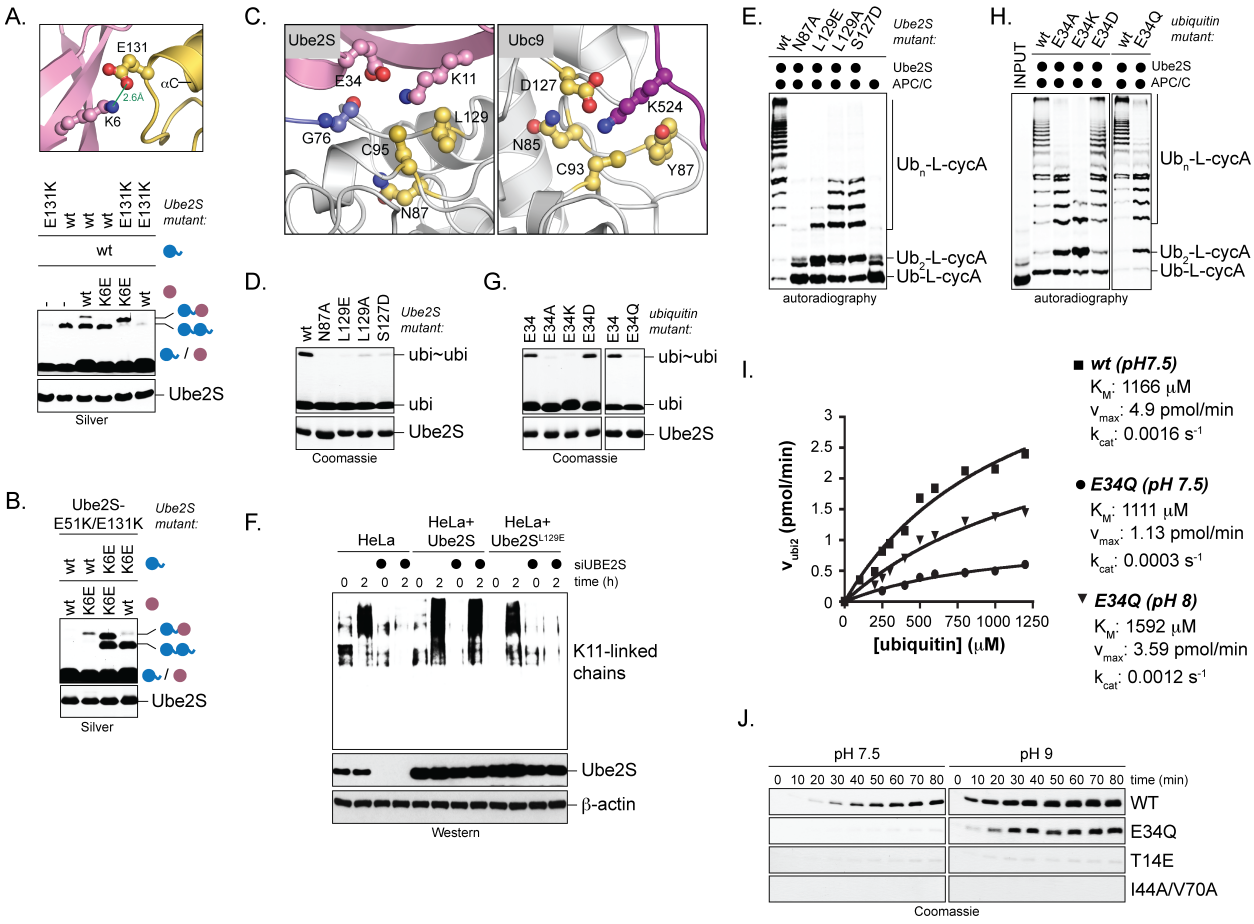
A.
E131
αC
2.6Å
K6
E131K
wt
wt
wt
E131K
E131K
Ube2S mutant:
wt
wt
wt
K6E
K6E
wt
Ube2S
Silver
B.
Ube2S-
E51K/E131K
Ube2S mutant:
wt
wt
K6E
K6E
wt
K6E
K6E
wt
Ube2S
Silver
C.
Ube2S
E34
K11
L129
G76
C95
N87
Ubc9
D127
K524
N85
C93
Y87
D.
wt
N87A
L129E
L129A
S127D
Ube2S mutant:
ubi~ubi
ubi
Ube2S
Coomassie
G.
E34
E34A
E34K
E34D
E34
E34Q
ubiquitin mutant:
ubi~ubi
ubi
Ube2S
Coomassie
F.
HeLa
HeLa+ Ube2S
HeLa+ Ube2S^L129E
siUBE2S
0 2 0 2 0 2 0 2 0 2 0 2
time (h)
K11-linked chains
Ube2S
β-actin
Western
E.
wt
N87A
L129E
L129A
S127D
Ube2S mutant:
Ube2S
APC/C
Ub_n-L-cycA
Ub_2-L-cycA
Ub-L-cycA
autoradiography
H.
INPUT
wt
E34A
E34K
E34D
wt
E34Q
ubiquitin mutant:
Ube2S
APC/C
Ub_n-L-cycA
Ub_2-L-cycA
Ub-L-cycA
autoradiography
I.
v_ubi2 (pmol/min)
3
2.5
2
1.5
1
0.5
0
0 250 500 750 1000 1250
[ubiquitin] (μM)
■ wt (pH7.5)
K_M: 1166 μM
v_max: 4.9 pmol/min
k_cat: 0.0016 s^-1
● E34Q (pH 7.5)
K_M: 1111 μM
v_max: 1.13 pmol/min
k_cat: 0.0003 s^-1
▼ E34Q (pH 8)
K_M: 1592 μM
v_max: 3.59 pmol/min
k_cat: 0.0012 s^-1
J.
pH 7.5
pH 9
0 10 20 30 40 50 60 70 80 0 10 20 30 40 50 60 70 80 time (min)
WT
E34Q
T14E
I44A/V70A
Coomassie

Figure S1

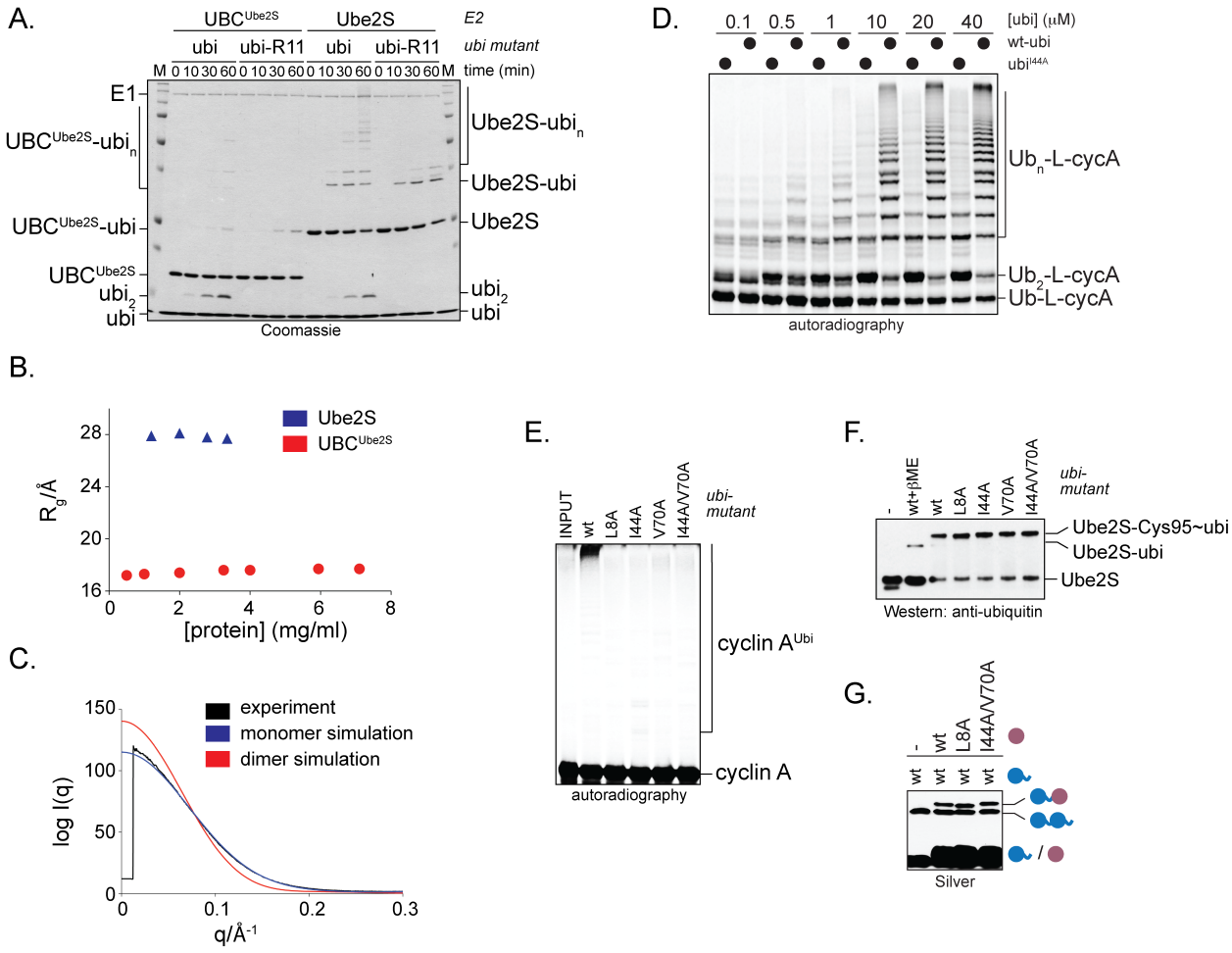
A.
UBC^Ube2S
Ube2S
E2
ubi
ubi-R11
ubi mutant
time (min)
E1
UBC^Ube2S-ubi_n
UBC^Ube2S-ubi
UBC^Ube2S
ubi_2
ubi
Ube2S-ubi_n
Ube2S-ubi
Ube2S
ubi_2
ubi
Coomassie
D.
[ubi] (μM)
wt-ubi
ubi^I44A
Ub_n-L-cycA
Ub_2-L-cycA
Ub-L-cycA
autoradiography
B.
Ube2S
UBC^Ube2S
R_g/Å
[protein] (mg/ml)
C.
experiment
monomer simulation
dimer simulation
log I(q)
q/Å^-1
E.
INPUT
wt
L8A
I44A
V70A
I44A/V70A
ubi-mutant
cyclin A^Ubi
cyclin A
autoradiography
F.
wt+βME
Ube2S-Cys95~ubi
Ube2S-ubi
Ube2S
Western: anti-ubiquitin
G.
Silver

Figure S2

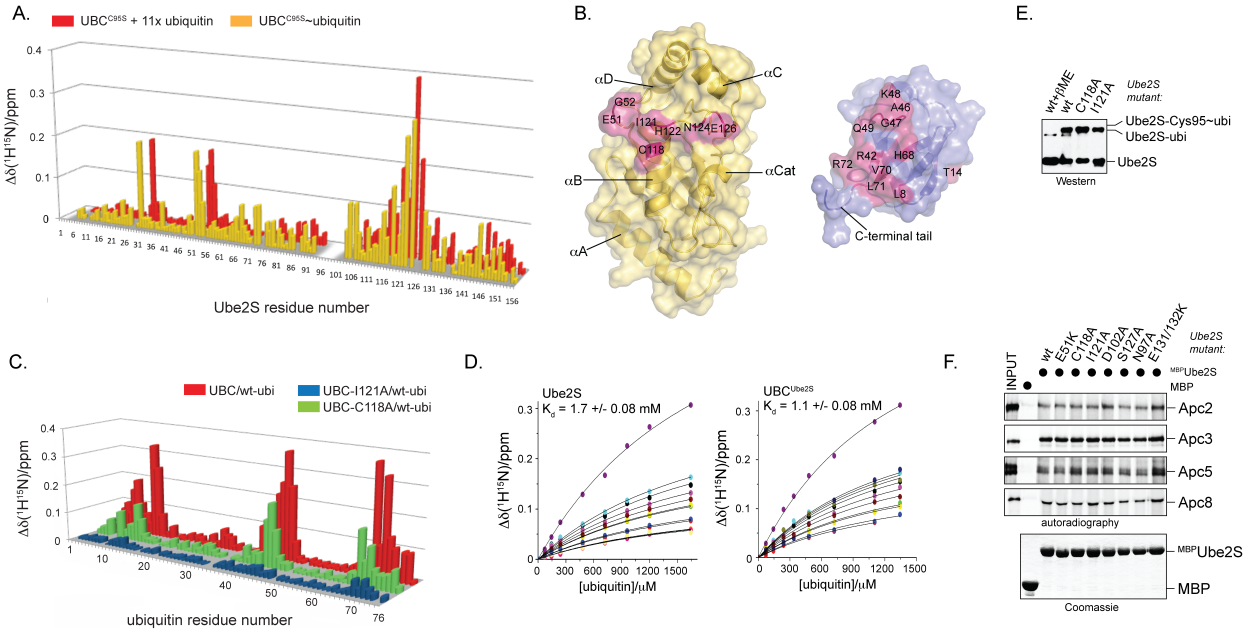
A.
UBC^C95S + 11x ubiquitin
UBC^C95S~ubiquitin
Δδ('H15N)/ppm
Ube2S residue number
B.
αD
αC
αB
αCat
αA
C-terminal tail
E.
wt+flME
wt
C118A
I121A
Ube2S mutant:
Ube2S-Cys95~ubi
Ube2S-ubi
Ube2S
Western
C.
UBC/wt-ubi
UBC-I121A/wt-ubi
UBC-C118A/wt-ubi
Δδ('H15N)/ppm
ubiquitin residue number
D.
Ube2S
Kd = 1.7 +/- 0.08 mM
UBCUbe2S
Kd = 1.1 +/- 0.08 mM
Δδ('H15N)/ppm
[ubiquitin]/μM
F.
INPUT
wt
E51K
C118A
I121A
D102A
S127A
N97A
E131/132K
Ube2S mutant:
MBPUbe2S
MBP
Apc2
Apc3
Apc5
Apc8
autoradiography
MBPUbe2S
MBP
Coomassie

Figure S3

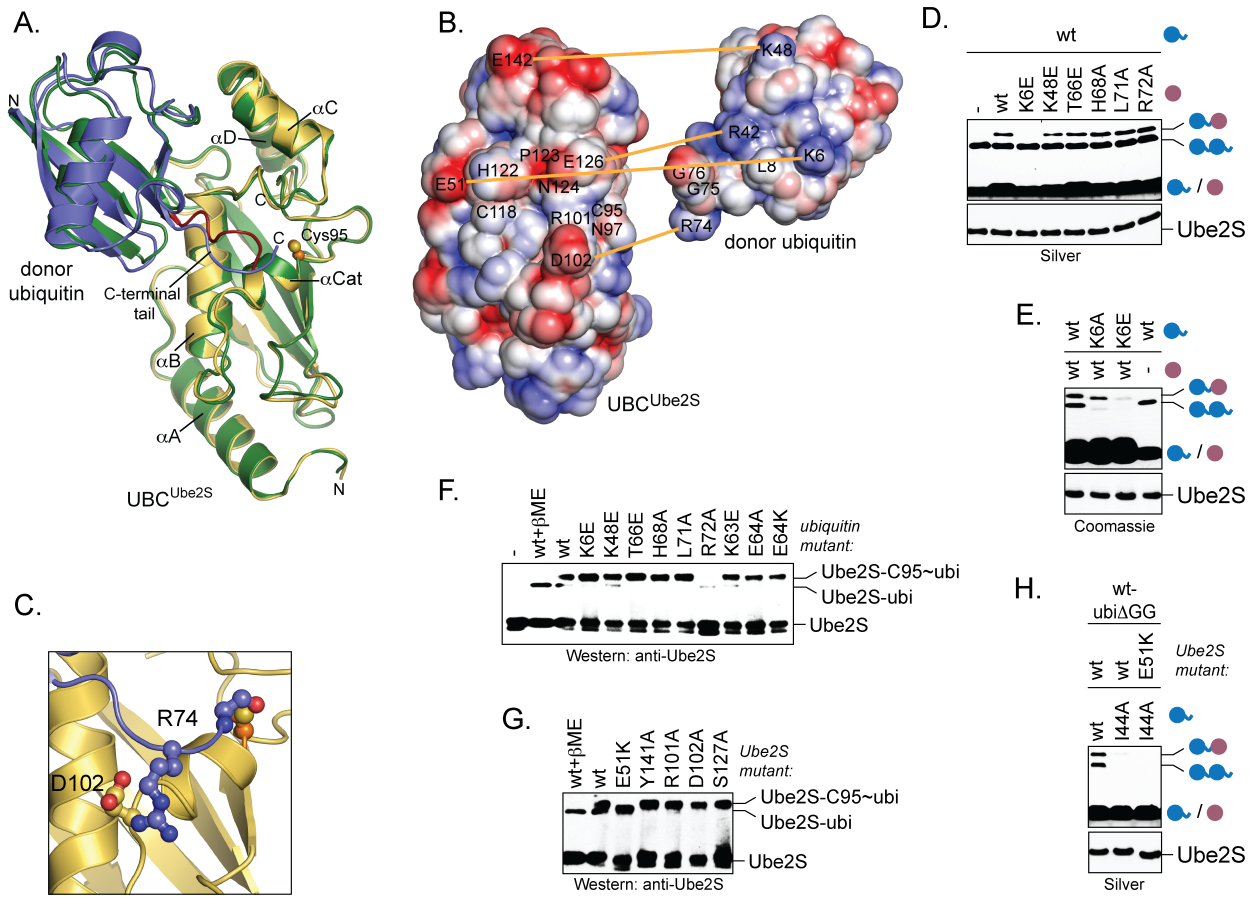
A.
N
αC
αD
C
C
Cys95
donor ubiquitin
C-terminal tail
αCat
αB
αA
UBC Ube2S
N
B.
E142
K48
R42
P123
E126
H122
K6
E51
N124
G76
G75
L8
C118
R101
C95
N97
R74
D102
donor ubiquitin
UBC Ube2S
D.
wt
-
wt
K6E
K48E
T66E
H68A
L71A
R72A
/
Ube2S
Silver
E.
wt
K6A
K6E
wt
wt
wt
wt
-
/
Ube2S
Coomassie
C.
R74
D102
F.
-
wt+βME
wt
K6E
K48E
T66E
H68A
L71A
R72A
K63E
E64A
E64K
ubiquitin mutant:
Ube2S-C95~ubi
Ube2S-ubi
Ube2S
Western: anti-Ube2S
G.
wt+βME
wt
E51K
Y141A
R101A
D102A
S127A
Ube2S mutant:
Ube2S-C95~ubi
Ube2S-ubi
Ube2S
Western: anti-Ube2S
H.
wt-ubiΔGG
wt
wt
E51K
Ube2S mutant:
wt
I44A
I44A
/
Ube2S
Silver

Figure S4

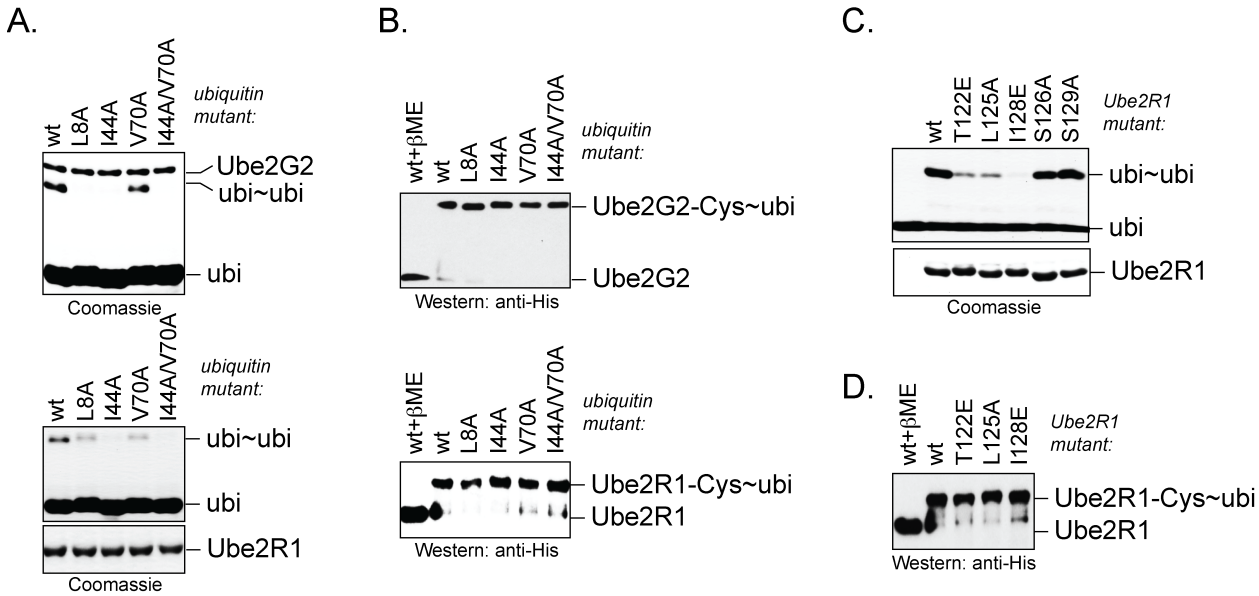
A.
wt
L8A
I44A
V70A
I44A/V70A
ubiquitin mutant:
Ube2G2
ubi~ubi
ubi
Coomassie
ubi~ubi
ubi
Ube2R1
Coomassie
B.
wt+βME
wt
L8A
I44A
V70A
I44A/V70A
ubiquitin mutant:
Ube2G2-Cys~ubi
Ube2G2
Western: anti-His
Ube2R1-Cys~ubi
Ube2R1
Western: anti-His
C.
wt
T122E
L125A
I128E
S126A
S129A
Ube2R1 mutant:
ubi~ubi
ubi
Ube2R1
Coomassie
D.
wt+βME
wt
T122E
L125A
I128E
Ube2R1 mutant:
Ube2R1-Cys~ubi
Ube2R1
Western: anti-His

Figure S5

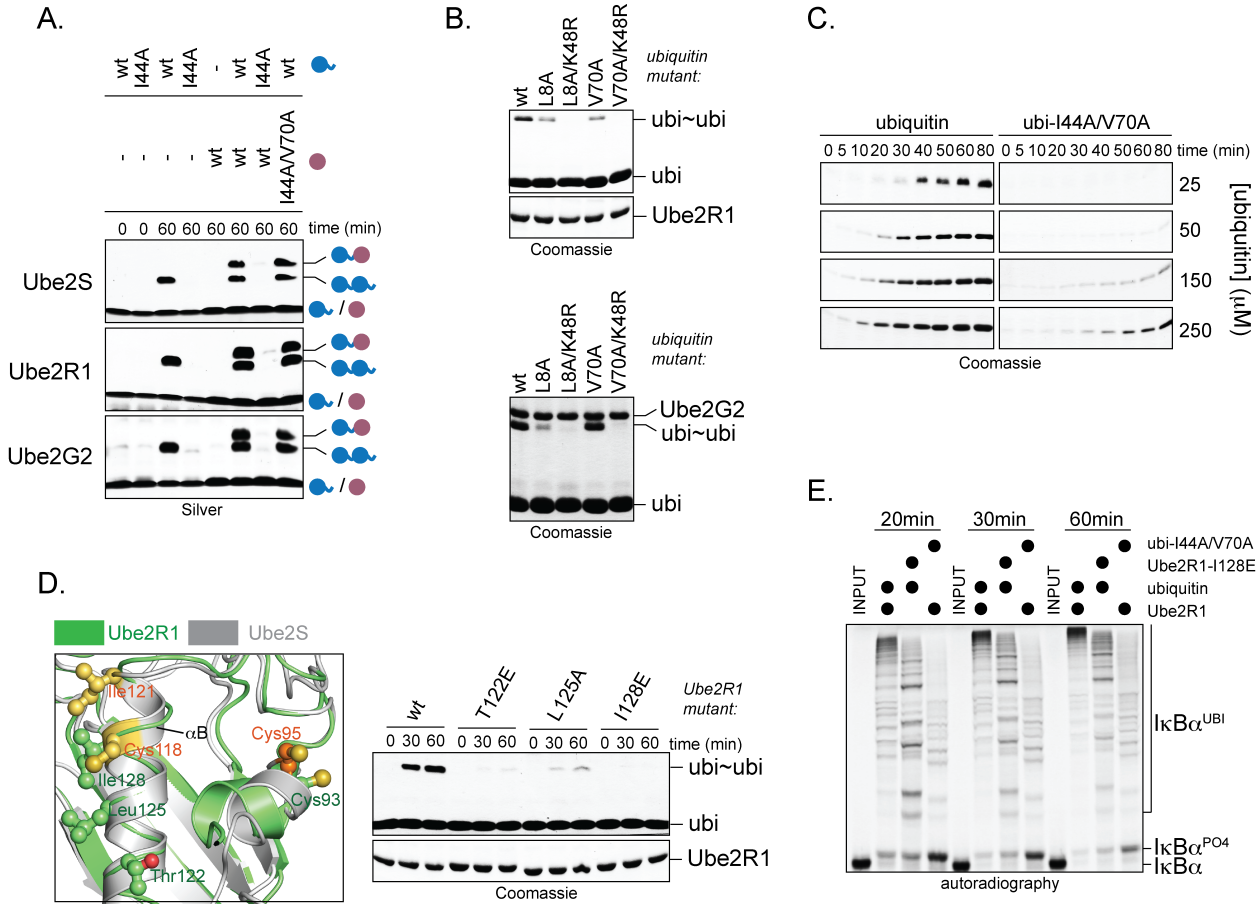
A.
wt
I44A
wt
I44A
-
wt
I44A
wt
I44A/V70A
0 0 60 60 60 60 60 60 time (min)
Ube2S
Ube2R1
Ube2G2
Silver
B.
ubiquitin mutant:
wt
L8A
L8A/K48R
V70A
V70A/K48R
ubi~ubi
ubi
Ube2R1
Coomassie
Ube2G2
ubi~ubi
ubi
C.
ubiquitin
ubi-I44A/V70A
0 5 10 20 30 40 50 60 80 0 5 10 20 30 40 50 60 80 time (min)
25
50
150
250
[ubiquitin] (μM)
Coomassie
D.
Ube2R1
Ube2S
Ile121
αB
Cys95
Cys118
Ile128
Leu125
Cys93
Thr122
Ube2R1 mutant:
wt
T122E
L125A
I128E
0 30 60 0 30 60 0 30 60 0 30 60 time (min)
ubi~ubi
ubi
Ube2R1
Coomassie
E.
20min
30min
60min
INPUT
INPUT
INPUT
ubi-I44A/V70A
Ube2R1-I128E
ubiquitin
Ube2R1
IκBα^UBI
IκBα^PO4
IκBα
autoradiography

Figure S6

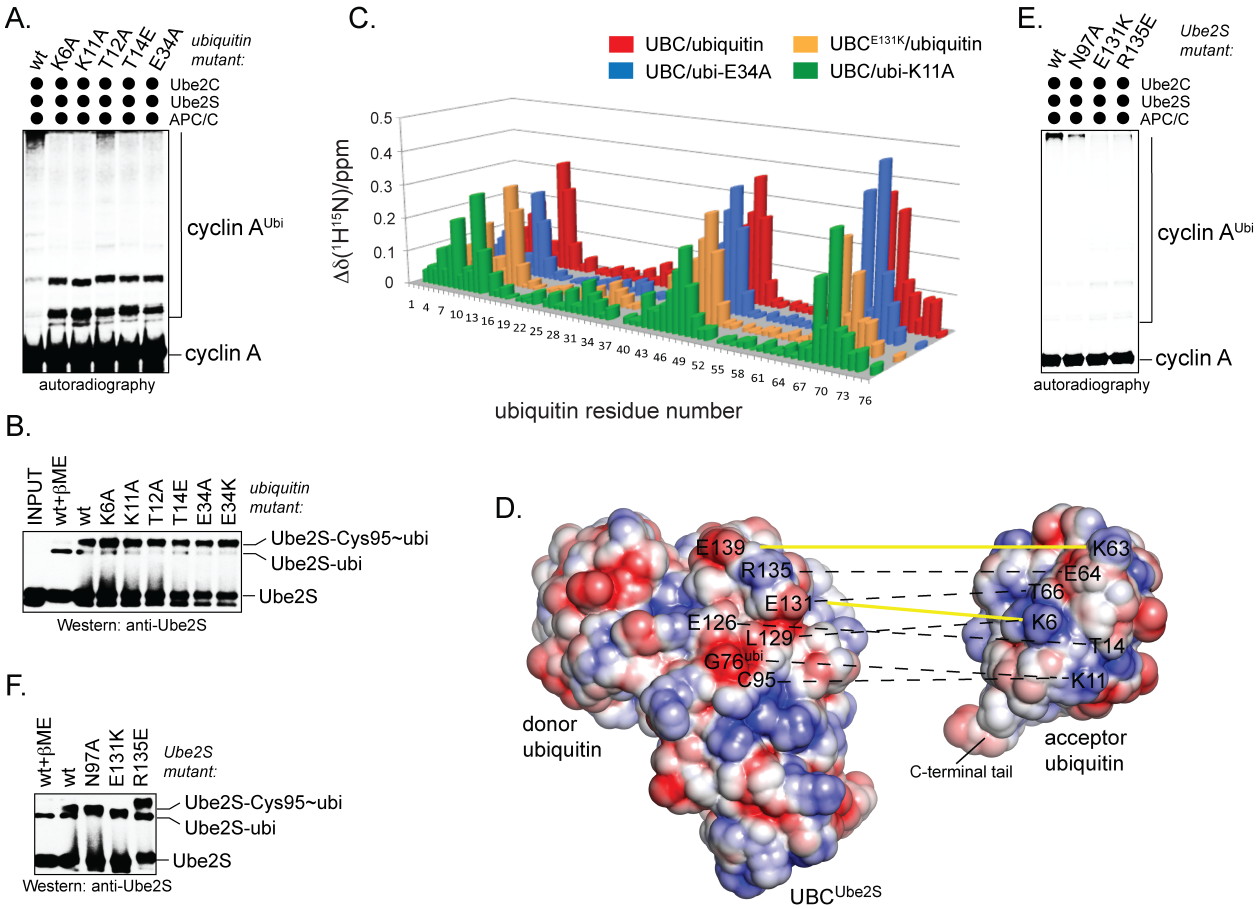
A.
wt
K6A
K11A
T12A
T14E
E34A
ubiquitin mutant:
Ube2C
Ube2S
APC/C
cyclin A^Ubi
cyclin A
autoradiography
B.
INPUT
wt+βME
wt
K6A
K11A
T12A
T14E
E34A
E34K
ubiquitin mutant:
Ube2S-Cys95~ubi
Ube2S-ubi
Ube2S
Western: anti-Ube2S
C.
UBC/ubiquitin
UBC^E131K/ubiquitin
UBC/ubi-E34A
UBC/ubi-K11A
Δδ(¹H¹⁵N)/ppm
ubiquitin residue number
D.
E139
R135
E131
E126
L129
G76^ubi
C95
K63
E64
T66
K6
T14
K11
donor ubiquitin
acceptor ubiquitin
C-terminal tail
UBC^Ube2S
E.
wt
N97A
E131K
R135E
Ube2S mutant:
Ube2C
Ube2S
APC/C
cyclin A^Ubi
cyclin A
autoradiography
F.
wt+βME
wt
N97A
E131K
R135E
Ube2S mutant:
Ube2S-Cys95~ubi
Ube2S-ubi
Ube2S
Western: anti-Ube2S

Figure S7

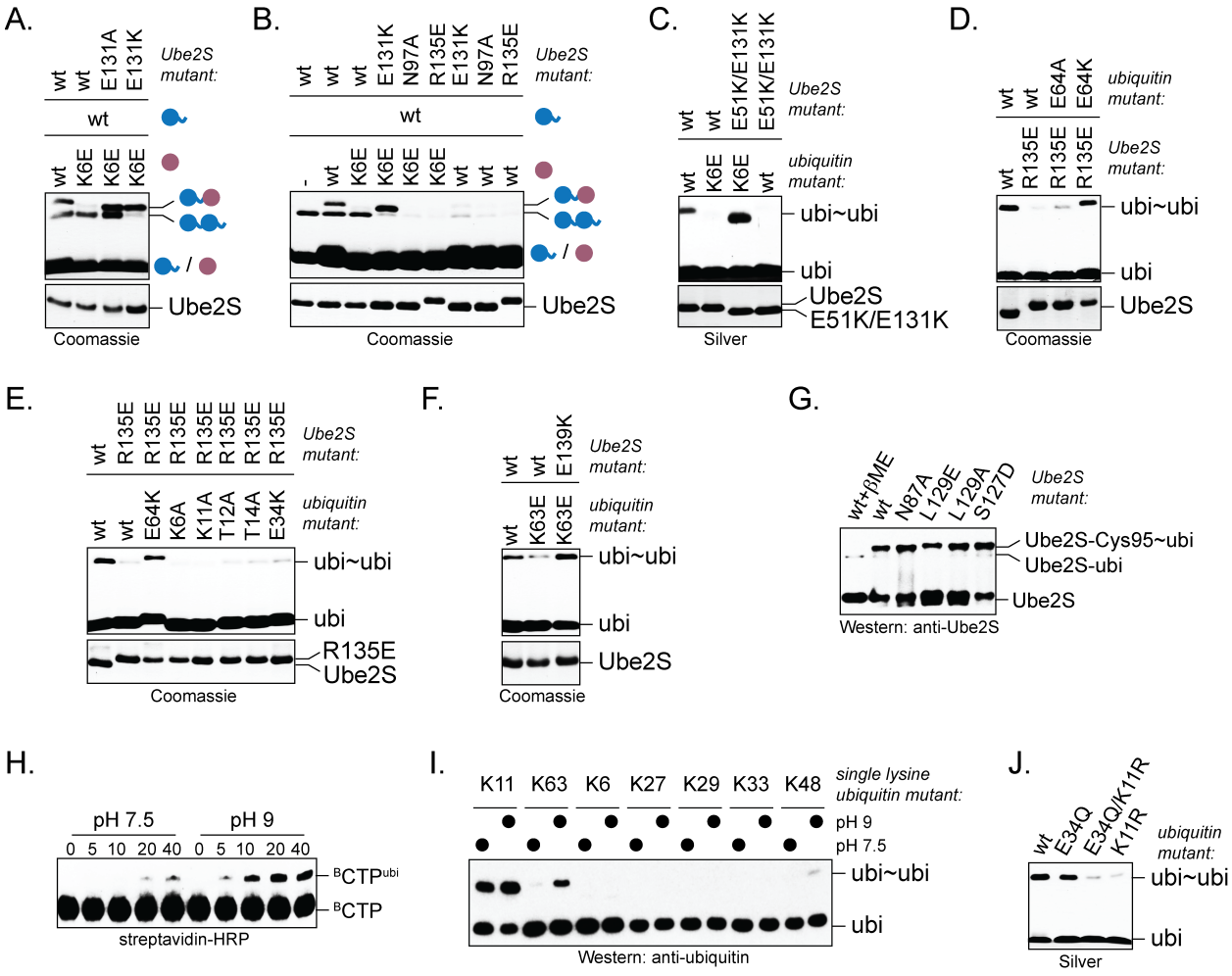
A.
wt
wt
E131A
E131K
Ube2S mutant:
wt
wt
K6E
K6E
K6E
Ube2S
Coomassie
B.
wt
wt
wt
E131K
N97A
R135E
E131K
N97A
R135E
Ube2S mutant:
wt
-
wt
K6E
K6E
K6E
K6E
wt
wt
wt
Ube2S
Coomassie
C.
wt
wt
E51K/E131K
E51K/E131K
Ube2S mutant:
wt
K6E
K6E
wt
ubiquitin mutant:
ubi~ubi
ubi
Ube2S
E51K/E131K
Silver
D.
wt
wt
E64A
E64K
ubiquitin mutant:
wt
R135E
R135E
R135E
Ube2S mutant:
ubi~ubi
ubi
Ube2S
Coomassie
E.
wt
R135E
R135E
R135E
R135E
R135E
R135E
Ube2S mutant:
wt
wt
E64K
K6A
K11A
T12A
T14A
E34K
ubiquitin mutant:
ubi~ubi
ubi
R135E
Ube2S
Coomassie
F.
wt
wt
E139K
Ube2S mutant:
wt
K63E
K63E
ubiquitin mutant:
ubi~ubi
ubi
Ube2S
Coomassie
G.
wt+βME
wt
N87A
L129E
L129A
S127D
Ube2S mutant:
Ube2S-Cys95~ubi
Ube2S-ubi
Ube2S
Western: anti-Ube2S
H.
pH 7.5
pH 9
0 5 10 20 40 0 5 10 20 40
BCTPubi
BCTP
streptavidin-HRP
I.
K11 K63 K6 K27 K29 K33 K48
single lysine ubiquitin mutant:
pH 9
pH 7.5
ubi~ubi
ubi
Western: anti-ubiquitin
J.
wt
E34Q
E34Q/K11R
K11R
ubiquitin mutant:
ubi~ubi
ubi
Silver

Figure S8

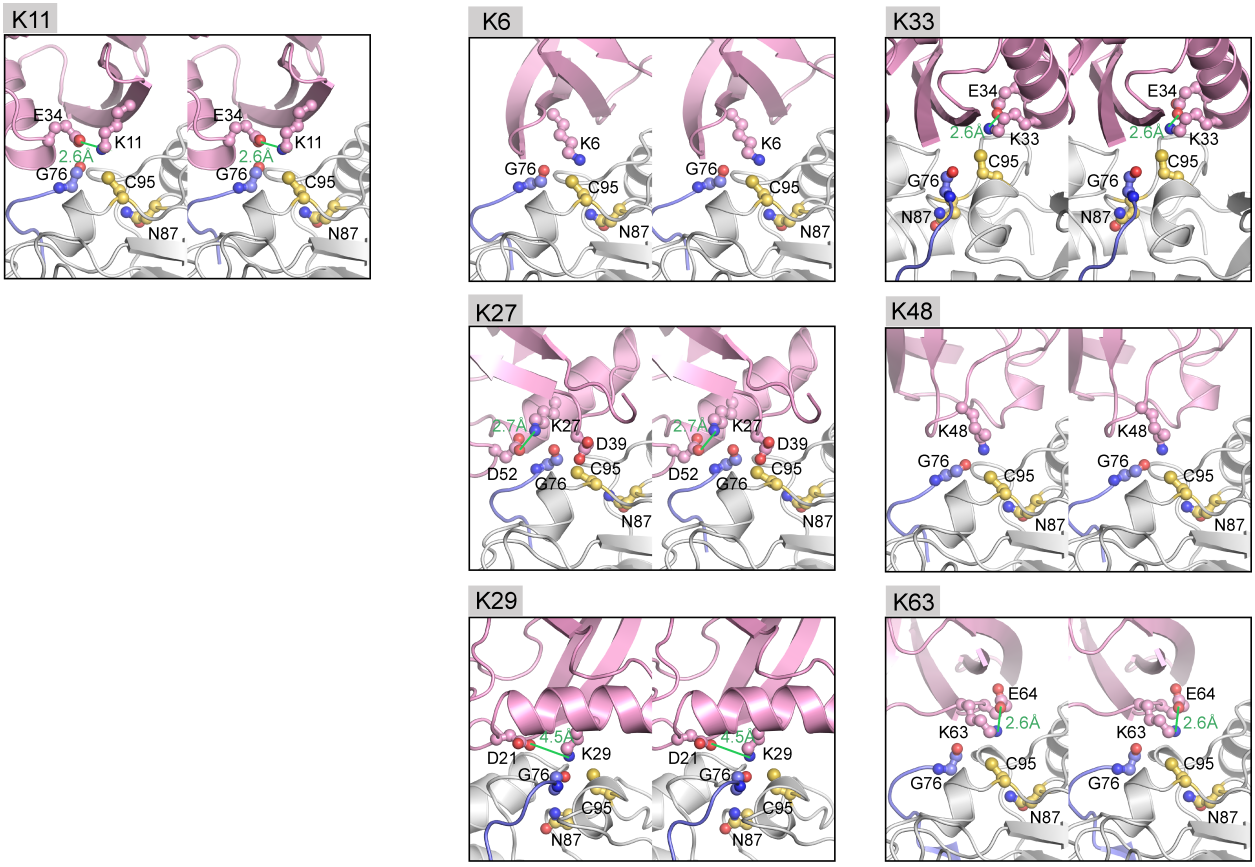
K11
E34
K11
2.6Å
G76
C95
N87
K6
K6
G76
C95
N87
K33
E34
2.6Å
K33
C95
G76
N87
K27
2.7Å
K27
D39
D52
C95
G76
N87
K48
K48
G76
C95
N87
K29
4.5Å
D21
K29
G76
C95
N87
K63
E64
2.6Å
K63
C95
G76
N87

Chapter 4

K11-Linked Polyubiquitination in Cell Cycle Control Revealed by a K11 Linkage-Specific Antibody

Marissa L. Matsumoto*, Katherine E. Wickliffe*, Ken C. Dong, Christine Yu, Ivan Bosanac, Daisy Bustos, Lilian Phu, Donald S. Kirkpatrick, Sarah G. Hymowitz, Michael Rape, Robert F. Kelley, Vishva M. Dixit

Molecular Cell (2010) *39*, 477-484

* equal contribution

Summary

Polyubiquitination is a posttranslational modification where ubiquitin chains containing isopeptide bonds linking one of seven ubiquitin lysines with the C terminus of an adjoining ubiquitin are covalently attached to proteins. While functions of K48- and K63-linked polyubiquitin are understood, the role(s) of noncanonical K11-linked chains is less clear. A crystal structure of K11-linked diubiquitin demonstrates a distinct conformation from K48- or K63-linked diubiquitin. We engineered a K11 linkage-specific antibody and use it to demonstrate that K11 chains are highly upregulated in mitotic human cells precisely when substrates of the ubiquitin ligase anaphase-promoting complex (APC/C) are degraded. These chains increased with proteasomal inhibition, suggesting they act as degradation signals in vivo. Inhibition of the APC/C strongly impeded the formation of K11-linked chains, suggesting that a single ubiquitin ligase is the major source of mitotic K11-linked chains. Our results underscore the importance of K11-linked ubiquitin chains as critical regulators of mitotic protein degradation.

Introduction

Ubiquitin is a 76 amino acid protein that is highly conserved from yeast to humans. Covalent linkage of the C terminus of ubiquitin to the ε-amino group of a lysine on a substrate plays an essential role in many cellular pathways, including the DNA-damage response, protein turnover, receptor downregulation, cell cycle progression, NF-κB signaling, and apoptosis (Hershko and Ciechanover, 1998).Three enzymes mediate ubiquitination—an E1 ubiquitin-activating enzyme, an E2 ubiquitin-conjugating enzyme, and an E3 ubiquitin ligase (Deshaies and Joazeiro, 2009; Schulman and Harper, 2009; Ye and Rape, 2009) whereas deubiquitinating enzymes (DUBs) reverse it (Reyes-Turcu et al., 2009).

Multiple forms of ubiquitination exist (Komander, 2009). Monoubiquitination refers to the attachment of a single ubiquitin to one or more lysines within the substrate, while polyubiquitin chains are formed when additional ubiquitins are linked to lysines or the N terminus of ubiquitin itself. Despite having identical subunits, ubiquitin chains linked through K48 and K63 have distinct structures. K48-linked polyubiquitin forms a compact structure where its hydrophobic patch, centered around I44, is buried (Cook et al., 1992; Eddins et al., 2007; Phillips et al., 2001; Tenno et al., 2004; Varadan et al., 2002). In contrast, K63-linked polyubiquitin forms extended chains lacking intersubunit interfaces (Datta et al., 2009; Komander et al., 2009; Tenno et al., 2004; Varadan et al., 2004). These conformational differences influence the fate of the modified protein by promoting interactions with distinct ubiquitin-binding proteins (Dikic et al., 2009). K48-linked chains target proteins for proteasomal degradation (Hershko and Ciechanover, 1998), whereas K63-linked chains typically facilitate protein-protein interactions required for signaling (Skaug et al., 2009). The structure and function of polyubiquitin chains linked through K6, K11, K27, K29, and K33 are less understood.

Ubiquitin chains linked through K11 were identified as critical regulators of cell division (Jin et al., 2008; Kirkpatrick et al., 2006) and were proposed to signal degradation of ubiquitin ligase anaphase-promoting complex (APC/C) substrates, which is essential for eukaryotic cell division (Jin et al., 2008; Williamson et al., 2009). The APC/C recruits two E2 enzymes, the ubiquitin chain-initiating UbcH10 and the chain-elongating Ube2S, which assemble K11-linked

chains with high specificity (Garnett et al., 2009; Williamson et al., 2009; Wu et al., 2010). Loss of this APC/C-specific E2 module leads to strong defects in mitotic progression (Song and Rape, 2010; Williamson et al., 2009). While these results suggest that K11-linked chains drive protein degradation during mitosis, characterization of ubiquitin chains assembled by the APC/C, UbcH10, and Ube2S has relied largely on in vitro experiments. Direct evidence of K11-linked chains regulating protein degradation in cells is lacking. In addition, it is unclear the extent to which the APC/C assembles K11-linked chains compared to canonical K48-linked chains.

The advent of antibodies capable of recognizing endogenous K48- and K63-linked polyubiquitin chains provided a simple and direct means to interrogate polyubiquitin signaling (Newton et al., 2008). Here, we describe the engineering of a K11-linked polyubiquitin-specific antibody. We illustrate the utility of this antibody by demonstrating upregulation of K11-linked chains during mitosis when APC/C substrates are degraded. Unexpectedly, loss of APC/C activity interfered with the synthesis of most K11-linked chains in cells, suggesting that a single ubiquitin ligase, the APC/C, assembles the bulk of K11-linked chains. These results emphasize a crucial role for K11-linked ubiquitin chains as essential regulators of mitotic protein degradation.

Results

Crystal Structure of K11-Linked Diubiquitin

The generation of K48- and K63-linked polyubiquitin-specific antibodies (Newton et al., 2008) was possible because K48- and K63-linked chains adopt distinct structures, thus presenting different surfaces to binding partners. To determine whether K11-linked chains also adopt a unique conformation, we crystallized enzymatically synthesized K11-linked diubiquitin (Figure S2). The structure, which was solved to 2.2 Å (Table 1), reveals that K11-linked diubiquitin can adopt a compact structure in which I44 of the hydrophobic patch of each ubiquitin is solvent accessible and on the same face of the dimer (Figures 1A and 1B). This structure differs markedly from that of extended K63-linked chains (Datta et al., 2009; Komander et al., 2009; Tenno et al., 2004; Varadan et al., 2004) and compact K48-linked chains, where I44 residues are buried within the interface (Cook et al., 1992; Eddins et al., 2007; Phillips et al., 2001; Tenno et al., 2004; Varadan et al., 2002) (Figure 1B). The interface between the K11-linked ubiquitins is composed primarily of residues from loops L1 and L3 and the C-terminal tail (Figure S1A) and has a hydrophobic core (Figure S1B). Given the distinct conformation adopted by K11-linked diubiquitin, we hypothesized that antibodies specific for K11-linked polyubiquitin could be engineered.

Generation of a K11-Linked Polyubiquitin-Specific Antibody

A synthetic bivalent Fab antibody fragment phage display library (Lee et al., 2004) was sorted using a competitive selection strategy (Figure S3A). A K11-linked diubiquitin-specific clone (G3), when produced as a soluble Fab fragment, had a dissociation constant (K_D) of 105 nM for binding K11-linked diubiquitin and demonstrated no detectable binding to either K48- or K63-linked diubiquitin (Table S1). This clone was used as a template for affinity maturation libraries encoding amino acid diversity within different combinations of complementarity-determining regions (CDRs). The highest-affinity K11-specific clone containing CDR L1 mutations, 2A3, had a K_D of 25 nM for K11-linked diubiquitin, while the highest-affinity K11-

specific clone containing CDR H2 mutations, 2E6, had a K_D of 47 nM (Table S1 and Figure S3B). Since the affinity maturation libraries generated were not designed to have both CDR L1 and H2 diversity, the light chain of 2A3 was combined with the heavy chain of 2E6. The resulting hybrid, 2A3/2E6, had a further improvement in affinity for K11-linked diubiquitin over both parental clones (K_D = 12 nM) and showed no detectable binding to K48- or K63-linked diubiquitin (Table S1).

Western Blot and Immunoprecipitation with the K11-Linked Polyubiquitin-Specific Antibody 2A3/2E6

2A3/2E6 detected as little as 16 ng of K11-linked diubiquitin by western blot without showing cross-reactivity to 1 μg of monoubiquitin, linear, K48-, or K63-linked diubiquitin (Figure 2A). It also detected enzymatically synthesized (Figure 2B) and endogenous K11-linked polyubiquitin (Figure 2C). To confirm 2A3/2E6 specificity, we synthesized polyubiquitin chains of multiple linkages in vitro with the E2 UbcH5c and E3 MuRF1. In the absence of a substrate, MuRF1 undergoes autoubiquitination with chains composed predominantly of K11, K48, and K63 linkages (Kim et al., 2007) Reactions were done using WT, K11R, K48R, or K63R ubiquitin (Figures 3A and 3B). Lysine-to-arginine mutations prevent the synthesis of polyubiquitin chains linked through that lysine, as confirmed by mass spectrometry (Figure 3C). Autoubiquitination reactions were immunoprecipitated by 2A3/2E6, and total ubiquitin was detected by western blot (Figure 3B). When 2A3/2E6 immunoprecipitated autoubiquitinated MuRF1 from the WT, K48R, and K63R reactions, the polyubiquitin linkage profiles remained similar to the input material (Figure 3C), suggesting the majority of MuRF1 molecules carry each of the primary linkages. By contrast, 2A3/2E6 failed to immunoprecipitate any polyubiquitin linkages from the K11R reaction, owing to the lack of the target linkage (Figure 3C). Next, we determined whether 2A3/2E6 could immunoprecipitate K11-linked polyubiquitin from HEK293T cells (Figure 3D). Immunoblotting revealed immunoprecipitation of ubiquitinated species, which was increased upon ubiquitin overexpression (Figure 3E). Mass spectrometry confirmed enrichment of K11 linkages in immunoprecipitates relative to the percentage of K11 linkages present in the input lysates (Figure 3F).

Upregulation of K11-Linked Chains Correlates with APC/C Substrate Degradation

Having established that 2A3/2E6 specifically recognizes K11-linked polyubiquitin, we used it to probe the formation of K11-linked chains in vivo. Asynchronous HeLa cells contained relatively little K11-linked polyubiquitin compared to K48-linked polyubiquitin (Figure 4A). By contrast, K11-linked chains were strongly upregulated in HeLa cells released from a nocodazole-induced prometaphase arrest. This increase correlated precisely with the degradation of APC/C substrates securin, cyclin B1, Aurora A, and Plk1 and was enhanced by proteasomal inhibition (Figures 4A and 4B). In contrast, K48- and K63-linked chains did not increase dramatically upon proteasome inhibition in cells exiting from mitosis (Figure 4B). These data suggest that activation of the APC/C results in a sharp increase in the overall concentration of K11-linked chains and that these function as degradation signals in vivo.

The aforementioned experiments relied on drug-induced synchronization. To determine whether the abundance of K11-linked chains is cell-cycle regulated in cells never exposed to spindle toxins, we analyzed the levels of K11-linked chains by immunofluorescence microscopy.

Confirming the immunoblotting, K11-linked chains were upregulated in mitosis (Figure 4C). Interestingly, we observed a strong accumulation of K11-linked chains at the spindle midbody from late anaphase on, consistent with a role for the APC/C in targeting Plk1 and passenger complex proteins for degradation (Figure 4C). These experiments further suggest that K11-linked chains act in mitotic control, in a manner consistent with being assembled by the APC/C.

The human APC/C synthesizes K11-linked chains on its substrates to promote their degradation (Jin et al., 2008; Williamson et al., 2009; Wu et al., 2010); however, most experiments to date have been performed in vitro with ubiquitin mutants. To determine whether the APC/C is responsible for formation of K11-linked chains in cells, we knocked down the APC/C-specific E2s, *UbcH10* and *Ube2S*, or the APC/C subunits *Cdc27*, *Apc11*, and *Cdh1*. As reported (Williamson et al., 2009), simultaneous depletion of *UbcH10* and *Ube2S* strongly impaired APC/C activity in cells, leading to stabilization of all APC/C substrates tested (Figure 4D). Strikingly, loss of these E2s also blocked upregulation of K11-linked chains in synchronized cells while having no effect on K48-linked chains (Figure 4D). Similar results were obtained upon depletion of APC/C subunits (Figure 4E). To exclude the possibility that the decrease in K11-linked chains resulted from a cell-cycle arrest, rather than from APC/C inhibition, we released the *UbcH10*/*Ube2S*-siRNA-treated cells from mitosis in the presence of a CDK inhibitor, roscovitine, which allows mitotic exit in the absence of APC/C activity (Potapova et al., 2006). Under these conditions, depletion of *UbcH10* and *Ube2S* caused a striking decrease in the abundance of K11-linked chains (Figure 4F). Furthermore, APC/C activation by overexpression of both Cdh1 and Ube2S in asynchronous HeLa cells resulted in upregulation of K11-linked chains (Figure 4G). This demonstrates that the E2s UbcH10 and Ube2S and the E3 APC/C are the major contributors to K11-linked polyubiquitin synthesis in mitosis and underscores the importance of K11-linked chain formation by the APC/C.

Consistent with the critical role of the APC/C in assembling K11-linked ubiquitin chains, we found this chain type to be highly enriched in affinity-purified APC/C (Figure 4H). To directly test whether APC/C assembles K11-linked chains, we investigated the kinetics of K11-linked polyubiquitin synthesis in cell extracts where APC/C activity can be controlled by addition of activator or inhibitor proteins. In synchronized HeLa cell lysates, where the APC/C is relatively inactive due to the spindle assembly checkpoint, long K11-linked chains were formed, and addition of APC/C-inhibitors $UbcH10^{C114S}$ and Emi1 proved that chain formation was APC/C dependent (Figure 4I). When p31 and UbcH10 were added to fully activate the APC/C, cyclin B1 was degraded and there was a dramatic increase in the abundance of K11-linked chains (Figure 4I). The abundance of K48-linked ubiquitin chains was not altered by these treatments. More detailed kinetic analysis revealed that K11-linked chains formed in two distinct phases (Figure 4J), both of which depended on APC/C activity (Figure 4). Together, our K11 linkage-specific antibody allowed us to demonstrate that APC/C assembles K11-linked chains in extracts as well as in cells. As activation of the APC/C, a single ubiquitin ligase, led to a dramatic increase in the bulk of K11-linked chains, our experiments suggest that the APC/C is a major source for this chain type in human cells.

Discussion

We describe the crystal structure of K11-linked diubiquitin and demonstrate that it can adopt a conformation distinct from diubiquitins of other linkages. While the structure has captured a single conformation, it is likely that there is some flexibility in the diubiquitin such

that other conformations could be adopted, as seen with K48-linked chains (Eddins et al., 2007; Varadan et al., 2002). Given its unique structure, it is likely that K11-specific binding proteins and DUBs will be identified.

Analysis of the crystal-packing contacts suggests how K11-linked tetraubiquitin might be formed (Figure S1C). Two diubiquitins in the asymmetric unit are packed in a single plane with their free K11 and C termini pointing toward each other. Tetraubiquitin could be formed by linking the four adjacent ubiquitin subunits into a ring. This arrangement represents a structure distinct from K48-linked tetraubiquitin (PDB 2O6V), where the first two ubiquitins are oriented 90° relative to the last two ubiquitins. Longer K11-linked chains could be formed with multiple rings stacked against each other, forming a coil-like structure. Each turn of the coil would be made up of four ubiquitins, and the connectivity between the turns would occur at the center of the coil.

The unique conformation adopted by K11-linked diubiquitin prompted efforts to engineer a K11 linkage-specific antibody using a phage display strategy. Specificity was ensured through counter-selection with monoubiquitin and alternative-linkage forms of polyubiquitin. The resulting antibody, 2A3/2E6, should prove critical for studying K11-linked polyubiquitination not only in mitosis but also other cellular pathways.

When we analyzed K11-linked ubiquitin chain abundance in human cells with 2A3/2E6, we recognized a striking cell-cycle-dependent regulation of chain assembly. While K11-linked chains were relatively low in asynchronous cells, they increased significantly as cells exited mitosis. As this is the time of the cell cycle when the majority of substrates of the ubiquitin ligase APC/C are degraded (Peters, 2006), our results suggest an unexpectedly strong link between activation of a single E3, the APC/C, and formation of K11-linked chains.

K11-linked chains were recently proposed to drive the degradation of APC/C substrates during mitosis (Jin et al., 2008; Williamson et al., 2009). Switching APC/C on and off in extracts, we confirmed these earlier findings, which were largely based on the use of ubiquitin mutants. Similar to the experiments in cells, the extract assays suggested that the APC/C is a major E3 for K11-linked chains during mitosis, a finding we confirmed by depleting APC/C subunits from cells. In addition, the E2s UbcH10 and Ube2S have to date only been shown to collaborate with the APC/C, suggesting it is their major, if not only, partner E3. Loss of *UbcH10* and *Ube2S* ablates APC/C activity in cells (Song and Rape, 2010; Williamson et al., 2009) (Figure 4D) and, strikingly, also abrogates the upregulation of mitotic K11-linked chain formation. Interestingly, both APC/C-specific E2s are tightly cell-cycle regulated. Ube2S binds to the APC/C coactivator Cdc20 in early mitosis and to Cdh1 in late mitosis and early G1, and this interaction is required for Ube2S activity (Williamson et al., 2009). In addition, both UbcH10 and Ube2S undergo APC/C-dependent degradation during G1, which occurs subsequent to the degradation of most, if not all, known APC/C substrates (Rape and Kirschner, 2004; Williamson et al., 2009). As seen here, the time window of UbcH10 and Ube2S activity on APC/C coincides with the time in the cell cycle when most K11-linked chains are formed. Together, our observations support the surprising view that a single ubiquitin ligase, the APC/C, is a major source of K11-linked chain formation in cells. The APC/C can intimately regulate K11-linked chain formation by controlling both K11-specific E2s, UbcH10 and Ube2S.

Our results demonstrate that K11- and K48-linked chains differ in many aspects, including their abundance, regulation, synthesis, and structure. However, chains of both topologies promote degradation by the 26S proteasome, which raises the important question of why the APC/C assembles K11-linked chains, especially to the extent seen here. Human APC/C

likely targets more than a hundred substrates for degradation, and we speculate that dedicating a specific ubiquitin chain type for this overburdened E3 might allow this degradation to be completed in the short time span of mitosis and early G1 (Rape et al., 2006). It is also possible that K11-linked chains support functions other than proteasomal degradation, which may be required for APC/C activity at certain locations or cell cycle stages. Our structure implies that specific, yet-to-be identified proteins recognize K11-linked chains, and our K11-specific antibody provides a powerful tool for their identification.

Methods

See online Supplemental Experimental Procedures for more detail:
http://www.sciencedirect.com/science/article/pii/S109727651000523X#app3

K11-Linked Diubiquitin

K11-linked polyubiquitin was produced using a modification of the procedure described (Pickart and Raasi, 2005). Purified diubiquitin was crystallized in 0.2 M ammonium sulfate and 20% polyethylene glycol 3350. The structure was solved by molecular replacement.

Phage Display

Phage display libraries were generated and sorted as described previously (Lee et al., 2004)with later rounds containing soluble monoubiquitin, linear diubiquitin, K48-linked polyubiquitin, and K63-linked polyubiquitin for counter-selection. Surface plasmon resonance (SPR), Fab conversion to IgGs, and purification were done as before (Newton et al., 2008).

Western Blots with the 2A3/2E6 Antibody

Proteins were separated by SDS-PAGE and transferred at 30 V for 2 hr by wet transfer in 10% methanol to nitrocellulose. Nonspecific binding sites were blocked with 5% milk/PBS + 0.05% Tween 20 (PBST) and then incubated with 1 μg/ml 2A3/2E6 IgG in 5% milk/PBST for 1 hr at 25°C. Signal was detected by a goat anti-human peroxidase-conjugated $F(ab')_2$ secondary (Jackson ImmunoResearch).

MuRF1 Autoubiquitination and Immunoprecipitation

MuRF1 autoubiquitination reactions and immunoprecipitations were carried out as previously described (Newton et al., 2008). All immunoprecipitations with 2A3/2E6 were done in the presence of 4 M urea.

Mass Spectrometry

Mass spectrometry was performed as described previously (Blankenship et al., 2009; Kirkpatrick et al., 2006).

Immunofluorescence Microscopy

HeLa cells were methanol fixed, PBST permeabilized, Abdil blocked, and incubated with anti-K11 and anti-α-tubulin antibodies overnight at 4°C. After washing, cells were incubated with fluorescently labeled secondary antibodies and mounted on slides with ProLong Gold Antifade (Invitrogen).

Extract Experiments

Extracts of HeLa S3 cells synchronized in mitosis by thymidine/nocodazole arrest were prepared as described (Jin et al., 2008). The mitotic extracts were activated by addition of UbcH10, $p31^{comet}$, ubiquitin, and energy mix, as indicated. Reactions were incubated for 2 hr at room temperature, stopped by addition of gel loading buffer, and analyzed by western blotting using antibodies against K11-linked chains, cyclin B1, or Ube2S.

Acknowledgments

We thank G. Fuh for the VH Fab phage display library, W. Wang for X-ray data collection, I. Wertz for helpful discussions, and K. Newton for editorial assistance. M. Matsumoto, K. Dong, C. Yu, I. Bosanac, D. Bustos, L. Phu, D. Kirkpatrick, S. Hymowitz, R. Kelley, and V. Dixit are all employees of Genentech, Inc.

Accession Numbers

Coordinates have been deposited in the Protein Data Bank (code 3NOB).

Figure Legends

Figure 1. Crystal Structure of K11-Linked Diubiquitin (A) The structure of K11-linked diubiquitin with the proximal ubiquitin (provides K11 to the isopeptide bond) in light orange and the distal ubiquitin (provides the C terminus) in dark orange. The K11 side chains and the C-terminal glycines are shown as spheres, and the isopeptide bond is labeled. The figure on the right is rotated 180° about a vertical axis relative to the figure on the left. **(B)** The structures of K11-, K48- (from tetraubiquitin, PDB code 2O6V), and K63-linked diubiquitin (PDB code 2JF5) are shown in orange, blue, and green, respectively. The side chains of I44 are shown as spheres, lysines as sticks, and isopeptide bonds circled. Superposition of the three structures with proximal ubiquitins aligned is shown.

Figure 2. The 2A3/2E6 Antibody Is Specific for K11-Linked Polyubiquitin in Western Blots (A) Monoubiquitin, linear diubiquitin, K48-linked diubiquitin, and K63-linked diubiquitin (1 μg/lane) and K11-linked diubiquitin (2-fold dilutions, 16–1000 ng/lane gradient) were immunoblotted with 2A3/2E6 (right) or Coomassie stained (left). **(B)** Monoubiquitin, K48-linked polyubiquitin 2–7 (2–7 ubiquitins), K63-linked polyubiquitin 2–7, and K11-linked polyubiquitin (1 μg/lane) were immunoblotted with a pan-ubiquitin antibody (middle) or with 2A3/2E6 (right) or were Coomassie stained (left). **(C)** K11-linked diubiquitin (50 ng), K48-linked diubiquitin (1 μg), K63-linked diubiquitin (1 μg), and HEK293T cell lysate (100 μg) were immunoblotted with 2A3/2E6 (right) or Coomassie stained (left).

Figure 3. The 2A3/2E6 Antibody Is Specific for K11-Linked Polyubiquitin in Immunoprecipitations (A–C) MuRF1 autoubiquitination reactions with WT, K11R, K48R, or K63R ubiquitin were immunoprecipitated with 2A3/2E6 (K11) or an isotype control antibody and then analyzed by western blot with a pan-ubiquitin antibody (B) and mass spectrometry (C). Numbers in parentheses in (A) indicate relevant lanes and columns in (B) and (C). Red lines in (B) indicate the region excised for mass spectrometry. **(D–F)** Cell lysates from HEK293T cells either mock transfected or transfected with WT human ubiquitin were immunoprecipitated with 2A3/2E6 (K11) or an isotype control antibody and then analyzed by western blot with a pan-ubiquitin antibody (E) and mass spectrometry (F). Numbers in parentheses in (D) indicate the relevant lanes in (E). Red lines in (E) indicate the region excised for mass spectrometry. The percentage of K11 linkages relative to total ubiquitin linkages measured in the cell lysates (input) and immunoprecipitations (anti-K11) are compared (F).

Figure 4. The 2A3/2E6 Antibody Reveals Cell-Cycle Regulation of K11-Linked Polyubiquitination (A) Western blots of asynchronous (A) or synchronized and released HeLa cells. **(B)** Western blots of synchronized and released HeLa cells with or without MG132. **(C)** Immunofluorescence microscopy of HeLa cells. K11-linked polyubiquitin staining is shown in green, α-tubulin in red, and Hoechst DNA staining in blue. **(D)** Western blots of synchronized and released control or *UbcH10*/*Ube2S* siRNA-transfected HeLa cells. **(E)** Western blots of synchronized and released control or *Cdc27*/*Apc11*/*Cdh1* siRNA-transfected HeLa cells. **(F)** Western blots of synchronized and released control or *UbcH10*/*Ube2S* siRNA-transfected HeLa cells, with or without roscovitine treatment. **(G)** Western blots of asynchronous HeLa cells mock transfected or overexpressing Cdh1 and Ube2S. **(H)** Western blots of immunoprecipitations with an anti-Cdc27 or isotype control IgG from synchronized HeLa cells 2 hr after release. **(I and J)**

Western blots of synchronized HeLa cell extracts incubated with buffer alone, p31 and UbcH10, or p31, Emi1, and UbcH10^{C114S} for the times indicated.

Figure S1. K11-Linked Diubiquitin Interfaces (A) The amino acid sequence of ubiquitin is aligned with a map of the secondary structure observed in the K11-linked diubiquitin. An open book surface model of K11-linked diubiquitin is shown with the proximal ubiquitin in light orange and the distal ubiquitin in dark orange. Residues of the L1 loop (blue), L3 loop (red), and C-terminal tail (green) that participate in the diubiquitin interface are highlighted in both the primary amino acid sequence as well as on the surface model of K11-linked diubiquitin. **(B)** The hydrophobic core of the K11-linked diubiquitin interface is highlighted. The proximal ubiquitin subunit is shown in light orange and the distal ubiquitin subunit in dark orange. Side chains of hydrophobic residues participating in the interaction are shown as sticks with residue numbers labeled in the left panel and as space-filled spheres in the right panel. **(C)** Crystal packing of two K11-linked diubiquitins with their K11 side chains shown as space- filled spheres in the left panel. The proximal red and distal orange ubiquitins are covalently linked forming one diubiquitin and the proximal yellow and distal green ubiquitins are covalently linked forming the second diubiquitin. Free K11 residues and C-termini point to the center of the tetramer. Connectivity could be possible linking red-orange-yellow-green where the red ubiquitin would have a free C-terminus (most proximal subunit) and the green ubiquitin would have a free K11 residue (most distal subunit). This is compared to the crystal structure of K48-linked tetraubiquitin (PDB code 2O6V) on the right where K48 side chains are shown as space-filled spheres. Connectivity is also red-orange-yellow-green with red being the most proximal subunit and green being the most distal.

Figure S2. Synthesis and Quantitative Mass Spectrometry Analysis of K11-linked Diubiquitin (A) Polyubiquitin chains synthesized by Ube2S (input) were separated by cation exchange chromatography and collected fractions were analyzed by Coomassie-stained SDS-PAGE. Shown here are monoubiquitin (Ub), diubiquitin (Ub_2), and triubiquitin (Ub_3). **(B)** The 14 kDa band corresponding to diubiquitin was excised, trypsin digested, and assessed by quantitative mass spectrometry. The signal of each isotopically labeled internal standard control peptide was normalized to 1.0 and the abundance of each diglycine-modified lysine-containing peptide was measured relative to its corresponding labeled control peptide. The K11 linkage represents 99.1% of the linkages present in the diubiquitin.

Figure S3. Identification of K11-Linked Polyubiquitin-Specific Fab Antibody Fragments (A) Panning strategy for identifying K11 linkage-specific Fabs. K11-linked diubiquitin was immobilized on an ELISA plate whereas monoubiquitin, linear diubiquitin, K48-linked polyubiquitin 2-7, and K63-linked polyubiquitin 2-7 were added in solution for counter-selection. Unbound phages were washed from the plates and specific binders were eluted. After several rounds of amplification of specific binders, the sequences of the displayed Fabs were determined. **(B)** Sequence alignment of CDRs L1 and H2 of clones G3 and 2A3/2E6. Residues highlighted in red indicate sequence changes relative to the G3 parental clone. Positions are numbered according to the Kabat numbering system.

Figure 1

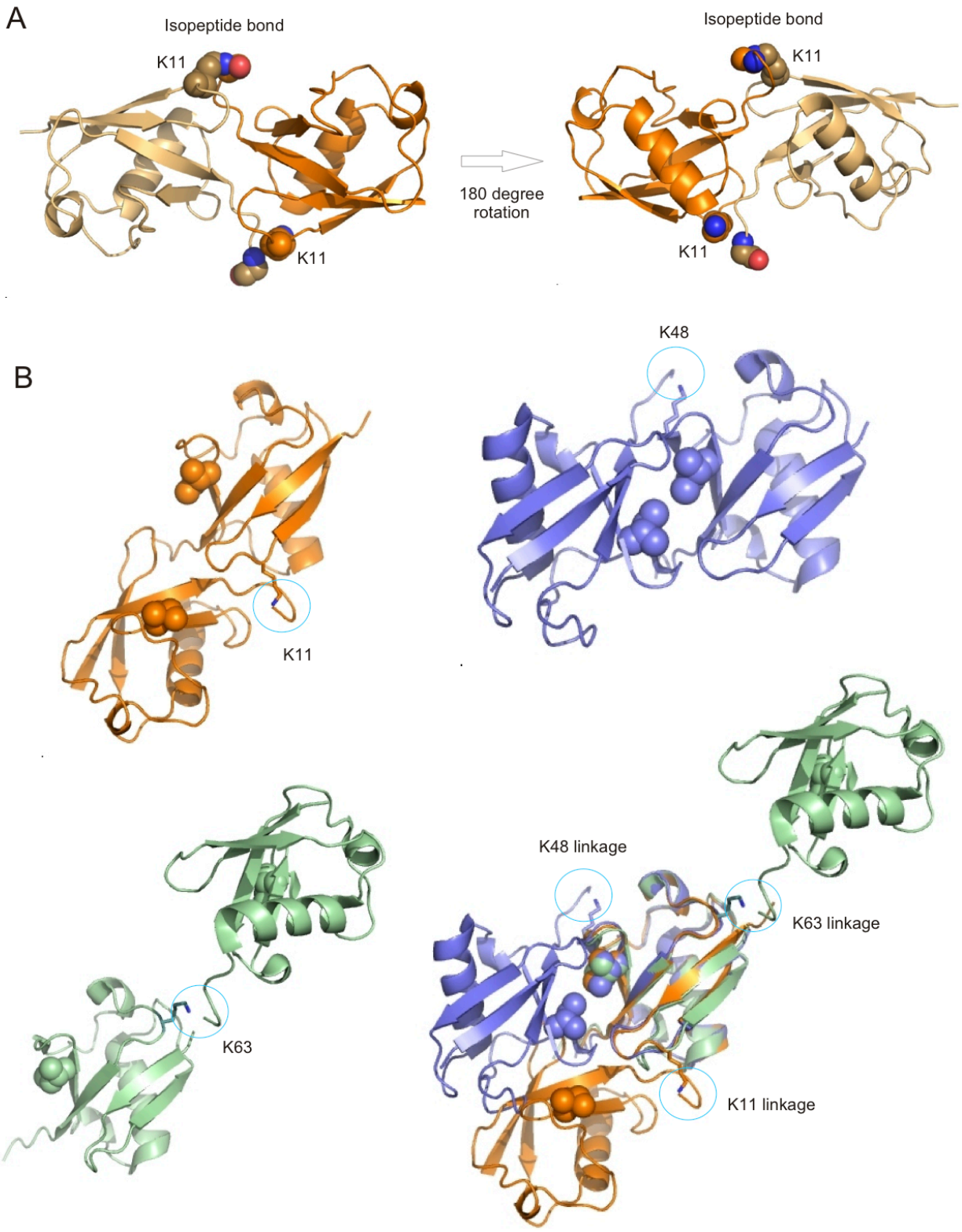
A
Isopeptide bond
K11
K11
180 degree
rotation
Isopeptide bond
K11
K11
B
K48
K11
K63
K48 linkage
K63 linkage
K11 linkage

Figure 2

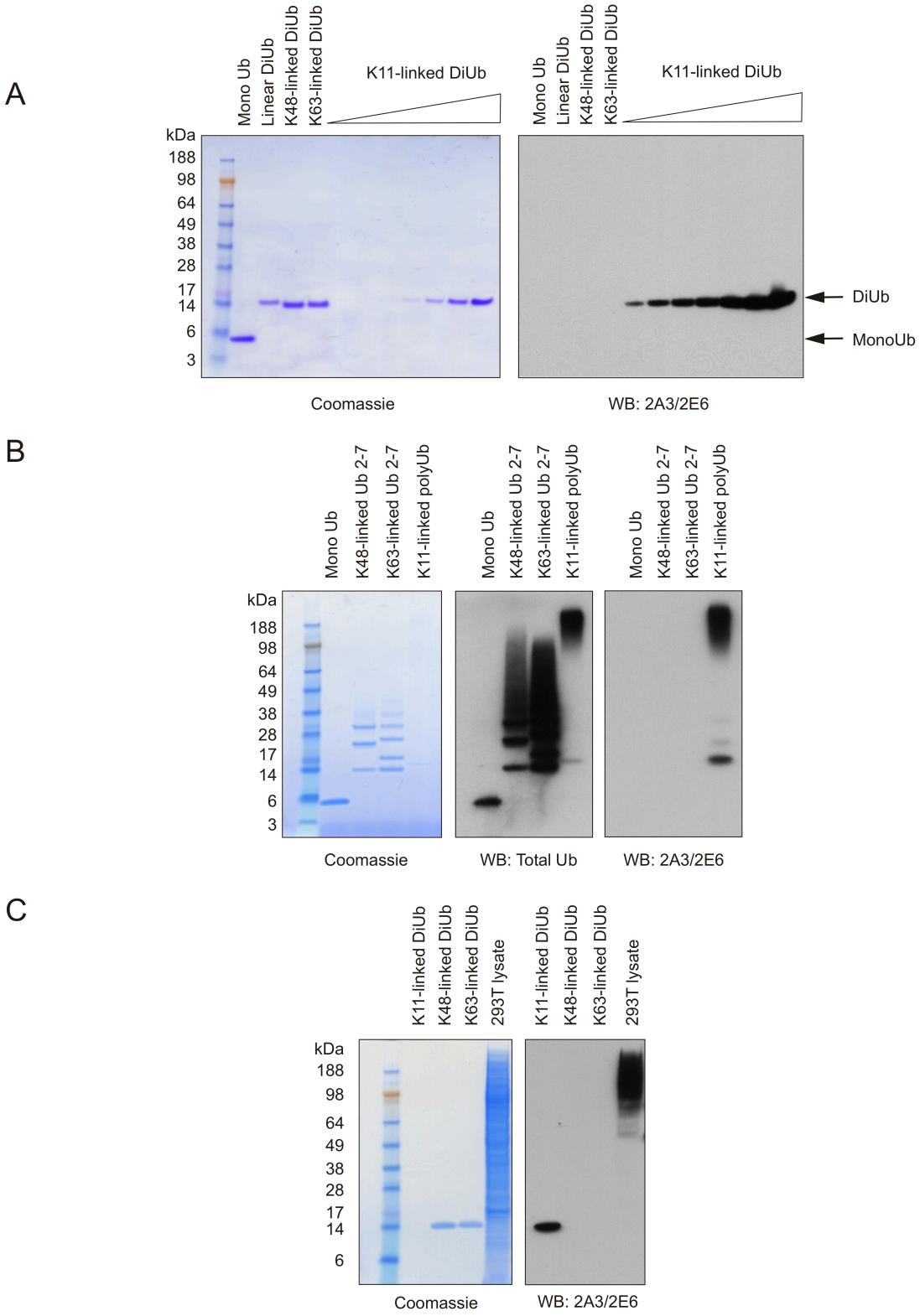
A
Mono Ub
Linear DiUb
K48-linked DiUb
K63-linked DiUb
K11-linked DiUb
kDa
188
98
64
49
38
28
17
14
6
3
DiUb
MonoUb
Coomassie
WB: 2A3/2E6
B
Mono Ub
K48-linked Ub 2-7
K63-linked Ub 2-7
K11-linked polyUb
Coomassie
WB: Total Ub
WB: 2A3/2E6
C
K11-linked DiUb
K48-linked DiUb
K63-linked DiUb
293T lysate
Coomassie
WB: 2A3/2E6

Figure 3

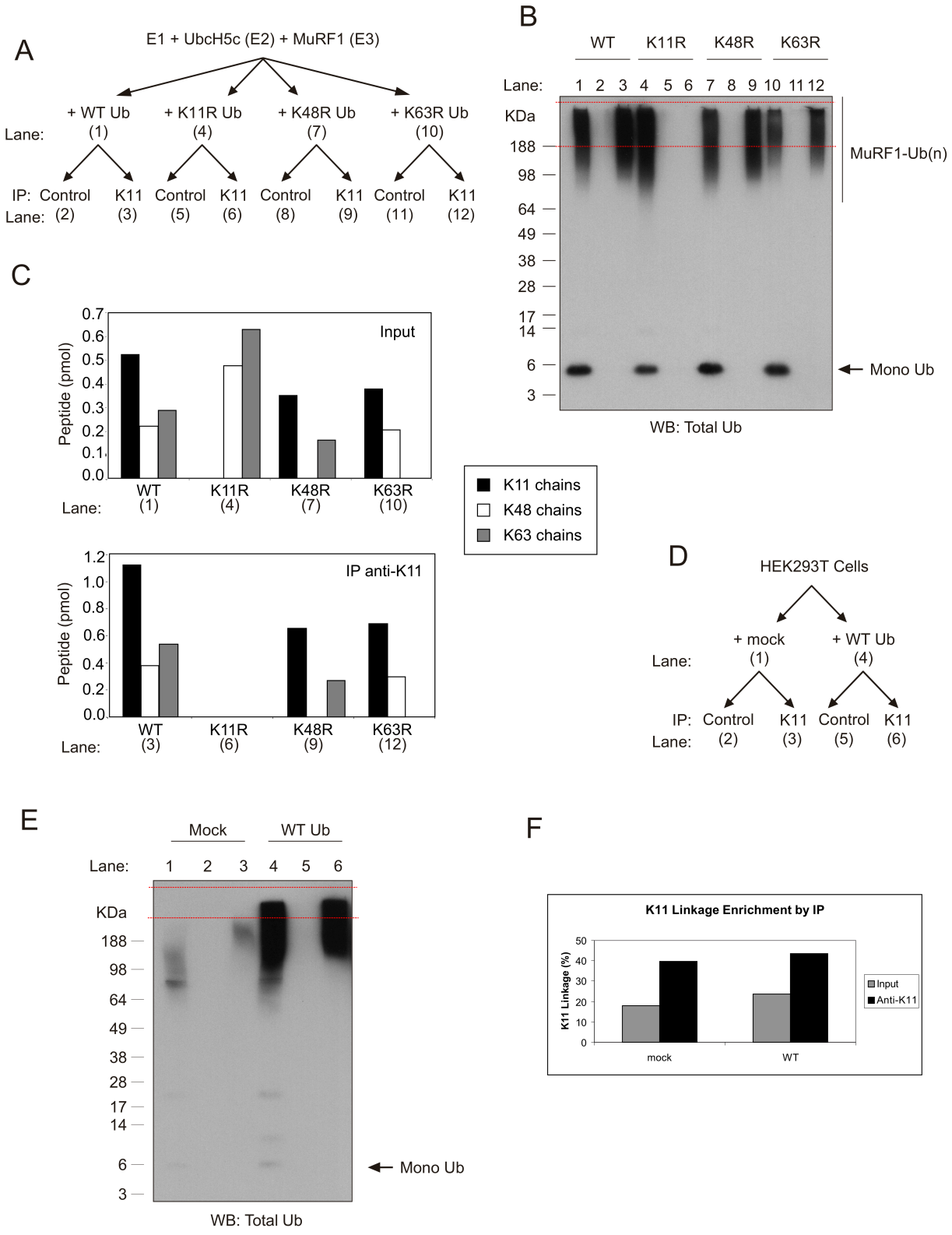

Figure 4

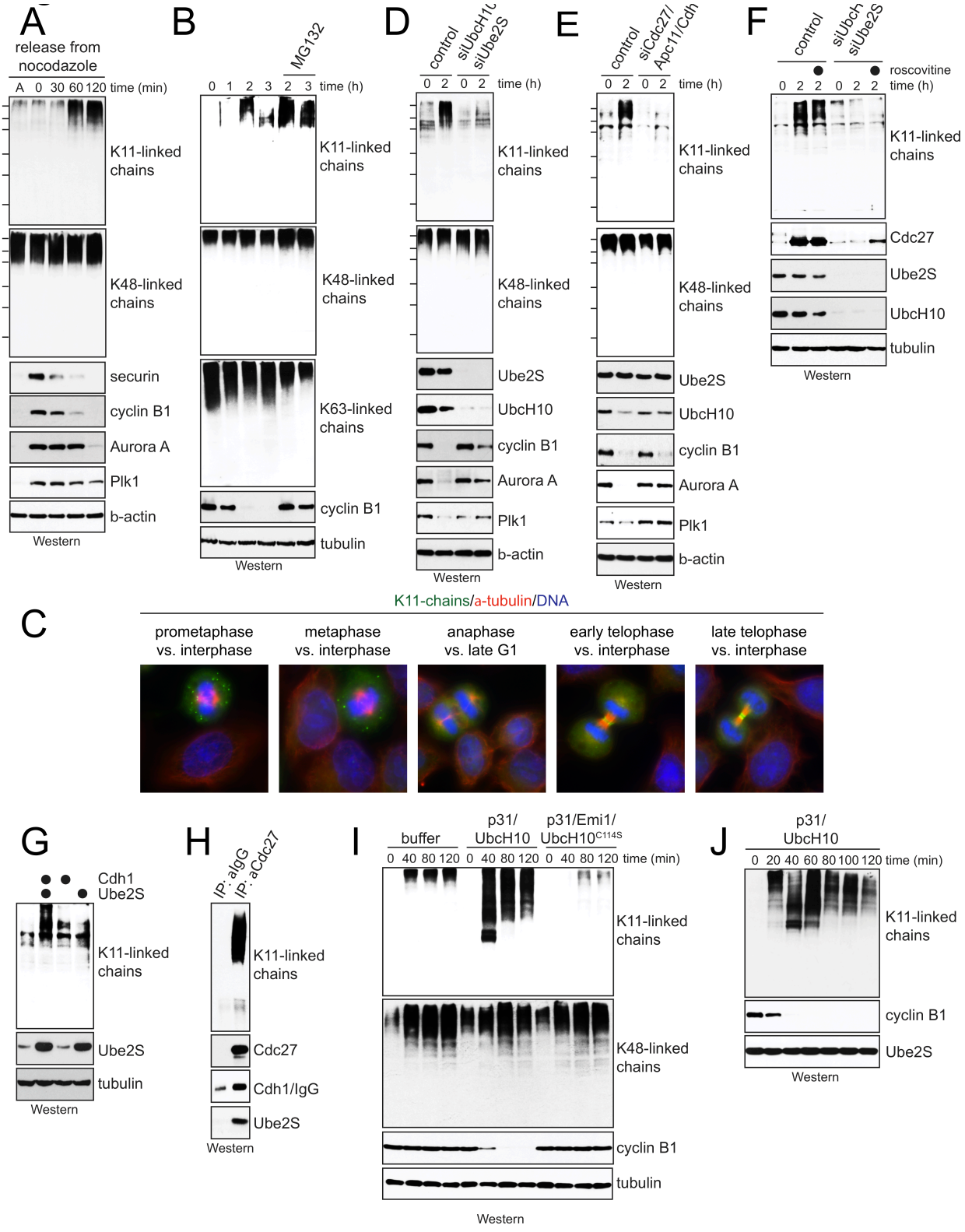
A
release from nocodazole
A 0 30 60 120 time (min)
K11-linked chains
K48-linked chains
securin
cyclin B1
Aurora A
Plk1
b-actin
Western
B
MG132
0 1 2 3 2 3 time (h)
K11-linked chains
K48-linked chains
K63-linked chains
cyclin B1
tubulin
Western
D
control
siUbcH10
siUbe2S
0 2 0 2 time (h)
K11-linked chains
K48-linked chains
Ube2S
UbcH10
cyclin B1
Aurora A
Plk1
b-actin
Western
E
control
siCdc27/ Apc11/Cdh
0 2 0 2 time (h)
K11-linked chains
K48-linked chains
Ube2S
UbcH10
cyclin B1
Aurora A
Plk1
b-actin
Western
F
control
siUbch
siUbe2S
roscovitine
0 2 2 0 2 2 time (h)
K11-linked chains
Cdc27
Ube2S
UbcH10
tubulin
Western
C
K11-chains/a-tubulin/DNA
prometaphase vs. interphase
metaphase vs. interphase
anaphase vs. late G1
early telophase vs. interphase
late telophase vs. interphase
G
Cdh1
Ube2S
K11-linked chains
Ube2S
tubulin
Western
H
IP: aIgG
IP: aCdc27
K11-linked chains
Cdc27
Cdh1/IgG
Ube2S
Western
I
buffer
p31/ UbcH10
p31/Emi1/ UbcH10C114S
0 40 80 120 0 40 80 120 0 40 80 120 time (min)
K11-linked chains
K48-linked chains
cyclin B1
tubulin
Western
J
p31/ UbcH10
0 20 40 60 80 100 120 time (min)
K11-linked chains
cyclin B1
Ube2S
Western

Figure S1

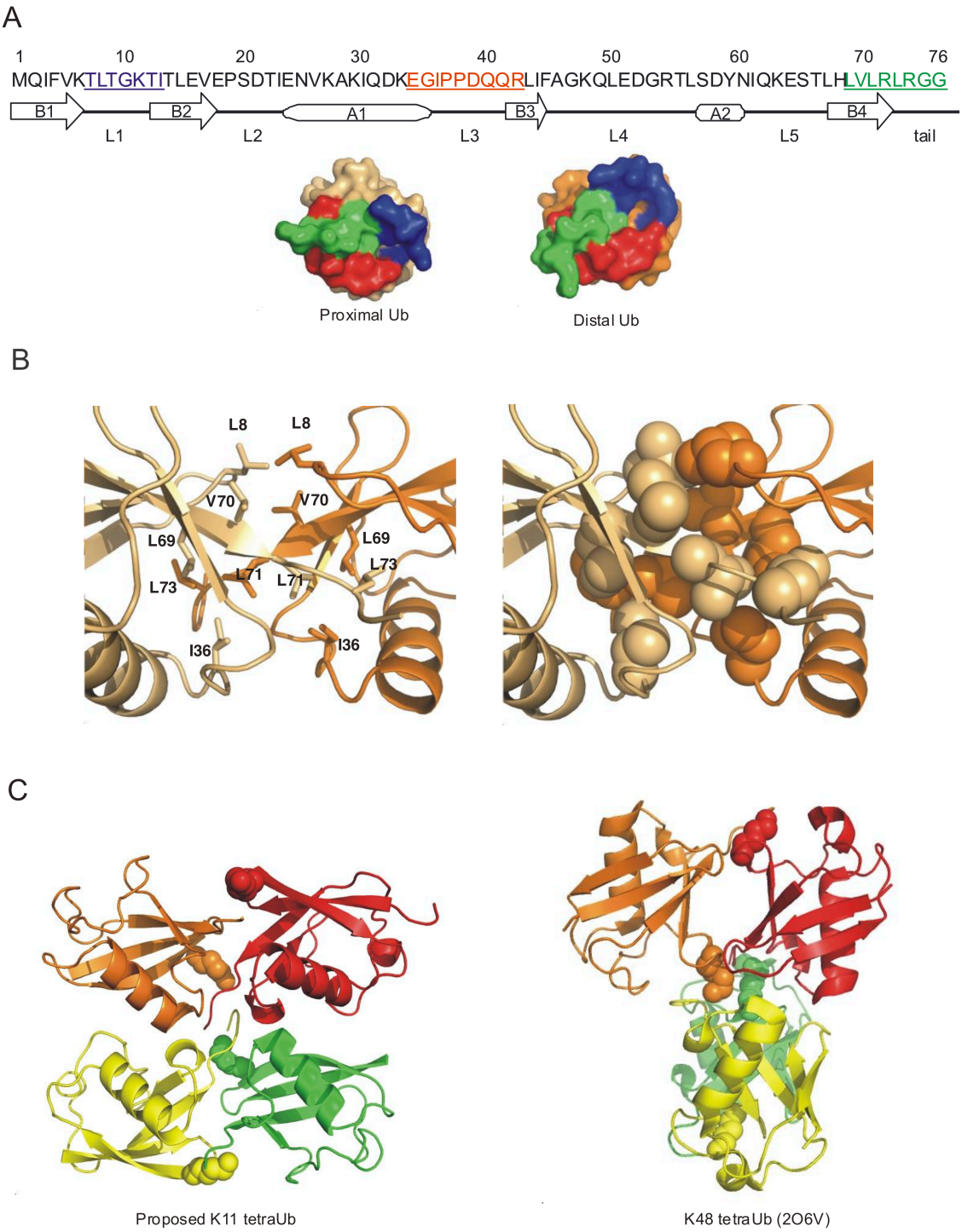
A
1 10 20 30 40 50 60 70 76
MQIFVKTLTGKTITLEVEPSDTIENVKAKIQDKEGIPPDQQRLIFAGKQLEDGRTLSDYNIQKESTLHLVLRLRGG
B1 B2 A1 B3 A2 B4
L1 L2 L3 L4 L5 tail
Proximal Ub
Distal Ub
B
L8 L8
V70 V70
L69 L69
L73 L71 L71 L73
I36 I36
C
Proposed K11 tetraUb
K48 tetraUb (2O6V)

Figure S2

A

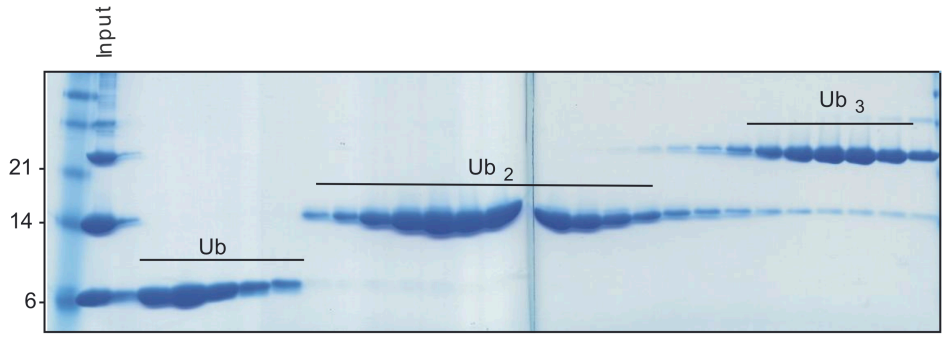

B

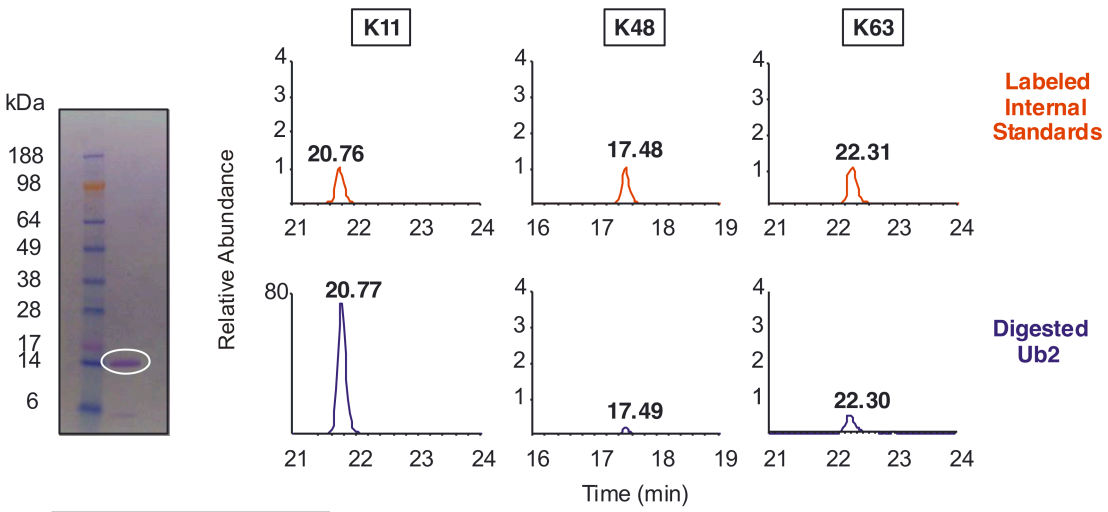

Linkage	Pmol
K11	68.8
K48	0.17
K63	0.44
Σ K6,K27,K29,K33	0.01

Figure S3

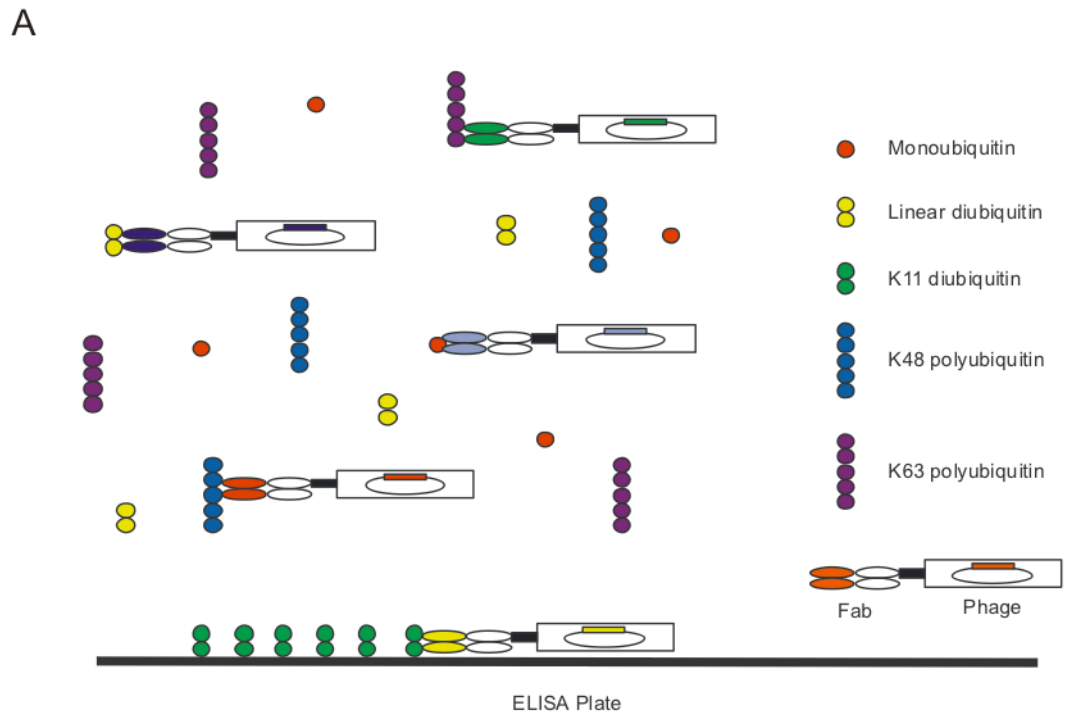

B

	CDR L1											CDR H2																			
	24										34	50		52		52a														65
G3	R	A	S	Q	D	V	S	T	A	V	A	G	I	N	P	N	G	G	Y	T	Y	Y	A	D	S	V	K	G	
2A3/2E6	R	A	S	Q	I	V	G	T	F	V	A	A	I	N	P	A	G	G	Y	T	Y	Y	A	D	S	V	K	G	

Table S1

SPR Analysis of the K11-Specific Fabs

Fab	k_a (1/Ms)	k_a SD (1/Ms)	k_d (1/s)	k_d SD (1/s)	K_d (nM)	K_d SD (nM)	Mutant CDRs
G3	3.02E+05	4.34E+04	3.16E-02	3.87E-03	105	3.00E+00	N/A
2A3	6.53E+05	5.32E+04	1.60E-02	1.51E-03	25	3.21E+00	L1
2E6	3.60E+05	3.20E+04	1.69E-02	8.89E-04	47	4.36E+00	H2
2A3/2E6	6.48E+05	3.95E+04	7.45E-03	2.19E-04	12	1.15E+00	L1/H2

Fabs were analyzed by surface plasmon resonance (SPR) for binding immobilized K11-, K48-, or K63-linked diubiquitin. Mean on-rate (k_a), off-rate (k_d), binding constant (K_D), and standard deviations (SD) of three experimental measurements for binding K11-linked diubiquitin are given. All clones showed no detectable binding to K48- or K63-linked diubiquitin. Complementarity determining regions (CDRs) containing mutations relative to clone G3 are indicated.

Chapter 5

Conclusions and Outlook

In the Chapters above, I presented our discoveries that human APC/C uses an E2 module to build Lys11-linked ubiquitin chains on its substrates. The chain initiation E2 Ube2C forms short ubiquitin chains on APC/C substrates, which are then rapidly elongated by the Lys11-specific E2 Ube2S (Chapter 2). We then went on to define the molecular mechanism through which Ube2S catalyzes specific ubiquitylation. We found that Ube2S binds donor ubiquitin to achieve processivity and uses a residue of ubiquitin to achieve Lys11 specificity, in a mechanism we term substrate-assisted catalysis (Chapter 3). Finally, we developed a Lys11-linkage specific antibody and used the antibody to show that levels of Lys11-linked ubiquitin chains increase as human cells enter mitosis in a manner dependent on Ube2S and Ube2C (Chapter 4). Together, this work cements the link between Lys11-linked ubiquitin chains, human APC/C, and mitosis, and reveals new mechanisms by which E2 enzymes promote ubiquitylation.

Work in my thesis has answered many questions about how human APC/C and Ube2S form Lys11-linked chains, but also opened up additional avenues of research. Ube2S is thus far the only known E2 that does not require the RING domain of an E3. Instead, we showed that Ube2S binds relatively stably to APC/C co-adapters Cdc20 and Cdh1 (Chapter 2). Our lab is currently investigating how Ube2S binds to the APC/C and how this affects E2 activity.

In all other reported examples of chain initiation and elongation E2 pairs, the two E2s are thought to bind, and therefore compete for, the same RING binding site on the E3. Because Ube2C and Ube2S occupy different binding sites on the APC/C, they are truly able to cooperate in chain assembly. Additionally, Ube2S is a dedicated chain elongation E2, and it cannot modify substrate lysines. The only other known E2 to show such a striking specificity for recognition of ubiquitin lysines is Ube2N/UEV1A. Our lab has now also determined the molecular requirements for chain initiation by human APC/C and Ube2C and shown that this is the rate-limiting step in ubiquitylation. Conserved initiation motifs are present on APC/C substrates and control the efficiency with which Ube2C modifies substrate lysines (Williamson et al., 2011). Therefore, Ube2S and Ube2C not only bind to different sites on the APC/C, but also recognize different molecular surfaces on their respective substrates (Chapter 3). This clear division of labor has the potential to greatly enhance the processivity of chain formation by the APC/C, and it will be interesting to see whether other E2 modules function in a similar manner.

The identification of Ube2S as an E2 for the APC/C allowed us to examine how linkage specificity is generated in the context of a physiological E2/E3 pair (Chapter 3). Most investigations into the mechanism of ubiquitin chain formation by E2s focus on identifying catalytic surfaces of the E2. We show that the substrate acceptor ubiquitin itself contains residues critical for lysine specificity. It was recently shown that the non-specific E2 UbcH5 requires the TEK box of ubiquitin to assembly Lys11-linked ubiquitin chains (Bosanac et al., 2011), suggesting that the molecular requirements for this chain type are conserved. The binding between E2s and acceptor ubiquitin is inherently weak (Hofmann and Pickart, 2001; Petroski and Deshaies, 2005; Rodrigo-Brenni et al., 2010), and our findings show how a catalytic-based method of linkage-specificity can overcome these low binding affinities. Further studies are needed to determine whether other ubiquitylation enzymes use similar mechanisms to assemble ubiquitin chains.

We and others have shown that non-covalent donor ubiquitin/E2 binding is a conserved mechanism to increase E2 processivity (Chapter 3) (Saha et al., 2011). These studies highlight a growing appreciation that the donor ubiquitin actively participates in ubiquitylation reactions by contributing unique surfaces. Recently, structures of RING E3s and E2~ubiquitin conjugates

revealed that RING domains bind the donor ubiquitin non-covalently and that this interaction is critical for ubiquitin transfer (Dou et al., 2012; Plechanovova et al., 2012; Pruneda et al., 2012). These results provide an explanation for the observation that E3s increase the rate of discharge of donor ubiquitin from E2s. Mutational analyses suggest that the RING-interacting E2 Cdc34 interacts with donor ubiquitin in the absence of an E3. However, Cdc34 activity is enhanced in the presence of its E3, raising the question of whether E2/RING binding provides additional binding surfaces for donor ubiquitin or activates the E2 in a yet unknown mechanism. Ube2S binds donor ubiquitin itself and does not bind the RING domain, providing a unique opportunity to dissect mechanisms of RING-independent E2 activation by an E3. I have shown that the APC/C enhances the ability of Ube2S to catalyze the formation of ubiquitin dimers and discharge ubiquitin from its active site. I am currently investigating the mechanism by which this E2 activation is achieved.

Ubiquitin linkage types have been characterized *in vivo* and *in vitro* by the use of mass spectrometry, ubiquitin mutants, and, more recently, linkage-specific antibodies. The development of a Lys11-specific antibody (Chapter 4) provides an essential tool for further investigation into the cellular processes regulated by this chain type in cells. Since our lab's initial study linking Lys11 chains and the APC/C, several studies have linked these chains to other cellular processes. For example, Lys11-linked chains have been associated with the ER-associated degradation (ERAD) pathway in yeast (Xu et al., 2009), TNFα signaling (Dynek et al., 2010), Wnt signaling (Hay-Koren et al., 2011), and membrane trafficking (Boname et al., 2010; Goto et al., 2010). However, in the latter three cases it is important to stress that Lys11 linkages are seen in the context of mixed ubiquitin chains. The non-specific E2 UbcH5, and not the Lys11-specific Ube2S, has been implicated in these processes. Therefore, the functional relevance of Lys11 linkages in the context of a mixed chain is unknown. To date, homogenous Lys11-linked chains have only been firmly linked to the degradation of APC/C substrates.

The studies presented here represent a growing interest in the importance of "atypical" ubiquitin chains. Although these chains may be not be abundant in cells, our work shows that they can have dedicated roles and specific enzymatic machinery responsible for their assembly. Most mass spectrometry studies examining ubiquitin linkages *in vivo* have been performed on asynchronous and unperturbed cells, save for proteasome inhibition. Our work emphasizes the importance of looking at ubiquitin linkages in specific contexts, such as cell cycle stage, disease states, or following the activation of signaling pathways. For example, a recently developed linear-linkage specific antibody was used to show that this chain type is upregulated following TNFα stimulation, supporting their role in NFκB signaling (Matsumoto et al., 2012). It will be exciting to see what future research reveals about the cellular functions and formation of ubiquitin chains linked through Lys6, Lys27, Lys29, and Lys33.

Many questions remain about how Lys11-linked ubiquitin chains are "decoded" by effector molecules in cells. These chains bind proteasomal receptors and the protein kinase adaptor NF-κB essential modulator (NEMO), but no Lys11-specific binding proteins have been identified. Additionally, a Lys11-specific deubiquitylating enzyme has been reported (Bremm et al., 2010), but its physiological role is not well established.

More fundamentally, it is unclear why human, *Xenopus*, and *Drosophila* APC/C substrates are degraded by Lys11- and not the canonical Lys48-linked ubiquitin chains. Yeast have no Ube2C or Ube2S homologs, and their APC/C mediates degradation by forming Lys48-linked chains. Are Lys11-linked chains critical regulators of mitosis in higher eukaryotes because they are specifically better suited to orchestrate the degradation of many substrates in a

short time? More trivially, it is possible that the importance of Lys11-linked chains in mitosis is a byproduct of the conservation of Ube2S during evolution and that there is nothing advantageous *per se* about Lys11-linked chains. The specific role of Lys11-linked chains in mitosis is a open question currently under investigation in the lab.

Both Lys11-linked ubiquitin chains and the E2s that assemble these chains are associated with human diseases. Quantitative proteomics have revealed an accumulation of Lys11 linkages in neurodegenerative disorders, including Huntington's disease (Bennett et al., 2007) and Alzheimer's disease (Dammer et al., 2011). Moreover, Ube2C and Ube2S, the Lys11 E2 module, are overexpressed in a number of cancer types and associated with tumor progression (Berlingieri et al., 2007; Fujita et al., 2009; Tedesco et al., 2007; van Ree et al., 2010). This is not surprising given the importance of the APC/C in maintaining genomic integrity and coordinating the events of mitosis. Therefore, Ube2C and Ube2S are attractive targets for cancer therapy.

The only approved cancer chemotherapeutic targeting the ubiquitin system is an inhibitor of the 26S proteasome. A number of small molecule inhibitors of E3 are currently undergoing clinical trials (Cohen and Tcherpakov, 2010). Directly targeting ubiquitylation enzymes involved in disease will hopefully reduce the pleiotropic side effects caused by general proteasomal inhibition. As a prerequisite for increasing treatment specificity, the identification of important ubiquitylation enzymes must be combined with a molecular dissection of how they function. Work presented in this dissertation analyzing how Ube2S and the APC/C collaborate to build ubiquitin chains highlights how this may be accomplished.

References

Alexandru, G., Graumann, J., Smith, G.T., Kolawa, N.J., Fang, R., and Deshaies, R.J. (2008). UBXD7 binds multiple ubiquitin ligases and implicates p97 in HIF1 alpha turnover. Cell *134*, 804-816.

Baboshina, O.V., and Haas, A.L. (1996). Novel multiubiquitin chain linkages catalyzed by the conjugating enzymes E2(EPF) and RAD6 are recognized by 26 S proteasome subunit 5. Journal of Biological Chemistry *271*, 2823-2831.

Baker, N.A., Sept, D., Joseph, S., Holst, M.J., and McCammon, J.A. (2001). Electrostatics of nanosystems: Application to microtubules and the ribosome. Proceedings of the National Academy of Sciences of the United States of America *98*, 10037-10041.

Baumgarten, A.J., Felthaus, J., and Waesch, R. (2009). Strong inducible knockdown of APC/C-Cdc20 does not cause mitotic arrest in human somatic cells. Cell Cycle *8*, 643-646.

Bedford, L., Lowe, J., Dick, L.R., Mayer, R.J., and Brownell, J.E. (2011). Ubiquitin-like protein conjugation and the ubiquitin-proteasome system as drug targets. Nature reviews Drug discovery *10*, 29-46.

Bennett, E.J., Shaler, T.A., Woodman, B., Ryu, K.-Y., Zaitseva, T.S., Becker, C.H., Bates, G.P., Schulman, H., and Kopito, R.R. (2007). Global changes to the ubiquitin system in Huntington's disease. Nature *448*, 704-U711.

Berlingieri, M.T., Pallante, P., Sboner, A., Barbareschi, M., Bianco, M., Ferraro, A., Mansueto, G., Borbone, E., Guerriero, E., Troncone, G., *et al*. (2007). UbcH10 is overexpressed in malignant breast carcinomas. European Journal of Cancer *43*, 2729-2735.

Blankenship, J.W., Varfolomeev, E., Goncharov, T., Fedorova, A.V., Kirkpatrick, D.S., Izrael-Tomasevic, A., Phu, L., Arnott, D., Aghajan, M., Zobel, K., *et al*. (2009). Ubiquitin binding modulates IAP antagonist-stimulated proteasomal degradation of c-IAP1 and c-IAP2. Biochemical Journal *417*, 149-160.

Boname, J.M., Thomas, M., Stagg, H.R., Xu, P., Peng, J., and Lehner, P.J. (2010). Efficient Internalization of MHC I Requires Lysine-11 and Lysine-63 Mixed Linkage Polyubiquitin Chains. Traffic *11*, 210-220.

Bosanac, I., Phu, L., Pan, B., Zilberleyb, I., Maurer, B., Dixit, V.M., Hymowitz, S.G., and Kirkpatrick, D.S. (2011). Modulation of K11-Linkage Formation by Variable Loop Residues within UbcH5A. Journal of Molecular Biology *408*, 420-431.

Bremm, A., Freund, S.M.V., and Komander, D. (2010). Lys11-linked ubiquitin chains adopt compact conformations and are preferentially hydrolyzed by the deubiquitinase Cezanne. Nature Structural & Molecular Biology *17*, 939-U947.

Brzovic, P.S., Lissounov, A., Christensen, D.E., Hoyt, D.W., and Klevit, R.E. (2006). A UbcH5/ubiquitin noncovalent complex is required for processive BRCA1-directed ubiquitination. Molecular cell *21*, 873-880.

Burton, J.L., and Solomon, M.J. (2001). D box and KEN box motifs in budding yeast Hsl1p are required for APC-mediated degradation and direct binding to Cdc20p and Cdh1p. Genes & Development *15*, 2381-2395.

Chen, Z.J., and Sun, L.J. (2009). Nonproteolytic functions of ubiquitin in cell signaling. Molecular cell *33*, 275-286.

Christensen, D.E., Brzovic, P.S., and Klevit, R.E. (2007). E2-BRCA1 RING interactions dictate synthesis of mono- or specific polyubiquitin chain linkages. Nature Structural & Molecular Biology *14*, 941-948.

Cohen, P., and Tcherpakov, M. (2010). Will the ubiquitin system furnish as many drug targets as protein kinases? Cell *143*, 686-693.

Comeau, S.R., Kozakov, D., Brenke, R., Shen, Y., Beglov, D., and Vajda, S. (2007). ClusPro: Performance in CAPRI rounds 6-11 and the new server. Proteins-Structure Function and Bioinformatics *69*, 781-785.

Cook, W.J., Jeffrey, L.C., Carson, M., Chen, Z.J., and Pickart, C.M. (1992). Structure of a diubiquitin conjugate and a model for interaction with ubiquitin conjugating enzyme (E2). Journal of Biological Chemistry *267*, 16467-16471.

Dammer, E.B., Na, C.H., Xu, P., Seyfried, N.T., Duong, D.M., Cheng, D., Gearing, M., Rees, H., Lah, J.J., Levey, A.I., *et al*. (2011). Polyubiquitin linkage profiles in three models of proteolytic stress suggest the etiology of Alzheimer disease. The Journal of biological chemistry *286*, 10457-10465.

Das, R., Mariano, J., Tsai, Y.C., Kalathur, R.C., Kostova, Z., Li, J., Tarasov, S.G., McFeeters, R.L., Altieri, A.S., Ji, X., *et al*. (2009). Allosteric activation of E2-RING finger-mediated ubiquitylation by a structurally defined specific E2-binding region of gp78. Molecular cell *34*, 674-685.

Datta, A.B., Hura, G.L., and Wolberger, C. (2009). The Structure and Conformation of Lys63-Linked Tetraubiquitin. Journal of Molecular Biology *392*, 1117-1124.

De Vries, S.J., van Dijk, A.D.J., Krzeminski, M., van Dijk, M., Thureau, A., Hsu, V., Wassenaar, T., and Bonvin, A.M.J.J. (2007). HADDOCK versus HADDOCK: New features and performance of HADDOCK2.0 on the CAPRI targets. Proteins-Structure Function and Bioinformatics *69*, 726-733.

Deshaies, R.J., and Joazeiro, C.A.P. (2009). RING Domain E3 Ubiquitin Ligases. In Annual Review of Biochemistry, pp. 399-434.

Dikic, I., Wakatsuki, S., and Walters, K.J. (2009). Ubiquitin-binding domains - from structures to functions. Nature Reviews Molecular Cell Biology *10*, 659-671.

Dolinsky, T.J., Czodrowski, P., Li, H., Nielsen, J.E., Jensen, J.H., Klebe, G., and Baker, N.A. (2007). PDB2PQR: expanding and upgrading automated preparation of biomolecular structures for molecular simulations. Nucleic Acids Res *35*, W522-W525.

Dolinsky, T.J., Nielsen, J.E., McCammon, J.A., and Baker, N.A. (2004). PDB2PQR: an automated pipeline for the setup of Poisson-Boltzmann electrostatics calculations. Nucleic Acids Res *32*, W665-W667.

Dou, H., Buetow, L., Sibbet, G.J., Cameron, K., and Huang, D.T. (2012). BIRC7-E2 ubiquitin conjugate structure reveals the mechanism of ubiquitin transfer by a RING dimer. Nat Struct Mol Biol *19*, 876-883.

Dye, B.T., and Schulman, B.A. (2007). Structural mechanisms underlying posttranslational modification by ubiquitin-like proteins. In Annual Review of Biophysics and Biomolecular Structure, pp. 131-150.

Dynek, J.N., Goncharov, T., Dueber, E.C., Fedorova, A.V., Izrael-Tomasevic, A., Phu, L., Helgason, E., Fairbrother, W.J., Deshayes, K., Kirkpatrick, D.S.*, et al*. (2010). c-IAP1 and UbcH5 promote K11-linked polyubiquitination of RIP1 in TNF signalling. Embo Journal *29*, 4198-4209.

Eddins, M.J., Carlile, C.M., Gomez, K.M., Pickart, C.M., and Wolberger, C. (2006). Mms2-Ubc13 covalently bound to ubiquitin reveals the structural basis of linkage-specific polyubiquitin chain formation. Nature Structural & Molecular Biology *13*, 915-920.

Eddins, M.J., Varadan, R., Flushman, D., Pickart, C.M., and Wolberger, C. (2007). Crystal structure and solution NMR studies of Lys48-linked tetraubiquitin at neutral pH. Journal of Molecular Biology *367*, 204-211.

Finley, D. (2009). Recognition and Processing of Ubiquitin-Protein Conjugates by the Proteasome. In Annual Review of Biochemistry, pp. 477-513.

Fujita, T., Ikeda, H., Kawasaki, K., Taira, N., Ogasawara, Y., Nakagawara, A., and Doihara, H. (2009a). Clinicopathological relevance of UbcH10 in breast cancer. Cancer science *100*, 238-248.

Fujita, T., Ikeda, H., Taira, N., Hatoh, S., Naito, M., and Doihara, H. (2009b). Overexpression of UbcH10 alternates the cell cycle profile and accelerate the tumor proliferation in colon cancer. BMC cancer *9*, 87.

Garnett, M.J., Mansfeld, J., Godwin, C., Matsusaka, T., Wu, J., Russell, P., Pines, J., and Venkitaraman, A.R. (2009). UBE2S elongates ubiquitin chains on APC/C substrates to promote mitotic exit. Nature Cell Biology *11*, 1363-U1241.

Gazdoiu, S., Yamoah, K., Wu, K., and Pan, Z.Q. (2007). Human Cdc34 employs distinct sites to coordinate attachment of ubiquitin to a substrate and assembly of polyubiquitin chains. Mol Cell Biol *27*, 7041-7052.

Geley, S., Kramer, E., Gieffers, C., Gannon, J., Peters, J.M., and Hunt, T. (2001). Anaphase-promoting complex/cyclosome-dependent proteolysis of human cyclin a starts at the beginning of mitosis and is not subject to the spindle assembly checkpoint. Journal of Cell Biology *153*, 137-147.

Gimenez-Abian, J.F., Diaz-Martinez, L.A., Wirth, K.G., Andrews, C.A., Gimenez-Martin, G., and Clarke, D.J. (2005). Regulated separation of sister centromeres depends on the spindle assembly checkpoint but not on the anaphase promoting complex/cyclosome. Cell Cycle *4*, 1561-1575.

Goshima, G., Wollman, R., Goodwin, S.S., Zhang, N., Scholey, J.M., Vale, R.D., and Stuurman, N. (2007). Genes required for mitotic spindle assembly in Drosophila S2 cells. Science *316*, 417-421.

Goto, E., Yamanaka, Y., Ishikawa, A., Aoki-Kawasumi, M., Mito-Yoshida, M., Ohmura-Hoshino, M., Matsuki, Y., Kajikawa, M., Hirano, H., and Ishido, S. (2010). Contribution of lysine 11-linked ubiquitination to MIR2-mediated major histocompatibility complex class I internalization. The Journal of biological chemistry *285*, 35311-35319.

Haas, A.L., Reback, P.B., and Chau, V. (1991). Ubiquitin conjugation by the yeast RAD6 and CDC34 gene products. Comparison to their putative rabbit homologs, E2(20K) AND E2(32K). The Journal of biological chemistry *266*, 5104-5112.

Haldeman, M.T., Xia, G., Kasperek, E.M., and Pickart, C.M. (1997). Structure and function of ubiquitin conjugating enzyme E2-25K: The tail is a core-dependent activity element. Biochemistry *36*, 10526-10537.

Hamilton, K.S., Ellison, M.J., Barber, K.R., Williams, R.S., Huzil, J.T., McKenna, S., Ptak, C., Glover, M., and Shaw, G.S. (2001). Structure of a conjugating enzyme-ubiquitin thiolester intermediate reveals a novel role for the ubiquitin tail. Structure *9*, 897-904.

Hay-Koren, A., Caspi, M., Zilberberg, A., and Rosin-Arbesfeld, R. (2011). The EDD E3 ubiquitin ligase ubiquitinates and up-regulates beta-catenin. Mol Biol Cell *22*, 399-411.

Hershko, A., and Ciechanover, A. (1998). The ubiquitin system. Annual Review of Biochemistry *67*, 425-479.

Hoege, C., Pfander, B., Moldovan, G.L., Pyrowolakis, G., and Jentsch, S. (2002). RAD6-dependent DNA repair is linked to modification of PCNA by ubiquitin and SUMO. Nature *419*, 135-141.

Hoeller, D., Hecker, C.-M., Wagner, S., Rogov, V., Doetsch, V., and Dikic, I. (2007). E3-independent monoubiquitination of ubiquitin-binding proteins. Molecular cell *26*, 891-898.

Hofmann, R.M., and Pickart, C.M. (1999). Noncanonical MMS2-encoded ubiquitin-conjugating enzyme functions in assembly of novel polyubiquitin chains for DNA repair. Cell *96*, 645-653.

Hofmann, R.M., and Pickart, C.M. (2001). In vitro assembly and recognition of Lys-63 polyubiquitin chains. The Journal of biological chemistry *276*, 27936-27943.

Husnjak, K., and Dikic, I. (2012). Ubiquitin-binding proteins: decoders of ubiquitin-mediated cellular functions. Annu Rev Biochem *81*, 291-322.

Jin, L., Williamson, A., Banerjee, S., Philipp, I., and Rape, M. (2008). Mechanism of ubiquitin-chain formation by the human anaphase-promoting complex. Cell *133*, 653-665.

Jung, C.-R., Hwang, K.-S., Yoo, J., Cho, W.-K., Kim, J.-M., Kim, W.H., and Im, D.-S. (2006). E2-EPF UCP targets pVHL for degradation and associates with tumor growth and metastasis. Nature Medicine *12*, 809-816.

Kamadurai, H.B., Souphron, J., Scott, D.C., Duda, D.M., Miller, D.J., Stringer, D., Piper, R.C., and Schulman, B.A. (2009). Insights into Ubiauitin Transfer Cascades from a Structure of a UbcH5B similar to Ubiquitin-HECTNEDD4L Complex. Molecular cell *36*, 1095-1102.

Kerscher, O., Felberbaum, R., and Hochstrasser, M. (2006). Modification of proteins by ubiquitin and ubiquitin-like proteins. In Annual Review of Cell and Developmental Biology, pp. 159-180.

Kim, A.H., Puram, S.V., Bilimoria, P.M., Ikeuchi, Y., Keough, S., Wong, M., Rowitch, D., and Bonni, A. (2009). A Centrosomal Cdc20-APC Pathway Controls Dendrite Morphogenesis in Postmitotic Neurons. Cell *136*, 322-336.

Kim, H.T., Kim, K.P., Lledias, F., Kisselev, A.F., Scaglione, K.M., Skowyra, D., Gygi, S.P., and Goldberg, A.L. (2007). Certain pairs of ubiquitin-conjugating enzymes (E2s) and ubiquitin-protein ligases (E3s) synthesize nondegradable forked ubiquitin chains containing all possible isopeptide linkages. Journal of Biological Chemistry *282*, 17375-17386.

Kimata, Y., Baxter, J.E., Fry, A.M., and Yamano, H. (2008). A Role for the Fizzy/Cdc20 Family of Proteins in Activation of the APC/C Distinct from Substrate Recruitment. Molecular cell *32*, 576-583.

Kirkpatrick, D.S., Hathaway, N.A., Hanna, J., Elsasser, S., Rush, J., Finley, D., King, R.W., and Gygi, S.P. (2006). Quantitative analysis of in vitro ubiquitinated cyclin B1 reveals complex chain topology. Nature Cell Biology *8*, 700-U121.

Kittler, R., Putz, G., Pelletier, L., Poser, I., Heninger, A.K., Drechsel, D., Fischer, S., Konstantinova, I., Habermann, B., Grabner, H., *et al*. (2004). An endoribonuclease-prepared siRNA screen in human cells identifies genes essential for cell division. Nature *432*, 1036-1040.

Kleiger, G., Saha, A., Lewis, S., Kuhlman, B., and Deshaies, R.J. (2009). Rapid E2-E3 assembly and disassembly enable processive ubiquitylation of cullin-RING ubiquitin ligase substrates. Cell *139*, 957-968.

Komander, D. (2009). The emerging complexity of protein ubiquitination. Biochemical Society Transactions *37*, 937-953.

Komander, D., and Rape, M. (2012). The ubiquitin code. Annu Rev Biochem *81*, 203-229.

Komander, D., Reyes-Turcu, F., Licchesi, J.D.F., Odenwaelder, P., Wilkinson, K.D., and Barford, D. (2009). Molecular discrimination of structurally equivalent Lys 63-linked and linear polyubiquitin chains. Embo Reports *10*, 466-473.

Konarev, P.V., Volkov, V.V., Sokolova, A.V., Koch, M.H.J., and Svergun, D.I. (2003). PRIMUS: a Windows PC-based system for small-angle scattering data analysis. J Appl Crystallogr *36*, 1277-1282.

Kraft, C., Herzog, F., Gieffers, C., Mechtler, K., Hagting, A., Pines, J., and Peters, J.M. (2003). Mitotic regulation of the human anaphase-promoting complex by phosphorylation. Embo Journal *22*, 6598-6609.

Kraft, C., Vodermaier, H.C., Maurer-Stroh, S., Eisenhaber, F., and Peters, J.M. (2005). The WD40 propeller domain of Cdh1 functions as a destruction box receptor for APC/C substrates. Molecular cell *18*, 543-553.

Krissinel, E., and Henrick, K. (2007). Inference of macromolecular assemblies from crystalline state. Journal of Molecular Biology *372*, 774-797.

Lee, C.V., Liang, W.C., Dennis, M.S., Eigenbrot, C., Sidhu, S.S., and Fuh, G. (2004). High-affinity human antibodies from phage-displayed synthetic fab libraries with a single framework scaffold. Journal of Molecular Biology *340*, 1073-1093.

Li, W., Tu, D., Brunger, A.T., and Ye, Y. (2007). A ubiquitin ligase transfers preformed polyubiquitin chains from a conjugating enzyme to a substrate. Nature *446*, 333-337.

Li, W., Tu, D., Li, L., Wollert, T., Ghirlando, R., Brunger, A.T., and Ye, Y. (2009). Mechanistic insights into active site-associated polyubiquitination by the ubiquitin-conjugating enzyme Ube2g2. Proceedings of the National Academy of Sciences of the United States of America *106*, 3722-3727.

Mathe, E., Kraft, C., Giet, F., Deak, P., Peters, J.M., and Glover, D.M. (2004). The E2-C vihar is required for the correct spatiotemporal proteolysis of cyclin B and itself undergoes cyclical degradation. Current Biology *14*, 1723-1733.

Matsumoto, M.L., Dong, K.C., Yu, C., Phu, L., Gao, X., Hannoush, R.N., Hymowitz, S.G., Kirkpatrick, D.S., Dixit, V.M., and Kelley, R.F. (2012). Engineering and structural characterization of a linear polyubiquitin-specific antibody. J Mol Biol *418*, 134-144.

Matsumoto, M.L., Wickliffe, K.E., Dong, K.C., Yu, C., Bosanac, I., Bustos, D., Phu, L., Kirkpatrick, D.S., Hymowitz, S.G., Rape, M., *et al.* (2010). K11-Linked Polyubiquitination in Cell Cycle Control Revealed by a K11 Linkage-Specific Antibody. Molecular cell *39*, 477-484.

Meierhofer, D., Wang, X., Huang, L., and Kaiser, P. (2008). Quantitative analysis of global ubiquitination in HeLa cells by mass spectrometry. Journal of proteome research *7*, 4566-4576.

Meyer, H.J., and Rape, M. (2011). Processive ubiquitin chain formation by the anaphase-promoting complex. Seminars in cell & developmental biology *22*, 544-550.

Newton, K., Matsumoto, M.L., Wertz, I.E., Kirkpatrick, D.S., Lill, J.R., Tan, J., Dugger, D., Gordon, N., Sidhu, S.S., Fellouse, F.A., *et al*. (2008). Ubiquitin chain editing revealed by polyubiquitin linkage-specific antibodies. Cell *134*, 668-678.

Peng, J.M., Schwartz, D., Elias, J.E., Thoreen, C.C., Cheng, D.M., Marsischky, G., Roelofs, J., Finley, D., and Gygi, S.P. (2003). A proteomics approach to understanding protein ubiquitination. Nature Biotechnology *21*, 921-926.

Peters, J.-M. (2006). The anaphase promoting complex/cyclosome: a machine designed to destroy. Nature Reviews Molecular Cell Biology *7*, 644-656.

Petroski, M.D. (2008). The ubiquitin system, disease, and drug discovery. BMC biochemistry *9 Suppl 1*, S7.

Petroski, M.D., and Deshaies, R.J. (2005). Mechanism of lysine 48-linked ubiquitin-chain synthesis by the cullin-RING ubiquitin-ligase complex SCF-Cdc34. Cell *123*, 1107-1120.

Pfleger, C.M., and Kirschner, M.W. (2000). The KEN box: an APC recognition signal distinct from the D box targeted by Cdh1. Genes & Development *14*, 655-665.

Phillips, C.L., Thrower, J., Pickart, C.M., and Hill, C.P. (2001). Structure of a new crystal form of tetraubiquitin. Acta Crystallographica Section D-Biological Crystallography *57*, 341-344.

Pickart, C.M., and Raasi, S. (2005). Controlled synthesis of polyubiquitin chains. In Ubiquitin and Protein Degradation, Pt B, R.J. Deshaies, ed., pp. 21-36.

Pierce, N.W., Kleiger, G., Shan, S.-o., and Deshaies, R.J. (2009). Detection of sequential polyubiquitylation on a millisecond timescale. Nature *462*, 615-U685.

Plechanovova, A., Jaffray, E.G., Tatham, M.H., Naismith, J.H., and Hay, R.T. (2012). Structure of a RING E3 ligase and ubiquitin-loaded E2 primed for catalysis. Nature *489*, 115-120.

Potapova, T.A., Daum, J.R., Pittman, B.D., Hudson, J.R., Jones, T.N., Satinover, D.L., Stukenberg, P.T., and Gorbsky, G.J. (2006). The reversibility of mitotic exit in vertebrate cells. Nature *440*, 954-958.

Pruneda, J.N., Littlefield, P.J., Soss, S.E., Nordquist, K.A., Chazin, W.J., Brzovic, P.S., and Klevit, R.E. (2012). Structure of an E3:E2~Ub complex reveals an allosteric mechanism shared among RING/U-box ligases. Molecular cell *47*, 933-942.

Rape, M., and Kirschner, M.W. (2004). Autonomous regulation of the anaphase-promoting complex couples mitosis to S-phase entry. Nature *432*, 588-595.

Rape, M., Reddy, S.K., and Kirschner, M.W. (2006). The processivity of multiubiquitination by the APC determines the order of substrate degradation. Cell *124*, 89-103.

Reddy, S.K., Rape, M., Margansky, W.A., and Kirschner, M.W. (2007). Ubiquitination by the anaphase-promoting complex drives spindle checkpoint inactivation. Nature *446*, 921-925.

Reverter, D., and Lima, C.D. (2005). Insights into E3 ligase activity revealed by a SUMO-RanGAP1-Ubc9-Nup358 complex. Nature *435*, 687-692.

Reyes-Turcu, F.E., Ventii, K.H., and Wilkinson, K.D. (2009). Regulation and Cellular Roles of Ubiquitin-Specific Deubiquitinating Enzymes. In Annual Review of Biochemistry, pp. 363-397.

Rodrigo-Brenni, M.C., Foster, S.A., and Morgan, D.O. (2010). Catalysis of Lysine 48-Specific Ubiquitin Chain Assembly by Residues in E2 and Ubiquitin. Molecular cell *39*, 548-559.

Rodrigo-Brenni, M.C., and Morgan, D.O. (2007). Sequential E2s drive polyubiquitin chain assembly on APC targets. Cell *130*, 127-139.

Ryu, K.Y., Baker, R.T., and Kopito, R.R. (2006). Ubiquitin-specific protease 2 as a tool for quantification of total ubiquitin levels in biological specimens. Analytical Biochemistry *353*, 153-155.

Sadowski, M., Suryadinata, R., Lai, X., Heierhorst, J., and Sarcevic, B. (2010). Molecular Basis for Lysine Specificity in the Yeast Ubiquitin-Conjugating Enzyme Cdc34. Molecular and Cellular Biology *30*, 2316-2329.

Saha, A., Lewis, S., Kleiger, G., Kuhlman, B., and Deshaies, R.J. (2011). Essential role for ubiquitin-ubiquitin-conjugating enzyme interaction in ubiquitin discharge from Cdc34 to substrate. Molecular cell *42*, 75-83.

Schulman, B.A., and Harper, J.W. (2009). Ubiquitin-like protein activation by E1 enzymes: the apex for downstream signalling pathways. Nature Reviews Molecular Cell Biology *10*, 319-331.

Sheinerman, F.B., and Honig, B. (2002). On the role of electrostatic interactions in the design of protein-protein interfaces. Journal of Molecular Biology *318*, 161-177.

Sigismund, S., Polo, S., and Di Fiore, P.P. (2004). Signaling through monoubiquitination. Current topics in microbiology and immunology *286*, 149-185.

Skaug, B., Jiang, X., and Chen, Z.J. (2009). The Role of Ubiquitin in NF-kappa B Regulatory Pathways. In Annual Review of Biochemistry, pp. 769-796.

Smith, M.H., Ploegh, H.L., and Weissman, J.S. (2011). Road to ruin: targeting proteins for degradation in the endoplasmic reticulum. Science *334*, 1086-1090.

Somma, M.P., Ceprani, F., Bucciarelli, E., Naim, V., De Arcangelis, V., Piergentili, R., Palena, A., Ciapponi, L., Giansanti, M.G., Pellacani, C.*, et al*. (2008). Identification of Drosophila Mitotic Genes by Combining Co-Expression Analysis and RNA Interference. Plos Genetics *4*.

Song, L., and Rape, M. (2010). Regulated Degradation of Spindle Assembly Factors by the Anaphase-Promoting Complex. Molecular cell *38*, 369-382.

Stegmeier, F., Rape, M., Draviam, V.M., Nalepa, G., Sowa, M.E., Ang, X.L., McDonald, E.R., III, Li, M.Z., Hannon, G.J., Sorger, P.K., *et al*. (2007). Anaphase initiation is regulated by antagonistic ubiquitination and deubiquitination activities. Nature *446*, 876-881.

Summers, M.K., Pan, B., Mukhyala, K., and Jackson, P.K. (2008). The unique N terminus of the UbcH10 E2 enzyme controls the threshold for APC activation and enhances checkpoint regulation of the APC. Molecular cell *31*, 544-556.

Svergun, D., Barberato, C., and Koch, M.H.J. (1995). CRYSOL - A program to evaluate x-ray solution scattering of biological macromolecules from atomic coordinates. J Appl Crystallogr *28*, 768-773.

Svergun, D.I., Semenyuk, A.V., and Feigin, L.A. (1988). Small-Angle-Scattering-Data Treatment by the Regularization Method. Acta Crystallogr A *44*, 244-250.

Tang, Z.Y., Li, B., Bharadwaj, R., Zhu, H.H., Ozkan, E., Hakala, K., Deisenhofer, J., and Yu, H.T. (2001). APC2 cullin protein and APC11 RING protein comprise the minimal ubiquitin ligase module of the anaphase-promoting complex. Molecular Biology of the Cell *12*, 3839-3851.

Tedesco, D., Zhang, J., Trinh, L., Lalehzadeh, G., Meisner, R., Yamaguchi, K.D., Ruderman, D.L., Dinter, H., and Zajchowski, D.A. (2007). The ubiquitin-conjugating enzyme E2-EPF is overexpressed in primary breast cancer and modulates sensitivity to topoisomerase II inhibition. Neoplasia *9*, 601-613

Tenno, T., Fujiwara, K., Tochio, H., Iwai, K., Morita, E.H., Hayashi, H., Murata, S., Hiroaki, H., Sato, M., Tanaka, K., *et al*. (2004). Structural basis for distinct roles of Lys63- and Lys48-linked polyubiquitin chains. Genes to Cells *9*, 865-875.

Tugendreich, S., Tomkiel, J., Earnshaw, W., and Hieter, P. (1995). CDC27Hs colocalizes with CDC16Hs to the centrosome and mitotic spindle and is essential for the metaphase to anaphase transition. Cell *81*, 261-268.

Van Nocker, S., and Vierstra, R.D. (1991). Cloning and characterization of a 20-kDa ubiquitin carrier protein from wheat that catalyzes multiubiquitin chain formation in vitro. Proceedings of the National Academy of Sciences of the United States of America *88*, 10297-10301.

van Ree, J.H., Jeganathan, K.B., Malureanu, L., and van Deursen, J.M. (2010). Overexpression of the E2 ubiquitin-conjugating enzyme UbcH10 causes chromosome missegregation and tumor formation. The Journal of cell biology *188*, 83-100.

VanDemark, A.P., Hofmann, R.M., Tsui, C., Pickart, C.M., and Wolberger, C. (2001). Molecular insights into polyubiquitin chain assembly: Crystal structure of the Mms2/Ubc13 heterodimer. Cell *105*, 711-720.

Varadan, R., Assfalg, M., Haririnia, A., Raasi, S., Pickart, C., and Fushman, D. (2004). Solution conformation of Lys(63)-linked di-ubiquitin chain provides clues to functional diversity of polyubiquitin signaling. Journal of Biological Chemistry *279*, 7055-7063.

Varadan, R., Walker, O., Pickart, C., and Fushman, D. (2002). Structural properties of polyubiquitin chains in solution. Journal of Molecular Biology *324*, 637-647.

Visintin, R., Prinz, S., and Amon, A. (1997). CDC20 and CDH1: A family of substrate-specific activators of APC-dependent proteolysis. Science *278*, 460-463.

Wagner, K.W., Sapinoso, L.M., El-Rifai, W., Frierson, H.F., Butz, N., Mestan, J., Hofmann, F., Deveraux, Q.L., and Hampton, G.M. (2004). Overexpression, genomic amplification and therapeutic potential of inhibiting the UbcH10 ubiquitin conjugase in human carcinomas of diverse anatomic origin. Oncogene *23*, 6621-6629.

Walczak, H., Iwai, K., and Dikic, I. (2012). Generation and physiological roles of linear ubiquitin chains. BMC biology *10*, 23.

Walker, A., Acquaviva, C., Matsusaka, T., Koop, L., and Pines, J. (2008). UbcH10 has a rate-limiting role in G1 phase but might not act in the spindle checkpoint or as part of an autonomous oscillator. Journal of Cell Science *121*, 2319-2326.

Wei, W., Ayad, N.G., Wan, Y., Zhang, G.J., Kirschner, M.W., and Kaelin, W.G. (2004). Degradation of the SCF component Skp2 in cell-cycle phase G1 by the anaphase-promoting complex. Nature *428*, 194-198.

Wickliffe, K., Williamson, A., Jin, L., and Rape, M. (2009). The multiple layers of ubiquitin-dependent cell cycle control. Chemical reviews *109*, 1537-1548.

Williamson, A., Banerjee, S., Zhu, X., Philipp, I., Iavarone, A.T., and Rape, M. (2011). Regulation of Ubiquitin Chain Initiation to Control the Timing of Substrate Degradation. Molecular cell *42*, 744-757.

Williamson, A., Wickliffe, K.E., Mellone, B.G., Song, L., Karpen, G.H., and Rape, M. (2009). Identification of a physiological E2 module for the human anaphase-promoting complex. Proceedings of the National Academy of Sciences of the United States of America *106*, 18213-18218.

Wojcik, C., Yano, M., and DeMartino, G.N. (2004). RNA interference of valosin-containing protein (VCP/p97) reveals multiple cellular roles linked to ubiquitin/proteasome-dependent proteolysis. Journal of Cell Science *117*, 281-292.

Wu, K., Kovacev, J., and Pan, Z.-Q. (2010a). Priming and Extending: A UbcH5/Cdc34 E2 Handoff Mechanism for Polyubiquitination on a SCF Substrate. Molecular cell *37*, 784-796.

Wu, P.Y., Hanlon, M., Eddins, M., Tsui, C., Rogers, R.S., Jensen, J.P., Matunis, M.J., Weissman, A.M., Wolberger, C., and Pickart, C.M. (2003). A conserved catalytic residue in the ubiquitin-conjugating enzyme family. The EMBO journal *22*, 5241-5250.

Wu, T., Merbl, Y., Huo, Y., Gallop, J.L., Tzur, A., and Kirschner, M.W. (2010b). UBE2S drives elongation of K11-linked ubiquitin chains by the Anaphase-Promoting Complex. Proceedings of the National Academy of Sciences of the United States of America *107*, 1355-1360.

Xu, P., Duong, D.M., Seyfried, N.T., Cheng, D., Xie, Y., Robert, J., Rush, J., Hochstrasser, M., Finley, D., and Peng, J. (2009). Quantitative Proteomics Reveals the Function of Unconventional Ubiquitin Chains in Proteasomal Degradation. Cell *137*, 133-145.

Ye, Y., and Rape, M. (2009). Building ubiquitin chains: E2 enzymes at work. Nature Reviews Molecular Cell Biology *10*, 755-764.

Yu, H. (2007). Cdc20: A WD40 activator for a cell cycle degradation machine. Molecular cell *27*, 3-16.

Yunus, A.A., and Lima, C.D. (2006). Lysine activation and functional analysis of E2-mediated conjugation in the SUMO pathway. Nature Structural & Molecular Biology *13*, 491-499.